UNIVERSITAS MUHAMMADIYAH PROF. DR. HAMKA
FAKULTAS FARMASI DAN SAINS
Jl. Limau II, Kebayoran Baru, Jakarta 12130 Tel. (021) 7208177, 722886, Fax. (021) 7261226, 7256620
Islamic Centre, Jl. Delima II/IV, Klender, Jakarta Timur Tlp.: (021) 8611070, Fax. (021) 86603233
Website: www.ffs-uhamka.ac.id; E-mail: ffs@uhamka.ac.id

SURAT TUGAS
MELAKUKAN KEGIATAN PENELITIAN DAN PUBLIKASI
NO. 220/F.03.08/2022

Bismillahirrohmanirrohiim,
Yang bertanda tangan di bawah ini

N a m a	**Dr. apt. Hadi Sunaryo, M.Si.**
NIDN	0325067201
Pangkat /Jabatan Akademik	Penata Tk. I, III/d / Lektor Kepala
Jabatan	Dekan
Unit Kerja	Fakultas Farmasi dan Sains UHAMKA Jakarta

Memberikan tugas Penelitian dan Publikasi pada **tahun akademik 2021/2022** kepada:

N a m a	**Dr. apt. Hariyanti, M.Si.**
NID/NIDN	D.03.0606/ 0311097705
Pangkat /Jabatan Akademik	Penata/ III-C
Jabatan Fungsional	LEKTOR
Unit Kerja	Fakultas Farmasi dan Sains UHAMKA Jakarta

Untuk Melaksanakan Penelitian dan Publikasi sebagai berikut:

NO	JUDUL PENELITIAN DAN PUBLIKASI
1.	**In Vitro Release of Metformin HCl from Polyvinyl Alcohol (PVA) - Gelatin Hydrogels Prepared by Gamma Irradiation"**

Demikian surat tugas ini diberikan kepada yang bersangkutan untuk dilaksanakan dengan penuh amanah dan tanggung jawab

Jakarta, 09 Maret 2022
Dekan,

Dr. apt. Hadi Sunaryo, M.Si., Apt.

Tembusan Yth:
1. Rektor UHAMKA Jakarta
2. Wakil Rektor I dan II UHAMKA Jakarta
3. Arsip

Atom Indonesia

Journal homepage: http://aij.batan.go.id

In Vitro Release of Metformin HCl from Polyvinyl Alcohol (PVA) - Gelatin Hydrogels Prepared by Gamma Irradiation

Hariyanti[1*], Erizal[2], E. Mustikarani[1], I. Lestari[3], F. Lukitowati[2]

[1]*Faculty Pharmacy and Science, Muhammadiyah Prof. Dr. Hamka University (UHAMKA), Islamic Center, Jl. Delima II/IV Perumnas Klender, Jakarta 13640, Indonesia*
[2]*Centre for Applications of Isotopes and Radiation, National Nuclear Energy Agency (BATAN), Jl. Lebak Bulus Raya No. 49, Jakarta 12440, Indonesia*
[3]*Department of Physics, Faculty of Mathematics and Natural Sciences, Universitas Indonesia, Jl. Margonda Raya, Depok 16424, Indonesia*

ARTICLE INFO

Article history:
Received 4 February 2021
Received in revised form 31 January 2022
Accepted 5 February 2022

Keywords:
Gelatin
Hydrogel
PVA
Metformin HCl
Irradiation
Freeze-thaw

ABSTRACT

The aim of this present work is to use polyvinyl alcohol (PVA) – gelatin-based hydrogel prepared by γ-rays irradiation with different gelatin concentrations ranging from 0.5 - 2 %w/v for immobilization of Metformin HCl (MH) at dose range of 0 - 30 mg. The mixture were freezed-thawed for 3 cycles, irradiated using γ-rays with sterilization dose at 25 kGy (dose rates 5 kGy/h). Gel fraction and water absorption were determined gravimetrically. The surface morphology of hydrogels were observed using Scanning Electron Microscope (SEM). In vitro release of MH were taken using UV-Vis spectrophotometer. After evaluated, it was found that with increasing gelatin concentrations, gel fraction increases and water absorption decreases. With increasing gelatin concentration and drug dosage, the cumulative drug released decreases. From SEM observation, the hydrogel had a heterogeneous porous. The hydrogel based on PVA-gelatin can be considered as a matrix for controlled drug release and safe for humans since both PVA and gelatin are non-toxic.

INTRODUCTION

Metformin HCl is a type-II antidiabetic drug that works to reduce excessive sugar levels in blood plasma. The advantages of metformin as a water-soluble drug are the low risk of hypoglycemia, and able to reduce the probability of heart damage and death. Metformin is an anti-hyperglycemia drug that is not completely absorbed in the intestine with a bioavailability of about 50 - 60 % in a half-life of 1.5 to 4.5 hours. The disadvantage of metformin is its usage frequency of 2 to 3 times a day with relatively large doses, which can reduce patient compliance. A formula that can maintain the plasma level of metformin and can last for 10 - 16 hours may be adequate in a single dose of metformin. Therefore, sustained products release are needed to entrap metformin which is useful for extending drug working time and improving patient compliance [1].

Recent progress and attempts were made on the oral sustained or controlled release formulation for metformin. Various methods are available to formulate water-soluble drugs into sustained release dosage forms by retarding the dissolution rate such as matrix tablets, coated tablets, floating tablets, slow release granules, sustained release oily matrix, sustained-release microparticles, and elementary osmotic pump [2-6]. For all these purposes, synthetic or natural polymers are used i.e. ethylcellulose, methylcellulose, PVP, gum, agar, microparticle, HPMC, etc. All the controlled release dosage forms available for metformin claims to release the drug up to 8 hours. These required the drug administration for 2 to 3 times a day, which is unfeasible for a single dose formulation. In some cases, the optimum release of drug was shown but only as an in vitro data. In vivo release was studied

*Corresponding author.
E-mail address: hariyanti@uhamka.ac.id
DOI: https://doi.org/10.17146/aij.2022.1123

under animals only. Further clinical studies are needed to assess the benefit of these systems for patients suffering from hypotension. Extensive studies are required to examine the factors that play a role in development of controlled release formulations of metformin. Surprisingly, despite all these research works, there are likely to be no well established metformin controlled release formulations reported to be available in the market. One candidate that has good prospects as a matrix for drug immobilization is a hydrogel. The development of the metformin in the form of immobilization has several advantages, for example reducing the frequency of drug use and minimizing the fluctuations in blood concentrations of drugs that reduce the side effect, among others [7].

Hydrogels are hydrophilic polymers with three-dimensional polymeric network, large molecular weights, and are insoluble in water. They have porous structure, which means that water and small molecules can easily diffuse across the pores. Their unique properties such as biocompatibilty, biodegradability, sensitivity to various stimuli and the ability to be conjugated easily with hydrophilic and hydrophobic therapeutic compounds, have made them important candidates in drug immobilization [8-11].

Drug immobilization technique of the hydrogel is one of the drug delivery methods currently being developed intensively in pharmaceutical industries as well as in medicine [12]. Drug immobilization is one of the techniques for an entrapped drug in hydrogels and released in a medium that can be controlled for a certain period of time. In general, immobilization of drugs in hydrogels can be done in two ways, namely post loading and in situ loading [13,14]. For post loading, the drug is entrapped after the hydrogels is formed. Whereas for in situ loading, the drug is simultaneously entrapped during synthesis process. Basically, drug immobilization technique is physically entrapping the drug in the matrix; the drug does not undergo chemical reactions with the hydrogels and the drug can be separated from the hydrogels in a controlled time interval [15]. One of the potential hydrogels to be used as a drug delivery is gelatin.

Gelatin is a natural, non-toxic, inexpensive polymer compound, biodegradable polymer, denatured protein obtained from the collagen acid and base process [16]. Gelatin has popular properties in the biomedical field including easily degraded, low immunogenicity and toxicity, a very large potential capacity to be modified on the active site of its amino-amino acids [17]. Gelatin can be easily form hydrogels via temperature changes, but the result is unstable and has poor mechanical properties [18]. The stability and mechanical properties of gelatin hydrogel can be improved via chemical crosslinking processes using crosslinkers such as genipin, glutaraldehyde, and carbodiimide [19,20]. However, the crosslinker is toxic. One method that is promising, safe, and inexpensive to modify gelatin into hydrogel is to form a physical crosslinking through the freeze-thaw process which is blended with polyvinyl alcohol (PVA) polymers [21] or by combined freezing-thawing and gamma ray irradiation [22,23].

Polyvinyl alcohol (PVA) is a potential hydrophilic polymer raw material for use in the biomedical field, especially in the form of injectable liquid gels [23,24]. PVA is biocompatible, non-toxic, non-carcinogenic, and shows good elasticity and compressive strength. In addition, PVA has the advantage of being able to easily form a physically crosslinked hydrogel with a freeze-thaw process treatment [25]. In the freezing process, water molecules will form ice crystals that are trapped in the PVA matrix. With the thaw treatment, ice crystals trapped in the hydrogel melt out from PVA hydrogel and form pores in hydrogel that are useful for the diffusion of water, drugs, or other molecules. Numerous research has utilized this PVA-based technique which is combined with other polymers/monomers to make hydrogels or other forms [1]. Thus, gelatin should be combined with PVA to obtain new hydrogels as a matrix for drug immobilization such as metformin HCl, which is then sterilized by gamma irradiation.

Drug immobilization method in hydrogel matrix using gamma irradiation technique has advantages such as polymers or monomers as hydrogel matrix can undergo crosslinking reactions, drugs can be trapped in hydrogel matrix simultaneously, there is no need for crosslinkers, and the resulting products are sterile. Based on the previous study, PVA-gelatin hydrogels exhibited the best swelling through gamma rays irradiation at a single dose of 25 kGy [26,27]. In addition, to ensure that the drug does not degrade, the use of PVA as a matrix can be supported with the freeze-thaw process before the irradiation process in the drug-polymer solution mixture.

Based on the description above, PVA-gelatin copolymer hydrogel containing metformin as a model of drug using freezing-thawing and irradiation technique process simultaneously. The hydrogel PVA-gelatin can prolong the release of metformin as well as the effect of irradiation dose or drug compositions.

METHODOLOGY

The PVA was made by Kuraray, Japan. The gelatin fish scales was prepared by PAIR BATAN. The metformin HCl was made in Mumbai, India. Distilled water was used for drug dissolution.

Gamma irradiation sources

The samples were irradiated using Co-60 gamma ray facility in IRPASENA, BATAN. The dose rate was 5 kGy/hour and the process was carried out at room temperature. The irradiation doses were calibrated using a Frieke dosimeter.

Determination of water absorption [9]

Hydrogel samples were dried in an oven at temperature of 60 °C until constant weight, then weighed (Wo). The dried hydrogels were afterward immersed in 25 ml of distilled water. After 1 hour, the hydrogels were removed from the soaking medium. Then, after removing the water on the hydrogel surfaces with filter paper, subsequently the hydrogel were weighed (Ws). Afterwards, the hydrogels were immersed again in water with the same container to test the water absorption for 1 hour. The same treatment was done for testing water absorption in different time intervals. Finally, the hydrogels were dried in an oven at 60 °C until constant weight. Water absorption can be calculated using the following Eq. (1),

$$\text{Water absorption} = \frac{Ws - Wo}{Wo} \text{ x } 100\ \% \qquad (1)$$

where
Ws = the weight of swollen hydrogel (g)
Wo = the weight of dry hydrogel (g)

Determination of gel fraction [9]

The dried hydrogels were placed in a tea bag and dried in an oven at temperature of 60 °C until constant weight, then weighed (Wo). In addition, the tea bags were immersed in distilled water and shaked in an shaker incubator at 100 rpm for 24 hours at room temperature to extract unreacted compounds due to radiation treatment. Then, the tea bags were removed from shaker incubator and dried under vacuum at 60 °C, then weighed (W_1). The gel fraction can be calculated by Eq. (2).

$$\text{Gel fraction} = \frac{W1}{W0} \text{x } 100\ \% \qquad (2)$$

where,
W_o = the initial weight of dry hydrogel (g)
W_1 = the weight of dry hydrogel after extraction (g)
Note: All works were carried in triplicate

Extraction of gelatin from fish scales

An approximately 200 g of dried fish scales were washed with tap water to remove impurities from the surface. Then it was soaked in a solution of lime soap to remove the fat from its surface. It was then washed again with running water to clean the remaining soap left. Fish scales that have been cleaned were immersed in ± 300 ml of distilled water, and the bottle was closed and put in an autoclave. Afterward, it was heated at a temperature of 121 °C and pressure of 1 atm for 15 minutes. The extracted solution was poured into a plastic tray with a 0.5 cm thickness, and dried in the air for 2 days. Drying products were in the form of gelatin sheets.

Immobilization of metformin HCl in PVA-gelatin hydrogels

Different amount of gelatin (0.5 g, 1 g, 1.5 g, and 2 g) were dissolved in 100 ml of distilled water. A total of 10 g of PVA was added into 100 ml of distilled water and mixed with the gelatin solutions. Then, the PVA-gelatin solutions were packed in a polypropylene (PP) plastics and heated in an autoclave at 121 °C for 15 minutes. About 5 ml of the PVA-gelatin mixture solution was put into a series of vial containing 10, 20, and 30 mg of metformin, homogenized with a hand shaker. Subsequently the mixture was frezeed-thawed for 3 cycles (4 °C, 16 hours and 35 °C, 8 hours) and finally irradiated with gamma rays at a single dose of 25 kGy [26,27]. After irradiation, the vials were broken and the hydrogel were removed from within. Subsequently, the hydrogels were immersed in 100 ml of distilled water, shaked at 100 rpm using an incubator shaker at 37 °C. Every 1 hour interval, 5 ml of the metformin solution released from the hydrogels were measured using a UV-Vis spectrophotometer at a maximum wavelength λ = 232 nm. A total of 5 ml of new solvent was added to the measuring vessel. The amount of drug released was calculated as a cumulative percent. All experiments were carried out in triplicate.

Scanning electron microscopy (SEM)

The surface characteristics of the PVA-gelatin hydrogel were investigated using Zeiss Scanning

Electron Microscope (SEM), made in Germany. The dried samples were soaked in distilled water up to maximum swelling. Then, the hydrogels were frozen in the freezer at -25 °C for 48 hours. The hydrogels were then lyophilized using freeze drying at -40 °C for 24 hours. Dry hydrogels were then observed for their surface properties using SEM.

UV-Vis spectrophotometer

UV-Vis mini 1240 Shimadzu, made in Japan, was used to measure the maximum wavelength of the drug as well as measuring the concentration of the drug that were released from the hydrogel.

RESULTS AND DISCUSSION

Water absorption

The ability of hydrogels to absorb water is one of the important parameters to predict the capacity of hydrogel in releasing drug. Effect of gelatin concentration on water absorption of PVA-gelatin hydrogels produced from gamma irradiation at 25 kGy is presented in Fig. 1. It can be seen that the irradiated PVA-gelatin hydrogel immersed in water during in the first hour, they absorb water from 100 % to 240 %. By increasing the immersing time up to 12 hours of measurement, the ability of the hydrogel to absorb water was gradually increased to 420 % - 500 % along with decreasing gelatin concentration. In addition, with increasing gelatin concentration up to 2 %, water absorption of the PVA-gelatin hydrogel decreased from 500 % to 420 %. Chemically, the reaction that occurs between PVA and gelatin is the esterification reaction of the OH group from PVA with the COOH group aspartate group and glucose amino acid gelatin to form hydrogel through the crosslinking process [28]. Hence, by increasing gelatin concentration up to 2 % in a mixtures of PVA-gelatin (10:2,wt%) with a relatively large concentrations of PVA, more gelatin will react with PVA. As a result, hydrophilicity of PVA-gelatin hydrogel decreases following with decreasing ability of the hydrogel to absorb water. This might result that, with increasing gelatin concentration, water absorption capacity of the PVA-gelatin hydrogel decreases.

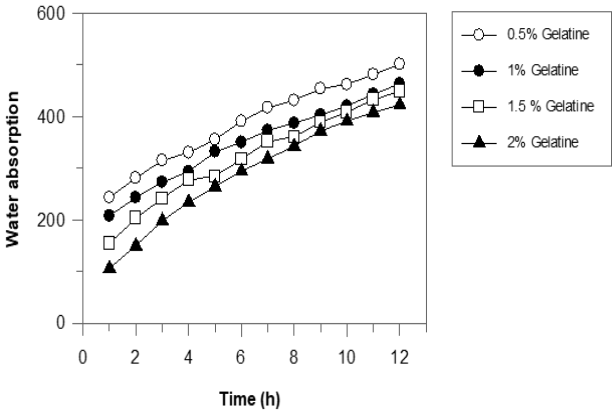

Fig. 1. Effect of immersion time on water absorption of PVA-gelatin hydrogel a result of irradiation at 25 kGy with different gelatin concentrations.

Gel fraction of hydrogel

Gel fraction is one of the important parameters generally used to determine physical properties of hydrogel. This parameter can also be used to determine crosslinking density of the hydrogels [29]. The results of the gel fraction determination of the PVA-gelatin hydrogel from gamma irradiation for various gelatin concentrations are presented in Fig. 2. It was observed that with increasing gelatin concentration from 0.5 % up to 2 %, gel fraction of the hydrogel increased from 83 % to 94 %. The gel fraction was increased approximately 10 % with the addition of 2 % gelatin at a concentration of 10 % PVA, and raw material wasted due to being dissolved in the water was about 6 %. The wasted material can be either degraded or unreacted PVA or gelatin in the synthesis process. This indicates that the synthesis reaction between PVA with gelatin through the freezing-thawing process combined with gamma irradiation is relatively efficient.

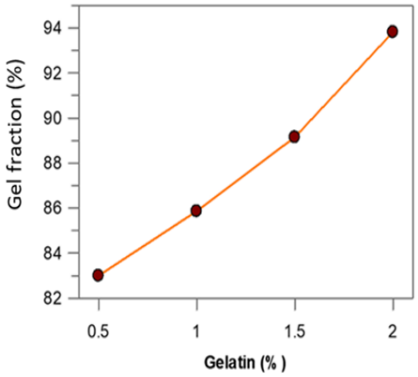

Fig. 2. Effect of gelatin concentration on gel fraction of PVA-gelatin hydrogel prepared using gamma irradiation at 25 kGy.

The mechanism of immobilization of metformin in the PVA-gelatin hydrogel through a combination freezing-thawing and irradiation process is illustrated in Fig. 3. In the freezing-thawing process, the metformin was randomly dispersed in the PVA-gelatin mixture, frozen on the surface and entrapped inside hydrogel, and reacted physically. If the metformin in the frozen form is irradiated, then the relatively small frozen metformin experienced a degradation reaction. This is one of the methods of choice for drug immobilization using irradiation techniques that can simultaneously strengthen the hydrogel matrix from being soluble in water through a radical crosslinking polymerization reaction.

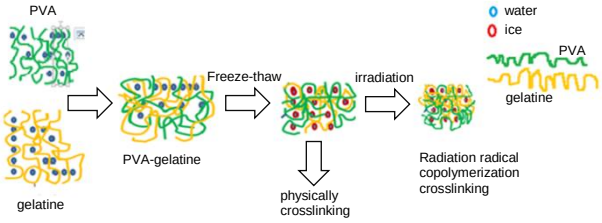

Fig. 3. Mechanism of freezing-thawing and irradiation of PVA-gelatin blended hydrogel preparation.

Effect of gelatin concentrations on in vitro release of metformin HCl (MH)

The results of the effect of immersion time on the cumulative in vitro release of MH from hydrogel matrix of PVA-gelatin as a function of gelatin concentrations of 1 %, 1.5 % ,and 2 % are presented in Fig. 4.

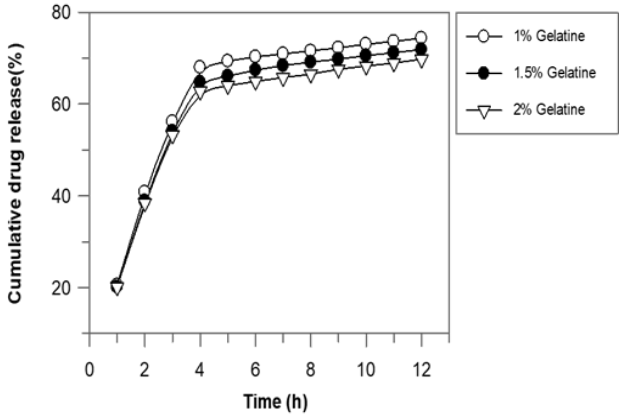

Fig. 4. Effect of immersion time vs cumulative in vitro release of MH from PVA-gelatin hydrogel measured at various gelatin concentrations.

During the first hour of the test, there was a higher cumulative percentage of MH release from hydrogels in the range of 20 - 21 %, known as the burst release. This is due to the release of MH on the surface of the hydrogel as a result of swelling [30]. Furthermore, with increasing immersion time from 1 hour to 4 hours, cumulative percentage of MH released from hydrogel increased rapidly to a maximum of 65 to 70 % with release rate of 10 - 20 % per hour. As for in vitro release of MH from the 4th to the 12th hours, the release from each hydrogel was slowly increased with a relatively small range of 0.4 - 1 % and tends to form a slope pattern with increasing immersion time. This release pattern of drug profile follows first-order release kinetics [30]. Hydrogels that are easily degraded (biodegradable) or nano hydrogel particles are generally profiled as an in vitro release kinetics. Drug release was caused by swelling and erosion [30]. This might occur in PVA-gelatin hydrogels. It can also be seen in Fig. 3 that, with an increase in gelatin concentration up to 2 %, in vitro release of MH decreased. This is due to an increase in the concentration of gelatin, so that swelling hydrogel decreased and thereby in vitro release was also decreased.

Effect of drug dosage on MH in vitro release

The dose of drug-loaded into the hydrogel and released from it is closely related to the capacity of the matrix. The effect of different MH doses from 10 mg to 30 mg immobilized in the PVA-gelatin hydrogel matrix on cumulative MH release is presented in Fig. 5. It appears that at the first hour test of the test, MH was released from the hydrogels as a burst drug release in a range of 9 - 20 %.

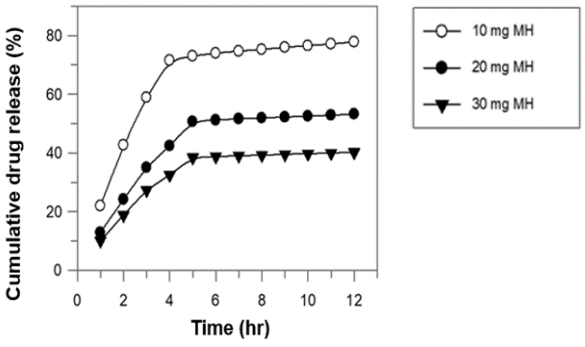

Fig. 5. Effect of immersion time vs cumulative MH release from PVA-gelatin as a function of different doses of MH.

Drug release from the 1st hour to the 5th hour was relatively rapid, reaching an optimum condition ranging from 33 % to 70 % with a release rate of 3 - 20 % per hour. Then, during measurement from the 5th to 12th hour, drug release gradually increased with the rate of 0.3 % - 0.6 % per hour, which is

relatively constant. In general, the profile of controlled release of MH drug is that the drug was released faster on the start, and then sloping slowly with smaller drug release rate. The pattern of drug release profile is known as release with first order kinetics [31]. In addition, in Fig. 4, it is clearly seen that as the increase in MH drug dosages to 30 mg, the percentage of drugs released from hydrogel decreased from 75 % to 36 %. This might be due to the increasingly dense hydrogel matrix with increasing MH dose, causing strong interactions between the drug and the hydrogel matrix both physically and chemically. Therefore, the diffusion of the drug within the hydrogel was reduced and its release decreased. It may also be caused by other causes that need further investigation.

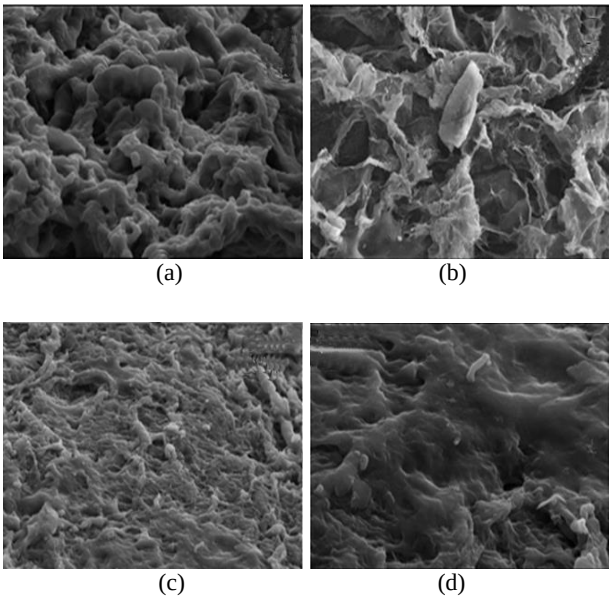

Fig. 6. SEM micrographs of PVA-g-gelatin hydrogels irradiated at 25 kGy with varying concentrations of gelatin; (a). 0.5 %; (b). 1 %; (c) 1.5 %; (d). 2 %.

SEM hydrogel

The Scanning Electron Microscopy (SEM) test was used to observe porosity or microscopic structures developed in irradiated PVA-gelatin hydrogels. By using SEM analysis, the microstructure of the hydrogel surface and the pores can be observed. The results of SEM observations on the PVA-gelatin hydrogel with magnification 1000 times are presented in Figs. 6a-6d. It can be seen that the mixture of PVA and gelatin resulted in a formation of hydrogel with irregular and porous structure. Increasing amount of gelatin produced a hydrogel with irregular structure as expressed in Fig. 6d.

The pores morphology of hydrogel can be related to their water absorption capacity. As shown in Fig. 3, the increase in gelatin concentration led to decreased in water absorption of PVA-gelatin hydrogels. The hydrogels with denser and tighter structures will have a smaller pore size and hinder the polymer chains, minimizing their water absorption capacity.

CONCLUSION

It can be concluded that gel fraction of the PVA-gelatin hydrogels increased with increasing gelatin concentration while water absorption decreased. Cumulative metformin releases decreased with inceasing gelatin concentrations and doses of metformin. PVA-gelatin hydrogels prepared by combining freeze-thaw and irradiation can be considered as a matrix for drug immobilization.

ACKNOWLEDGMENT

Thank you to Mr. Bonang and M. Yassin S.Si. at the IRPASENA irradiator, BATAN for helping us to irradiate the sample until the work was completed.

AUTHOR CONTRIBUTION

We declare that all contributors of this paper are equally contributed as main contributors. All authors read and approved the final version of the paper.

REFERENCES

1. K. J. Wadher, R. B. Kakde and M. J. Umekar, Int. J. Pharm. Investig. **1** (2011) 157.
2. J. Sauri, M Zachariah, R. Macovez *et al.*, J. Drug Delivery Sci. Technol. **42** (2017) 215.
3. J. L. J. Blanco, J. M. Benito, C. O. Mellet *et al.*, J. Drug Delivery Sci. Technol. **42** (2017) 18.
4. D. W. Kurniawan, D. A. Triyanto and V. V. F. R. Utami, Kartika: Jurnal Ilmiah Farmasi **6** (2018) 11. (in Indonesian)
5. K. V. R. N. S. Ramesh, S. Mohanalayam, O. Sarheed *et al.,* Asian J. Pharm. **11** (2017) 118.
6. M. T. R. Chikukwa, M. Wesoly, A. B. Korzeniowska *et al.,* Pharm. Dev. Technol. **25** (2020) 281.
7. X. Bai, M. Gao, S. Syed *et al.,* Bioact. Mater. **3** (2018) 401.

8. Y. C. Qian, P. C. Chen, G. J. He *et al.*, Molecules **19** (2014) 9850.
9. Erizal, E. W. Pratiwi, D. P. Perkasa *et al.*, Jurnal Kimia Kemasan **40** (2018) 47. (in Indonesian)
10. Z. Velkova, G. Kirova, M. Stoytcheva *et al.*, Eng. Life Sci. **18** (2018) 871.
11. D. Singh, A. Singh and R. Singh, J. Biomater. Sci., Polym. Ed. **26** (2015) 1269.
12. C. Vasile, D. Pamfil, E. Stoleru *et al.*, Molecules **25** (2020) 1539.
13. A. Chyzy, M. Tomczykowa and M. E. Plonska-Brzezinska, Materials **13** (2020) 188.
14. S. Amin, S. Rajabnezhad and K. Kohli, Sci. Res. Essay **3** (2009) 1175.
15. H. Hariyanti, Erizal, M. Y. Yunus *et al.*, Jurnal Sains Materi Indonesia **21** (2020) 143. (in Indonesian)
16. S. Mitura, A. Sionkowska and A. Jaiswal, J. Mater. Sci. - Mater. Med. **31** (2020) 50.
17. R. Song, M. W. Murphy, C. Li et al., Drug Des. Dev. Ther. **12** (2018) 3117.
18. Q. Xing, K. Yates, C. Vogt *et al.*, Sci. Rep. **4** (2014) 4706.
19. G. Thakur, F. C. Rodrigues and K. Singh, *Crosslinking Biopolymers for Advanced Drug Delivery and Tissue Engineering Applications,* in: Cutting-Edge Enabling Technologies for Regenerative Medicine, Advances in Experimental Medicine and Biology 1078, Springer, Singapore (2018) 213.
20. P. N. Charron, T. A. Braddish and R. A. Oldinski, J. Mech. Behav. Biomed. Mater. **92** (2019) 90.
21. K. R. Park and Y. C. Nho, J. Appl. Polym. Sci. **91** (2004) 1612.
22. Erizal, D. Pribadi, E. Yulianti *et al.*, Jurnal Sains Materi Indonesia **19** (2018) 139. (in Indonesian)
23. M. Kobayashi and H. S. Hyu, Materials. **3** (2010) 2753.
24. J. Tavakoli, A. J. Gascooke and Y. Tang, Top. Curr. Chem. **379** (2021) 1390.
25. Erizal and Z. Abidin, Jurnal Ilmiah Aplikasi Isotop dan Radiasi **7** (2011) 21. (in Indonesian)
26. K. Swaroop, M. J. Gaana, S. S. Shruthi *et al.*, *Studies on Swelling Behaviour of Radiolytically Synthesised PVA/Gelatin Hydrogels*, AIP Conference Proceedings 2115, 030050 (2019).
27. K. Swaroop, L. P. Shrikant and H. M. Somashekarappa, Curr. Perspect. Chem. Sci. **9** (2021) 125.
28. K. Pal, A. K. Banthia and D. K. Majumdar, AAPS PharmSciTech **8** (2007) E1.
29. L. Arens, D. Barther, J. Landsgesell *et al.*, Soft Matter **15** (2019) 9949.
30. Z. Xiang, P. Sarazin and B. D. Favis, Biomacromolecules **10** (2009) 2053.
31. M. Miotke, J. Strankowska, J. Kwela *et al.*, Polym. Bull. **77** (2019) 483.

UNIVERSITAS MUHAMMADIYAH PROF. DR. HAMKA
FAKULTAS FARMASI DAN SAINS
Jl. Limau II, Kebayoran Baru, Jakarta 12130 Tel. (021) 7208177, 722886, Fax. (021) 7261226, 7256620
Islamic Centre, Jl. Delima II/IV, Klender, Jakarta Timur Tlp.: (021) 8611070, Fax. (021) 86603233
Website: www.ffs-uhamka.ac.id; E-mail: ffs@uhamka.ac.id

SURAT TUGAS
MELAKUKAN KEGIATAN PENELITIAN DAN PUBLIKASI
NO. 221/F.03.08/2022

Bismillahirrohmanirrohiim,
Yang bertanda tangan di bawah ini

N a m a	**Dr. apt. Hadi Sunaryo, M.Si.**
NIDN	0325067201
Pangkat /Jabatan Akademik	Penata Tk. I, III/d / Lektor Kepala
Jabatan	Dekan
Unit Kerja	Fakultas Farmasi dan Sains UHAMKA Jakarta

Memberikan tugas Penelitian dan Publikasi pada **tahun akademik 2021/2022** kepada:

N a m a	**Dr. apt. Hariyanti, M.Si.**
NID/NIDN	D.03.0606/ 0311097705
Pangkat /Jabatan Akademik	Penata/ III-C
Jabatan Fungsional	LEKTOR
Unit Kerja	Fakultas Farmasi dan Sains UHAMKA Jakarta

Untuk Melaksanakan Penelitian dan Publikasi sebagai berikut:

NO	JUDUL PENELITIAN DAN PUBLIKASI
1.	**"Synthesis and in vitro cytotoxic activity of novel indazole analogues of curcumin against MCF-7, HeLa, WiDr, and vero cell lines"**

Demikian surat tugas ini diberikan kepada yang bersangkutan untuk dilaksanakan dengan penuh amanah dan tanggung jawab

Jakarta, 09 Maret 2022
Dekan,

Dr. apt. Hadi Sunaryo, M.Si., Apt.

Tembusan Yth:
1. Rektor UHAMKA Jakarta
2. Wakil Rektor I dan II UHAMKA Jakarta
3. Arsip

Journal of Applied Pharmaceutical Science Vol. 12(04), pp 179-184, April, 2022
Available online at http://www.japsonline.com
DOI: 10.7324/JAPS.2022.120420
ISSN 2231-3354

Synthesis and *in vitro* cytotoxic activity of novel indazole analogues of curcumin against MCF-7, HeLa, WiDr, and vero cell lines

Hariyanti Hariyanti[1], Arry Yanuar[2], Kusmardi Kusmardi[3], Hayun Hayun[2]*

[1]Department of Pharmacy, Faculty of Pharmacy and Science, Universitas Muhammadiyah Prof. DR. HAMKA, Jakarta, Indonesia.
[2]Laboratory of Pharmaceutical and Medicinal Chemistry, Faculty of Pharmacy, Universitas Indonesia, Depok, Indonesia.
[3]Department of Anatomic Pathology, Faculty of Medicine, Universitas Indonesia, Jakarta, Indonesia.

ARTICLE INFO

Received on: 01/08/2021
Accepted on: 01/12/2021
Available Online: 05/04/2022

Key words:
Curcumin indazole analogs, cytotoxicity, selectivity, MCF-7, HeLa, WiDr, vero.

ABSTRACT

We prepared six novel curcumin indazole analogs and confirmed their structures by Fourier transform infrared, nuclear magnetic resonance, and mass spectra. Subsequently, their cytotoxicity was tested using the Michigan Cancer Foundation (MCF-7) proliferation assay against the Michigan Cancer Foundation (MCF-7), HeLa, WiDr, and vero cell lines. This study found that the compounds we prepared were more active against WiDr than HeLa and MCF-7. The activity of 3b, 3c, 3d, and 5a against WiDr (colorectal carcinoma) cells was higher than curcumin and tamoxifen. Their selectivity index (SI) indicated that several synthesized compounds showed more selectivity (SI value > 2) than positive controls tamoxifen and doxorubicin (SI value < 2.00). Three compounds (3a, 3b, and 3c) showed high SI against WiDr cells (3.74, 5.27, and 4.39, respectively). Compound 3b produced the highest cytotoxic activity, especially against WiDr cells (IC_{50} = 27.20 µM) with excellent selectivity (SI = 5.27). Therefore, the compound should be further developed as an anticancer agent for colorectal carcinoma.

INTRODUCTION

The annual report in 2020 indicated a high prevalence of breast cancer, cervical cancer, and colorectal cancer worldwide (American Cancer Society, 2020). The development of monocarbonyl analogs of curcumin to be tetrahydro-indazole structures showed good antioxidant and antitumor against Michigan Cancer Foundation (MCF-7), WI38, Hep G2, and vero cells (Bayomi *et al*., 2015; Bayomi *et al*., 2013). Indazole compounds are scarcely found in nature, generally prepared by organic synthesis. The formation of the indazole ring significantly improved the biological activity of the molecules (Gaikwad *et al*., 2015; Plescia *et al*., 2010; Shrivastava *et al*., 2016; Thangadurai *et al*., 2012; Thirupalu *et al*., 2014; Zhang *et al*., 2018). Recently, *in silico* studies using pharmacophore modeling and docking methods indicated that several asymmetric hexahydro-2H-indazoles were potentially active as ERα inhibitors (Hariyanti *et al*., 2021). Therefore, we prepared six novel curcumin indazole analogs and evaluated them for their cytotoxicity against breast (MCF-7), cervical (HeLa), and colorectal (WiDr) cancer cells. To evaluate their selectivity, the compounds' cytotoxicity was also tested against normal vero cells.

*Corresponding Author
Hayun Hayun, Laboratory of Pharmaceutical and Medicinal Chemistry, Faculty of Pharmacy, Universitas Indonesia, Depok, Indonesia. E-mail: hayun @farmasi.ui.ac.id

MATERIALS AND METHODS

General procedures

All chemicals (E. Merck, Germany, or Sigma-Aldrich, USA) were obtained commercially. Purity tests and reactions monitoring were carried out using the thin layer chromatography procedure. Melting points (m.p.) were assessed by the melting point instrument (Bibby Sterilin, UK) and were not corrected. Infrared (IR) spectra were scanned in a Kalium Bromide mixture on the Shimadzu FTIR-8400S Spectrometer (Japan). Nuclear magnetic resonance (NMR) spectra were run in a $CDCl_3$ solution on a JEOL JNM 500 Spectrometer (Peabody, USA). Mass spectra were found using electrospray ionization (+) mode UNIFI-Waters Liquid Chromatography-Mass Spectrometry (MS)/MS (USA). 3–(4–Methoxyphenyl/3,4-dimethoxyphenyl)–3,3a,4,5,6,7–

hexahydro–2H–indazole (**1a-b**), cyclovalone (**4a**), and 2,6-bis-[(E)-4-hydroxybenzylidene]cyclohexanone (**4b**) used as starting materials were prepared according to the reported method (Hayun *et al*., 2017; Minu *et al*., 2009; Rahmawati *et al*., 2020).

Preparation of curcumin tetrahydro-indazole analogs (3a-d)

The preparation of **3a** with a yield of 61.0% has been reported previously (Hariyanti *et al*., 2020). Preparation of compounds **3b-d** was carried out according to the procedures of compound **3a** by reacting **1b** that replaced **1a** with *p*-methoxy-benzaldehyde, vanillin, or 3,4-dimethoxy-benzaldehyde (**2a-c**).

4-([(7E)-3–(3,4–dimethoxyphenyl)–4,5,6,7–tetrahydro–3aH–indazol-7-ylidene]methyl)-2-methoxyphenol (3b)

Pale yellow powder, yield 35.2%, and m.p. 240°C–242°C. Fourier Transform Infrared (FT-IR), υ/cm^{-1}: 3,217 (OH), 3,059 (C-H Ar stretch), 2,956 (C-H Al stretch), 1,582 (C=N), 1,519 (C=C ring Ar stretch), 1,460 C-H Al bend), 1,253 (C-O-Ar asymmetrical stretch), and 1,162 (C-O-Ar symmetrical stretch). ^{1}H-NMR, δ/ppm: 7.24 (d, 1H, *J* 3 Hz), 6.94 (d,02H, *J* 8 Hz), 7.17 (dd,01H, *J* 8 Hz), 6.89 (dd,02H, *J* 8 Hz), 3.85 (t,01H), 3.91 (d, 6H), 3.92 (s, 3H), 2.81 (m,04H), 1.97 (m,02H). ^{13}C-NMR, δ/ppm: 149.35 (1C), 149.21 (1C), 148.64 (1C), 148.36 (1C), 145.53 (1C), 144.13 (1C); 129.9 and 114.8 (C=$C_{ethylenic}$), 1,122.4 (2C_{Ar}); 123.9, 119.9, 112.8,0,111.1,0110.9, and 110.2 (1C_{Ar}, respectively); 56.0, 55.1, and 55.06 (1C_{O-Me}, respectively);227.2, 31.2, 24.2, and 22.2 (1C_{Al}, respectively). HR-MS:-m/z 393.18003 $[M+H]^+$; calculated for $C_{23}H_{24}N_2O_4$ = 392.17361 [M]; Error = - 2.3 ppm.

(7E)–3–(3,4–dimethoxyphenyl)–7–(4–methoxybenzylidene)–4,5,6,7–tetrahydro–3aH–indazole (3c)

Pale yellow powder, yield 74.3%, and m.p. 244°C–246°C. FT-IR, υ/cm^{-1}: 3,020 (C-H Ar stretch), 2,920 (C-H Al stretch), 1,561 (C=N), 1,519 (C=C ring Ar stretch), 1,460 (C-H Al bend), 1,261 (C-O-Ar asymmetrical stretch), and 1,136 (C-O-Ar symmetrical stretch). ^{1}H-NMR, δ/ppm: 7.23 (d, 1H, *J* 1.5 Hz), 6.89 (d, 2H, *J* 9 Hz), 7.17 (dd, 1H, *J* 8 Hz), 6.97 (s, 1H), 6.94 (dd, 1H, *J* 8 Hz), 6.87 (d, 1H, *J* 8.5 Hz),03.92 (s, 3H),03.91 (d,06H),02.81 (m, 4H), 1.88 (m,02H). ^{13}C-NMR, δ/ppm: 149.22 (1C), 148.65 (1C), 148.29 (1C), 145.73 (1C), 144.02 (1C); 129.6 and 122.4 (C=$C_{ethylenic}$); 126.2, 123.9, 119.9, 114.8, 112.8,0111.2,0111.1, 110.95, and 110.92 (1C_{Ar}, respectively); 56.1, 56.05, and 55.0 (1C_{O-Me}, respectively); 27.2, 31.2,024.7, and 22.3 (1C_{Al}, respectively). HR-MS:-m/z 409.21152 $[M+CH_3OH+H]^+$; calculated for $C_{23}H_{24}N_2O_3$= 376.17896 [M]; Error = 0.3 ppm.

(7E)–3–(3,4–dimethoxyphenyl)–7–(3,4–dimethoxybenzylidene)–4,5,6,7–tetrahydro–3aH–indazole (3d)

Pale yellow powder, yield 56.1%, and m.p. 236°C–238°C. FT-IR, υ/cm^{-1}: 3,020 (C-H Ar stretch), 2,947 (C-H Al stretch), 1,591 (C=N), 1,514 (C=C ring Ar stretch), 1,450 (C-H Al bend), 1,255 (C-O-Ar asymmetrical stretch), and 1,142 (C-O-Ar symmetrical stretch). ^{1}H-NMR, δ/ppm: 6.88-(s, 2H), 7.19 (dd,01H, *J* 8 Hz), 6.91 (s, 2H), 6.87 (s,01H), 6.94 (dd, 2H, *J* 8 Hz), 3.93 (s, 3H),03.92 (s, 3H), 3.91 (s, 3H), 3.89 (s, 3H), 2.81 (m, 4H), 1.88 (m, 2H). ^{13}C-NMR, δ/ppm: 149.27 (1C), 148.94 (1C), 148.71 (1C), 148.16 (1C),0129.85 (1C),0128.0 (1C); 122.12 and 121.3 (C=$C_{ethylenic}$); 119.42, 109.92, and 111.04 (2C_{Ar}, respectively); 112.66 and 111.28 (1C_{Ar}, respectively); 56.08 and 56.04 (2C_{O-Me}, respectively); 31.15, 27.24,024.81, and 22.38 (1C_{Al}, respectively). HR-MS :-m/z 407.19619 $[M+H]^+$; calculated for $C_{24}H_{26}N_2O_3$ = 406.18926 [M]; Error = - 0.7 ppm.

Preparation of curcumin hexahydro-indazole analogs (5a–b)

Preparation of **5a-b** was carried out by mixing 10 mmol of the synthesized cyclovalone (**4a**) for **5a** and its *p*-hydroxy analog (**4b**) for **5b**, with 100 mmol hydrazine monohydrate in 10 ml of glacial acetic acid, refluxed at 120°C for 3 hours until completed reaction, added on to crushed ice, filtered off till the suspension was obtained, and washed using cold water to afford the solid product. Recrystallization was done from a suitable solvent to provide the pure compound **5a–b**.

1-[(7E)-3-–(4-hydroxy,3–methoxyphenyl)–7–(4-hydroxy,3–methoxybenzylidene)-3,3a,4,5,6,7-hexahydro–2H–indazol-2-yl]-ethan-1-one (5a)

Pale yellow powder, yield 23.7%, and m.p. 105°C–107°C. FT-IR, υ/cm^{-1}: 3,200–3,525 (OH), 3,059 (C-H Ar stretch), 2,956 (C-H Al stretch), 1,635 (C=O), 1,599 (C=N), 1,518 (C=C ring Ar stretch), 1,450 (C-H Al bend), 1,273 (C-O-Ar asymmetrical stretch), and 1,150 (C-O-Ar symmetrical stretch). ^{1}H-NMR, δ/ppm: 7.14 (s, 1H), 6.92 (d, 2H, *J* 2-Hz), 6.75 (d,01H, *J* 2 Hz), 6.86 (s,01H), 6.78 (dd,01H, *J* 8Hz), 6.88 (d, 1H, *J* 8Hz), 3.90 (d, 6H), 2.19 (s, 3H), 4.83 (d, 1H), 3.06 (d, 1H), 2.39 (s, 2H), 2.32 (m, 1H), 2.43 (m, 1H), 2.96 (m, 1H), 1.94 (m, 2H). ^{13}C-NMR, δ/ppm: 170.64 (1$C_{C=O}$), 159.08 (1$C_{C=N}$);0146.82,0146.38, 145.61, 145.06 (1C_{Ar-O}, respectively); 0128.98 and 128.19 (C=$C_{ethylenic}$); 134.11, 128.64, 123.47, 118.63, 114.86, 114.46, 112.38, and 108.48 (1C_{Ar}, respectively); 67.99 (1C_{C-N}); 57.43 and 56.08 (1C_{O-Me}, respectively); 38.96, 30.15, 29.06,024.49, and 22,49 (1C_{Al}, respectively). HR-MS:-m/z 423.19132 $[M+H]^+$; calculated for $C_{24}H_{26}N_2O_5$ = 422.18417 [M]; Error = - 0.2 ppm.

1-[(7E)-3-(4-hydroxyphenyl)–7–(4-hydroxybenzylidene)-3,3a,4,5,6,7–hexahydro–2H–indazol-2-yl]-ethan-1-one (5b)

Pale yellow powder, yield 42.2%, and m.p. 146°C–148°C. FT-IR, υ/cm^{-1}: 3,200–3,500 (OH), 3,012 (C-H Ar stretch), 2,943 (C-H Al stretch), 1,647 (C=O), 1,579 (C=N), 1,512 (C=C ring Ar stretch), 1,450 (C-H Al bend), and 1,263 (C_{Ar}-O stretch). ^{1}H-NMR, δ/ppm: 6.74 (m,01H, *J* 2 Hz), 7.19 (dd, 2H, *J* 8 Hz), 6.91 (s,01H), 6.84 (dd,01H, *J* 6 Hz), 7.05 (m,01H, *J* 8 Hz), 6.78 (dd, 2H, *J* 8 Hz), 2.13 (s, 3H), 4.07 (m,01H), 3.06 (d,01H), 2.72 (m,02H), 2.0 (s,01H), 1.8 (m,01H), 1.21 (m, 2H). ^{13}C-NMR, δ/ppm: 170.6 (1$C_{C=O}$), 159.97 (1$C_{C=N}$); 156.63 and 155.55 (1C_{Ar-O}, respectively); 0114.16 and0115.20 (C=$C_{ethylenic}$); 131.36, 130.71, 128.88, 128.12, 126.99, 121.35, 115.70, 115. 63, 115. 28 and 115.20 (1C_{Ar}, respectively); 67.43 (1C_{C-N}); 30.05, 29.76, 29.13, 27.20 and 24.67 (1C_{Al}, respectively). HR-MS:-m/z 363.17051 $[M+H]^+$; calculated for $C_{23}H_{22}N_2O_3$ = 362.16304 [M]; Error = +0.8 ppm.

***In vitro* cytotoxicity**

The prepared compounds were tested for cytotoxicity against MCF-7, HeLa, WiDr, and vero cell lines (American Type

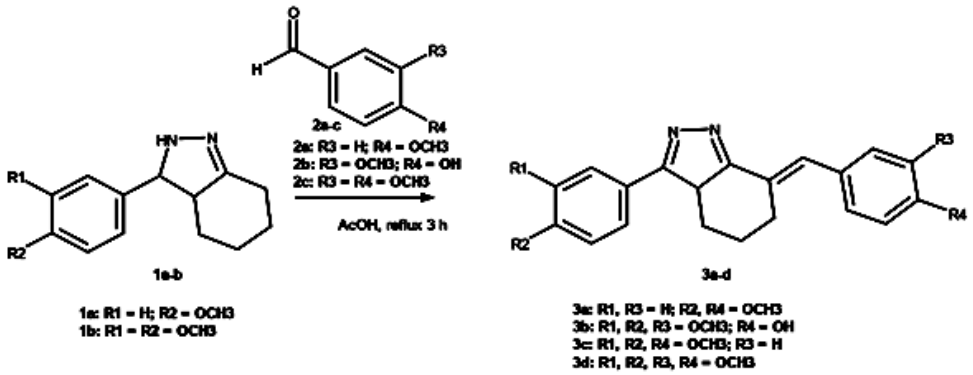

Figure 1. Preparation reaction of compounds **3a-d**.

Culture Collection ([ATCC) HTB-22, ATCC CCL-2, ATCC CCL-218, and ATCC CCL-81] using the 3-(4,5-dimethylthiazol-2-yl)-2,5-diphenyl-2H-tetrazolium bromide (MTT) assay procedure (ATCC, 2020). Fetal bovine serum (5%), penicillin (100 U/ml), and streptomycin (100 µg/ml) were added to the 96-well plates containing cultivated cells in suitable growth media (Dulbecco's Modified Eagle's medium for WiDr and vero and Roswell Park Memorial Institute 1640 medium for MCF-7 and HeLa) and incubated for 24 hours until the culture reached 60% confluence. After replacing the growth media with new media, a series of concentrations (3.125–200 µg/ml) of test compounds were added. The cells were reincubated for 48 hours (the growth media were replaced every day with new media). After that, a 10 µl MTT solution was added and incubated for 4 hours; the media were discarded and the formazan formed in 100 µl ethanol was dissolved. Finally, the dissolved formazan was measured using an Enzyme-Linked Immunosorbent Assay reader at λ 595 nm (Bahuguna *et al*., 2017). The IC_{50} values were determined from the curve of concentrations versus inhibitions (%). GraphPad Prism 8 v. 8.02 (www.graphpad.com) was used for analysis.

RESULTS AND DISCUSSION

Chemistry

Compounds **3b-d** were prepared by condensation **1b**-and-benzaldehyde derivatives-**2a-c** in a yield of 35.2%, 56.1%, and 74.3% (Fig 1), while compounds **5a-b** were prepared by condensation symmetrical bis-benzylidene-cyclohexanone **4a-b** and hydrazine monohydrate in a yield of 23.7% and 42.2% (Fig 2). The reactions were carried out in glacial acetic acid and reflux temperature to afford novel products 4,5,6,7-tetrahydro-3aH-indazole (**3b-d**) and 2-acetylated-3,3a,4,5,6,7-hexahydro-2H-indazole (**5a-b**). The high temperature applied in the reaction most likely lowered the stability of the starting materials (Weerawatanakorn *et al.,* 2015), causing low yields. The application of mild conditions resulted in a higher yield; however, the products were different from those above (Bayomi *et al*., 2015; Nuriev *et al*., 2016; Raut *et al*., 2020).

The prepared compound structures were elucidated based on spectral analysis. No sharp peak at 3,290–3,300 cm^{-1} appeared in the FT-IR spectra, indicating the disappearance of the amine group. The bands at 3,012–3,059 and 2,920–2,956 cm^{-1} confirmed the presence of C-H aromatic and aliphatic bonds. The C=N azole, C=C aromatic ring, and C-O-C ether bonds were observed at 1,732–1,734, 1,447–1,665, and 1,140–1,265 cm^{-1}, respectively. Broad peaks at 3,217 and 3,200–3,500 cm^{-1} indicated a hydroxyl group's presence in the **3b** and **5a-b** compounds, while a strong peak at 1,635–1,647 cm^{-1} confirmed the C=O of acetamide in the **5a** and **5b** compounds. In the ^{1}H-NMR spectra, 7–9 protons for the two aromatic rings and one ethenyl chain appeared at 6–7 ppm, and a typical proton OCH_3 group appeared at around 3.8 ppm. Structural analysis was also supported by ^{13}C-NMR and the mass spectral data, which confirmed the suitability to the targeted compounds (MarvinSketch 20.8.0, 2020; Silverstein *et al*., 2005).

In vitro cytotoxicity

The prepared compounds (**3a-d** and **5a-b**) were evaluated for their cytotoxicity against four cell lines (MCF-7, HeLa, WiDr, and vero) using an MTT assay procedure. Curcumin, tamoxifen, and doxorubicin were used as a comparable compound

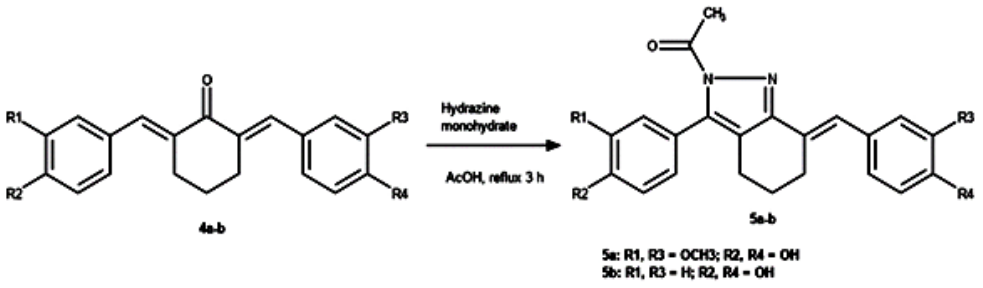

Figure 2. Preparation reaction of compounds **5a-b**.

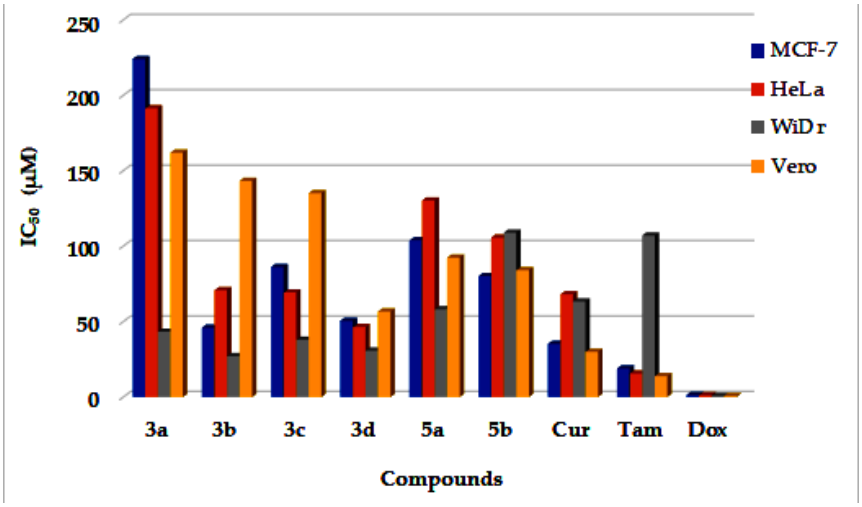

Figure 3. Cytotoxic activity (IC_{50}, µM) values for the prepared compounds, curcumin, tamoxifen, and doxorubicin on MCF-7, HeLa, WiDr, and vero cells, respectively.

Table 1. IC_{50} and SI values of the prepared compounds, curcumin, tamoxifen, and doxorubicin against MCF-7, HeLa, WiDr, and vero cell lines.

Compounds	IC_{500}(µM)[a]				SIb		
	HeLa	MCF-7	WiDr	Vero	HeLa	MCF-7	WiDr
3a	>100	>100	43.28	>100	<2	<2	3.74
3b	70.80	45.97	27.20	>100	2.02	3.12	5.27
3c	69.30	86.24	37.96	>100	<2	<2	4.39
3d	46.36	50.56	30.77	56.68	<2	<2	<2
5a	>100	>100	58.19	92.47	<2	<2	<2
5b	>100	80.26	>100	84.12	<2	<2	<2
Curcumin	68.09	35.30	63.41	30.01	<2	<2	<2
Tamoxifen	15.62	19.01	>100	13.91	<2	<2	<2
Doxorubicin	1.27	1.40	0.66	0.75	<2	<2	<2

[a]: Mean of triplicate experiments; [b] : SI value = ratio between IC_{50} of vero (normal) cell and IC_{50} of cancer cell.

and positive control. Tamoxifen is a drug commonly used in breast cancer treatment, while doxorubicin is most useful for treating broad cancers such as leukemia, neuroblastoma, and ovary, lung, and breast cancer (Thorn *et al*., 2011).

The results indicated that the prepared compounds had low to medium cytotoxic activity (Table 1 and Fig. 3). The IC_{50} values against MCF-7 cells were between 45.97 and 86.24 µM. Compound **3b** had the highest cytotoxicity against MCF-7, but its activity was lower than curcumin. In contrast, tamoxifen and doxorubicin exhibited high cytotoxicity against MCF-7. The IC_{50} values against HeLa cells were between 46.36 and 100 µM. Compound **3d** had the highest cytotoxicity against HeLa cells. The cytotoxicity of **3d** was higher than that of curcumin but lower than tamoxifen and doxorubicin. The IC_{50} values against WiDr cells were between 27.20 and 58.19 µM. These results indicated that the synthesized compounds were more cytotoxic against WiDr than against HeLa and MCF-7 cells. -Compound **3b** had the highest cytotoxicity against WiDr cells. This activity was better than curcumin and tamoxifen but lower than doxorubicin.

The cytotoxicity of compounds **3b**, **3c**, and **3d** containing three and four methoxy groups was higher than compounds **3a**, **5a**, and **5b** containing less than three methoxy groups. The results were in line with the finding previously reported in asymmetrical analogs of curcumin and 4-amino chalcone derivatives that the methoxy group's number and position influence cytotoxic activity (Prasetyaningrum *et al*., 2018; Novilla *et al*., 2019).

The IC_{50} values against vero cells were between 56.68 and >100 µM. These data indicated that most synthesized compounds had low toxicity against normal cells (Burger *et al*., 2004; Schmitz *et al*., 1993). Compound **3b** showed high selectivity against MCF-7, HeLa, and WiDr cells [selectivity index, (SI) = 3.12, 2.02, and 5.27]. In contrast, compounds **3a** and **3c** only showed selectivity against WiDr cells (SI = 3.74 and 4.39). The selectivity of these compounds was higher than curcumin and the positive controls (tamoxifen and doxorubicin). The compound with an SI less than two indicates general toxicity. The higher the SI, the more selective the compound (Burger *et al*., 2004; Badisa *et al*.,

2009; Kurnia *et al*., 2019). The IC_{50} value of curcumin against MCF-7 cells was 35.03 µM, whereas in a previous study it was 8.62 µM (Li *et al*., 2015). This difference may be due to the different methods used for the testing or different laboratory conditions. The resistance factor also affects the sensitivity of the drug to cells.

CONCLUSION

A series of six curcumin indazole analogs have been prepared. All the compounds showed low to moderate cytotoxicity against MCF-7, HeLa, and WiDr cells. Compounds **3b** exhibited the greatest cytotoxicity, especially against WiDr cells with excellent selectivity. The compound should be further developed as a cytotoxic agent for colorectal adenocarcinoma.

ACKNOWLEDGMENTS

The authors are grateful to the Chemical Research Center, LIPI, Tangerang, Indonesia, for NMR and MS measurements.

CONFLICT OF INTEREST

The authors confirm no conflicts of interest between the authors.

FUNDING

This research and APC were supported by the Ministry of Research and Technology/ BRIN, RI, 2020 (Assignment Agreement No. NKB-0373/UN2.RST/HKP.05.00/2020).

ETHICAL APPROVALS

This study does not involve experiments on animals or human subjects.

DATA AVAILABILITY

All data generated and analyzed are included within this research article.

PUBLISHER'S NOTE

This journal remains neutral with regard to jurisdictional claims in published institutional affiliation.

REFERENCES

American Cancer Society. Cancer facts & figures. American Cancer Society, pp 1–44, 2020. Available via https://www.cancer.org/research/cancer-facts-statistics/all-cancer-facts-figures/cancer-facts-figures-2020.html (Accessed 1 December 2020).

Badisa RB, Darling-Reed SF, Joseph P, Cooperwood JS, Latinwo LM, Goodman CB. Selective cytotoxic activities of two novel synthetic drugs on human breast carcinoma MCF-7 cells. Anticancer Res, 2009; 29:2993–6.

Bahuguna A, Khan I, Bajpai VK, Kang SC. MTT assay to evaluate cytotoxic potential of a drug. Bangladesh J Pharmacol, 2017; 12:115–8; doi:10.3329/bjp.v12i2.30892

Bayomi SM, El-kashef HA, El-ashmawy MB, Nasr MNA, El-sherbeny MA, Abdel-aziz NI, El-Sayed MA, Suddek GM, El-Messer SM, Ghaly MA. Synthesis and biological evaluation of new curcumin analogues as antioxidant and antitumor agents: molecular modelling study. Eur J Med Chem, 2015; 101:584–94; doi:10.1016/j.ejmech.2015.07.014

Bayomi SM, El-Kashef HA, El-Ashmawy MB, Nasr NA, El-Sherbeny MA, Badria A. Synthesis and biological evaluation of new curcumin derivatives as antioxidant and antitumor agents. Med Chem Res, 2013; 22:1147–62; doi:10.1007/s00044-012-0116-9

Burger AM, Fiebig HH. Preclinical screening for new anticancer agents. In: Figg WD, McLeod HL (eds.). Handbook of anticancer pharmacokinetics and pharmacodynamics, cancer drug discovery and development, Humana Press Inc, Totowa, NJ, pp 36–7, 2004; doi:10.1007/978-1-59259-734-5_2

Gaikwad DD, Warad KD, Chapolikar AD, Devkate CG, Tayade AP, Pawar RP, Domb AJ. Synthesis of indazole motifs and their medicinal importance: an overview. Eur J Med Chem, 2015; 90:707–31; doi:10.1016/j.ejmech.2014.11.029

GraphPad Software, Inc. Available via www.graphpad.com (Accessed 17 November 2020).

Hariyanti H, Kusmardi K, Yanuar A, Hayun H. Ligand based pharmacophore modeling, virtual screening, and molecular docking studies of asymmetrical hexahydro-2H-indazole analogs of curcumin (AIACs) to discover novel estrogen receptors alpha (ERα) inhibitor. Indones J Chem, 2021; 21(1):137–47; doi:10.22146/ijc.54745

Hariyanti H, Yanuar A, Kusmardi K, Hayun H. (7E)–3–(4–Methoxyphenyl)–7–[(4–methoxyphenyl) methylidene]–4,5,6,7–tetrahydro–3aH–indazole. Molbank, 2020; 2020:M1162; doi:10.3390/M1162

Hayun H, Jatmika C, Purwati EM, Salim S, Kurniawan R, Chandra EG, Fajriawan AA, Nareswara AD. Synthesis and free radical-scavenging activities of di-mannich bases of cyclovalone derivatives. Orient J Chem, 2017; 33(6):2742–57; doi:10.13005/ojc/330607

Kurnia A, Saputri FC, Hayun H. Synthesis and anticancer potential of aminomethyl derivatives of methyl-substituted asymmetrical curcumin mono-carbonyl. J Appl Pharm Sci, 2019; 9(08):018–24; doi.10.7324/JAPS.2019.90803

Li Q, Chen J, Luo S, Xu J, Huang Q, Liu T. Synthesis and assessment of the antioxidant and antitumor properties of asymmetric curcumin analogues. Eur J Med Chem, 2015; 93:461–9; doi:10.1016/j.ejmech.2015.02.005

MarvinSketch 20.8.0. ChemAxon Ltd., 1998–2020. Available via http://www.chemaxon.com

Minu M, Thangadurai A, Wakode SR, Agrawal SS, Narasimhan B. Synthesis, antimicrobial activity and QSAR studies of new 2,3-disubstituted-3,3a,4,5,6,7-hexahydro-2H-indazoles. Bioorg Med Chem Let, 2009; 19(11):2960–4; doi:10.1016/j.bmcl.2009.04.052

MTT cell proliferation assay. Available via https://www.atcc.org/~/media/ DA5285A1F52C414E864C966FD78C9A79.ashx (Accessed 28 November 2020).

Nuriev VN, Vatsadze IA, Sviridenkova NV, Vatsadze SZ. Synthesis of 3,7 disubstituted hexahydro and tetrahydro-2H-indazoles from cross-conjugated dienones. Russ J Org Chem, 2016; 52:389–96; doi:10.1134/S1070428016030167

Novilla A, Mustofa M, Astuti I, Jumina J, Suwito H. Cytotoxic activity of methoxy-4-amino chalcone derivatives against leukemia cell lines. Mol Cell Biomed Sci, 2019; 3(1):34–41; doi:10.21705/mcbs.v3i1.44

Plescia S, Raffa D, Plescia F, Casula G. Synthesis and biological evaluation of new indazole derivatives. ARKIVOC, 2010; (x):163–77; doi:10.3998/ark.5550190.0011.a14

Prasetyaningrum PW, Bahtiar A, Hayun H. Synthesis and cytotoxicity evaluation of novel asymmetrical mono-carbonyl analogs of curcumin. Sci Pharm, 2018; 86(2):25; doi:10.3390/scipharm86020025

Rahmawati N, Hariyanti H, Saputri FC, Hayun H. Synthesis and preliminary in vitro anti-inflammatory evaluation of mannich bases derivatives of 4-methoxy-substituted of asymmetrical cyclovalone analogs. Indones J Pharm, 2020; 31(1):35–41; doi:10.13005/ojc/330607.

Raut S, Dhotre B, Tidke A, Pathan MA. An operationally simple and efficient synthesis of 7-benzylidene-substitutedphenyl- 3,3a,4,5,6,7-hexahydro-2H-indazole by grinding method. Curr Org Syn, 2020; 17(4):313–21; doi: 10.2174/1570179417666200406142118

Schmitz FJ, Bourden BF, Toth SI. Antitumor and cytotoxic compounds from marine organisms. In: Attaway DH, Zaborsky OR (eds.).

Marine biotechnology, pharmaceutical and bioactive natural products, Plenum Press, New York, NY, 198 p, vol. 1, 1993.

Shrivastava A, Chakraborty AK, Upmanyu N, Singh A. Recent progress in chemistry and biology of indazole and its derivatives: a brief review. Austin J Anal Pharm Chem, 2016; 3(4):1076. Available via https://austinpublishinggroup.com/analytical-pharmaceutical-chemistry/fulltext/ajapc-v3-id1076.php

Silverstein RM, Webster FX, Kiemle DJ. 2005. Spectrometric identification of organic compounds. 7th ed, John Wiley & Sons, Inc, New York, NY.

Thangadurai A, Minu M, Wakode S, Agarwal S, Narasimhan B. Indazole: a medicinally important heterocyclic moiety. Med Chem Res, 2012; 21:1509–23; doi:10.1007/s00044-011-9631-3

Thirupalu RM, Hanuman RV, Chenna KRR, Krishna V, Rami RYV. Synthesis and molecular docking studies of new substituted indazole derivatives for anti-breast cancer activity. Der Pharm Chem, 2014; 6(6):411–7; Available via https://1library.net/document/zp033loq-synthesis-molecular-docking-studies-substituted-indazole-derivatives-activity.html

Thorn CF, Oshiro C, Marsh S, Hernandez-Boussard T, McLeod H, Klein TE, Altman RB. Doxorubicin pathways: pharmacodynamics and adverse effects. Pharmacogenet Genom, 2011; 21(7):440–6; doi:10.1097/FPC.0b013e32833ffb56

Weerawatanakorn M, Wu JC, Pan MH, Ho CT. Reactivity and stability of selected flavor compounds. J Food Drug Anal, 2015; 23(2):176–90; doi:10.1016/j.jfda.2015.02.001

Zhang SG, Liang CG, Zhang WH. Recent advances in indazole-containing derivatives: synthesis and biological perspectives. Molecules, 2018; 23:2783; doi:10.3390/molecules23112783

How to cite this article:
Hariyanti H, Yanuar A, Kusmardi K, Hayun H. Synthesis and in vitro cytotoxic activity of novel indazole analogues of curcumin against MCF-7, HeLa, WiDr, and vero cell lines. J Appl Pharm Sci, 2022; 12(04):179–184.

UNIVERSITAS MUHAMMADIYAH PROF. DR. HAMKA
FAKULTAS FARMASI DAN SAINS
Jl. Limau II, Kebayoran Baru, Jakarta 12130 Tel. (021) 7208177, 722886, Fax. (021) 7261226, 7256620
Islamic Centre, Jl. Delima II/IV, Klender, Jakarta Timur Tlp.: (021) 8611070, Fax. (021) 86603233
Website: www.ffs-uhamka.ac.id; E-mail: ffs@uhamka.ac.id

SURAT TUGAS
MELAKUKAN KEGIATAN PENELITIAN DAN PUBLIKASI
NO. 222/F.03.08/2022

Bismillahirrohmanirrohiim,
Yang bertanda tangan di bawah ini

N a m a	**Dr. apt. Hadi Sunaryo, M.Si.**
NIDN	0325067201
Pangkat /Jabatan Akademik	Penata Tk. I, III/d / Lektor Kepala
Jabatan	Dekan
Unit Kerja	Fakultas Farmasi dan Sains UHAMKA Jakarta

Memberikan tugas Penelitian dan Publikasi pada **tahun akademik 2021/2022** kepada:

N a m a	**Dr. apt. Hariyanti, M.Si.**
NID/NIDN	D.03.0606/ 0311097705
Pangkat /Jabatan Akademik	Penata/ III-C
Jabatan Fungsional	LEKTOR
Unit Kerja	Fakultas Farmasi dan Sains UHAMKA Jakarta

Untuk Melaksanakan Penelitian dan Publikasi sebagai berikut:

NO	JUDUL PENELITIAN DAN PUBLIKASI
1.	**"New Decahydroacridine-1,8-diones Derived From 3-Aminocyclohex-2-en-1-one: Synthesis, Characterization, Antioxidant, In Vitro, and In-Silico Anti-Inflammatory Activity"**

Demikian surat tugas ini diberikan kepada yang bersangkutan untuk dilaksanakan dengan penuh amanah dan tanggung jawab

Jakarta, 09 Maret 2022
Dekan,

Dr. apt. Hadi Sunaryo, M.Si., Apt.

Tembusan Yth:
1. Rektor UHAMKA Jakarta
2. Wakil Rektor I dan II UHAMKA Jakarta
3. Arsip

RJC

RASĀYAN *J. Chem.*
Vol. 15 | No. 2 |1241-1248| April - June | 2022
ISSN: 0974-1496 | e-ISSN: 0976-0083 | CODEN: RJCABP
http://www.rasayanjournal.com
http://www.rasayanjournal.co.in

NEW DECAHYDROACRIDINE-1,8-DIONES DERIVED FROM 3-AMINOCYCLOHEX-2-EN-1-ONE: SYNTHESIS, CHARACTERIZATION, ANTIOXIDANT, *In-vitro,* AND *In-silico* ANTI-INFLAMMATORY ACTIVITY

I. P. Sari[1], H. Hariyanti[2], A. Yanuar[1] and H. Hayun[1,✉]

[1]Faculty of Pharmacy, Universitas Indonesia, Depok16424, West Java, Indonesia.
[2]Faculty of Pharmacy and Sciences, Universitas Muhammadiyah Prof. DR. HAMKA, Jakarta, 13460, Indonesia
✉Corresponding Author: hayun@farmasi.ui.ac.id

ABSTRACT

New decahydroacridine-1,8-dione derivatives have been synthesized from 3-aminocyclohex-2-en-1-one. The compounds were characterized based on spectroscopic data and assessed their antioxidant and anti-inflammatory properties both *in-vitro* and *in-silico*. All the compounds exhibited poor *in-vitro* antioxidant activity but high *in-vitro* anti-inflammatory activity. *An in-silico* study using Autodock v 4.2 integrated LigandScout software 4.4.3. against the COX-1 (PBD ID: 1CQE) and COX-2 (PBD ID: 6COX) enzymes indicated that all the compounds could interact with both enzymes. Except for 3c against COX-1, the compounds' interaction with both enzymes exhibited binding energy lower than diclofenac and curcumin. The results confirm that the compounds have a high potential to be anti-inflammatory agents and deserve further development.

Keywords: Synthesis, Decahydroacridine-1,8-diones, Acridine-1,8-dione, Antioxidant, Anti-inflammatory, *In-vitro, In-silico.*

RASĀYAN *J. Chem.*, Vol. 15, No.2, 2022

INTRODUCTION

Nonsteroidal anti-inflammatory drugs (NSAIDs) are pain reliever drugs that are most frequently applied in adults to treat chronic health problems, such as arthritis and lupus. However, these drugs often exhibit adverse side effects, especially gastric irritation.[1-3] The carboxylic functional group in their molecular structures would enable gastric cyclooxygenase-1 (COX-1) inhibition and direct gastric mucosal irritation associated with oral administration of the drugs.[4] So, it is attractive to discover novel NSAIDs compounds that do not have the carboxylic functional group. The acridine-1,8-dione derivatives exhibit various biological activities such as anticancer, antimalarial, antimicrobial, antiglaucoma, carbonic anhydrase inhibitor, antioxidant, and anti-inflammatory.[5-12] The compounds are typically prepared using the Hantzsch procedure by reacting 5,5-dimethyl-1,3-cyclohexanedione, aldehydes, and nitrogen-containing compounds such as ammonium acetate, anilines, alkylamines, or other primary amines.[5-12] Various methods have been applied to synthesize the acridine-1,8-diones, but all the methods utilized 5,5-dimethyl-1,3-cyclohexanedione as starting material and resulted 3,3,6,6-tetramethyl-9-phenyl-3,4,6,7,9,10-hexahydroacridine-1,8-dione. [5-11, 13-14] To further explore the acridine-1-8-diones as an antioxidant and anti-inflammatory, we have synthesized new decahydroacridine-1,8-dione derivatives (without four methyl substitutions at positions 3, 3, 6, and 6) (Fig.-1) using 3-aminocyclohex-2-en-1-one as starting material. In addition, we report the molecular docking study to predict the compounds' binding affinity to cyclooxygenase enzymes.

EXPERIMENTAL

General Procedure

The chemicals we used were bought from Sigma/Merck with no purification further. Melting point measurements were carried out using the melting point device (Bibby Sterilin, UK). The compound's purity and reaction rates were observed by thin-layer chromatography (TLC). Infrared spectra measurements were performed on an FTIR-8400 Spectrometer (Shimadzu, Japan). Agilent Nuclear Magnetic Resonance

http://doi.org/10.31788/RJC.1526775

Spectrometer was utilized to obtain the compound's NMR spectra. LC-MS/MS with electrospray ionization (+) mode (UNIFI-Waters, Milford, MA, USA) was used to analyze the compound's mass spectra (MS).

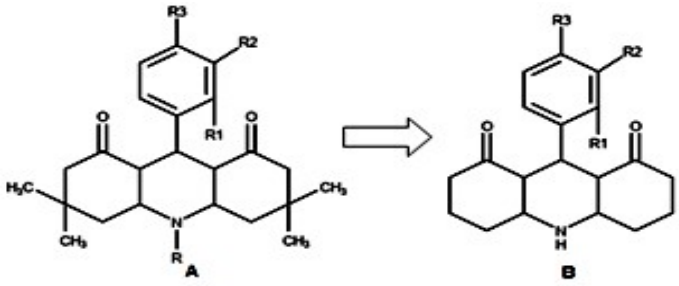

Fig.-1: The Typically Published Decahydroacridine-1,8-diones (A). The Title Compounds (B)

Synthesis of 9-phenyl-decahydroacridine-1,8-diones (3a-f).

A solution of equimolar of 3-aminocyclohex-2-en-1-one (1) and aromatic aldehydes (2a-f) in anhydrous acetic acid was heated under reflux for 2–5 h until completed reaction. Then the solution volume was reduced by evaporation to about one-third, cooled, and the precipitate formed was filtered off, washed up by cold distilled water, and dried. The purification by recrystallization from ethanol or column chromatography afforded pure compounds 3a-f. Replacement of 2a-f with aromatic aldehydes (2g-i) did not produce the target compounds 3g-i. Compound 3a. Yield 70%, m.p. 250-251ºC, FT-IR (υ/cm^{-1}): 3194, 3050, 2980, 1641, 1606, 1498, 1355, 1230, 1180, and 1130. ^{1}H-NMR (δ/ppm, *J*/Hz): 9.44 (s, 1H), 7.03 (m, *J*=3, 1H), 7.13 (t, *J*=3, 2H), 7.15 (d, *J*=3, 2H), 4.90 (s, 1H), 2.50 (m, overlap with DMSO, 4H), 1.91 (m, *J*=6, 2H),12.17 (m, *J*=5, 4H), 1.79 (m, *J*=4, 2H). ^{13}C-NMR (δ/ppm): 194.8 (2C=O), 151.3 (2C=C-N), 147.4 (1C_{Ar-C}), 127.8 (2C_{ArH}), 127.5 (2C_{ArH}), 125.4 (1C_{ArH}), 112.4 (2C=C-C), 36.8 (2C_{Al}), 32.1 (1C_{Al}), 26.3 (2C_{Al}), 20,8 (2C_{Al}). MS: m/zfobtained 294.14919 $[M+H]^+$, M= 293.14158, calculated mass for $C_{19}H_{19}NO_2$ = 293.14157, mass error = -0.03 ppm. The 2D-NMR (HSQC and HMBC) spectra of 3a can be seen in Fig.-2. Compound 3b. Yield 84%, m.p. 241-242ºC, FT-IR (υ/cm^{-1}): 3200, 3050, 2960, 1690, 1610, 1530 (NO_2), 1480, 1300, 1240, 1175, 1125. ^{1}H-NMR (δ/ppm, *J*/Hz): 9.80 (s, 1H), 7.49 (t, *J*=8, 1H), 7.59 (d, *J*=8, 1H), 7.94 (d, *J*=6, 1H), 7.97 (s, 1H), 4.99 (s, 1H), 2.56 (m, *J*=6, 4H), 2.22 (m, *J*=5, 4H), 1.91 (m, *J*=4, 2H), 1.79 (m, *J*=3, 2H). ^{13}C-NMR (δ/ppm): 194.9 (2C=O), 152.2 (1C_{Ar-NO}), 149.4 (2C=C-N), 147.5 (1C_{Ar-C}), 134.4 (1C_{ArH}), 129.5 (1C_{ArH}), 122.1 (1C_{ArH}), 120.1 (1C_{ArH}), 111.5 (2C=C-C), 36.7 (2C_{Al}), 32.9 (1C_{Al}), 26.3 (2C_{Al}), 20,8 (2C_{Al}). MS: m/z obtainedd339.13412 $[M+H]^+$; M=0338.12666, calculated mass for $C_{19}H_{18}N_2O_4$ = 338.126657, mass error = 0.009 ppm. Compound 3c. Yield 52%, m.p. 281-282ºC, FT-IR (υ/cm^{-1}): 3205, 3040, 2950, 1650, 1595, 1490, 1240, 1150, 1100, 1185, and 775 (CF_3). ^{1}H-NMR (δ/ppm, *J*/Hz): 9.39 (s, 1H), 7.22 (t, *J*=8, 1H), 7.30 (d, *J*=8, 1H), 7.39 (d, *J*=7, 1H), 7.43 (t, *J*=8, 1H), 5.35 (s, 1H), 2.50 (m, overlap with DMSO, 4H), 2.16 (m, *J*=6, 2H), 2.04 (t, *J*=5, 1H), 2.09 (t, *J*=5, 1H), 1.73 (m, *J*=6, 2H), 1.87 (m, *J*=6, 2H). ^{13}C-NMR (δ/ppm): 194.4 (2C=O), 151.1 (2C=C-N), 147.2 (1C_{Ar-C}), 131.7 (1C_{ArH}), 130.6 (1C_{Ar-CF}), 127.2 (1C_{ArH}), 126.8 (1C_{ArH}), 125.9 (2$C_{ArH, CF3}$), 113.6 (2C=C-C), 36.7 (2C_{Al}), 30.4 (1C_{Al}), 26.4 (2C_{Al}), 20.8 (2C_{Al}). MS: m/z obtained 362.13620 $(M+H)^+$; M= 361.12782, calculated mass for $C_{20}H_{19}F_3NO_2$ = 361.12896, mass error = 3.2 ppm. Compound 3d. Yield 30%, m.p. 253-254ºC, FT-IR (υ/cm^{-1}): 3205, 3045, 2989, 1645, 1597, 1490, 1355, 1242, 1178, and 1120. ^{1}H-NMR (δ/ppm, *J*/Hz): 9.40 (s, 1H), 6.71 (d, *J*=9, 2H), 7.04 (d, *J*=8, 2H), 3.65 (s, 3H), 4.84 (s, 1H), 2.48 (m, overlap with DMSO, 4H), 2.20 (m, *J*=5, 2H), 1.90 (m, *J*=4, 2H), 1.76 (m, *J*=3, 2H). ^{13}C-NMR (δ/ppm): 194.8 (2C=O), 157.1 (1C_{ArO}), 151.0 (2C=C-N), 139.7 (1C_{Ar-C}), 128.4 (2C_{ArH}), 113.1 (2C_{ArH}), 112.7 (2C=C-C), 54.9 (1CH_3O), 36.8 (2C_{Al}), 31.1 (1C_{Al}), 26.3 (2C_{Al}), 20, 8 (2C_{Al}). MS: m/z obtained 324.15850 $(M+H)^+$; M= 323.151224, calculated mass for $C_{20}H_{21}NO_3$ = 323.1521435, mass error = -2.8 ppm. Compound 3e. Yield 78%, m.p. 240-241ºC, FT-IR (υ/cm^{-1}): 3235, 3060, 2920, 2890, 1706, 1645, 1592, 1473, 1360, 1241, 1172, 1162, 1080 (C-Cl). ^{1}H-NMR (δ/ppm, *J*/Hz): 9.50 (s, 1H), 7.15 (d, *J*=7, 1H), 7.20 (t, *J*=8, 2H), 4.87 (s, 1H), 2.50 overlap DMSO, 4H), 2.20 (m, *J*=3, 4H), 1.91 (m, *J*=5, 2H), 1.78 (m, *J*=5, 2H). ^{13}C-NMR (δ/ppm): 194.8 (2C=O), 151.5 (2C=C-N), 146.3 (1C_{ArCl}), 130.0 (1C_{Ar-C}), 129.4 (2C_{ArH}), 127.7 (2C_{ArH}), 112.1 (2C=C-C), 36.4 (2C_{Al}), 31.9 (1C_{Al}), 26.3 (2C_{Al}), 20.8 (2C_{Al}). MS: m/z obtained 328.10874 $(M+H)^+$; M= 327.10078, calculated mass for $C_{19}H_{18}ClNO_2$ =

327.1026065, mass error = -3.6 ppm. Compound 3f. Yield 22%, m.p. 249-250°C, FT-IR (υ/cm^{-1}): 3230, 3005, 2963, 2915, 1665, 1646, 1605, 1460, 1355, 1240, 1178, and 1125. ^{1}H-NMR (δ/ppm, *J*/Hz): 9.40 (s, 1H), 6.94 (d, *J*=8, 2H), 7.05 (d, *J*=8, 2H), 4.85 (s, 1H), 2.62, m, *J*=5, 4H), 2.28 (m, *J*=6, f4H), 2.22 (s, 3H), 1.76 (m, *J*=5, 2H), 1.92 (m, *J*=5, 2H). ^{13}C-NMR (δ/ppm): 194.8 (2C=O), 151.1 (2C=C-N), 144.5 (1C_{Ar-C}), 134.3 (1C_{Ar-C}), 128.3 (2C_{ArH}), 127.4 (2C_{ArH}), 112.6 (2C_{ArH}), 36.8 (2C), 31.7 (1C_{Al}), 30.4 (1C_{Al}), 26.3 (2C_{Al}), 20.8 (2C_{Al}). MS: m/z obtained 308.16326 $(M+H)^+$; M= 307.155984, calculated mass for $C_{20}H_{21}NO_2$ = 307.1572289, mass error = -4.05 ppm.

Anti-inflammatory Assay

The title compounds (3a-f) were assessed at 15 μM in methanol (for preliminary) and at various concentrations (0.15 to 6 μM) (for IC_{50} determination) as anti-inflammatory agents by a procedure of thermal-induced denaturation of protein as previously reported.[15-16] The mixture of standard diclofenac sodium or test solutions (0.5 mL) and BSA solution 0.5% (w/v) in tris-buffer saline (pH to 6.3) (4.5 mL) was kept at 37°C for 15 min, heated at 70°C for 10 min, cooled, and the mixture's turbidity measured at 660 nm. To calculate the inhibition (%), we used the equation:

$$\text{Inhibition (\%)} = [(\text{Acs} - \text{Ats})/\text{Acs}] \times 100$$

Acs = control solution absorbance; Ats = test solution absorbance.

Antioxidant Assay

The title compounds (3a-f) were screened as antioxidants using DPPH radical scavenging technique and the Ferric Reducing Ability Potential (FRAP) method with curcumin as comparable, as earlier reported.[16-18]

DPPH Radical

The mixture of the title compounds (3a-f) or curcumin solution at 100 μg/mL (0.5 mL) and DPPH solution at 50 μg/ml (2 mL), both in methanol, was kept in the darkroom at r.t. for 30 min, then measured spectrometrically at 517 nm. To calculate the inhibition (%), we used the equation:

$$\text{Inhibition (\%)} = [(\text{Acs} - \text{Ats})/\text{Acs}] \times 100$$

Acs = control solution absorbance; Ats = test solution absorbance.

FRAP

The mixture of 0.1 mL of the title compounds (3a-f) or curcumin solution at 100 μg/mL in methanol and 0.9 mL of the fresh FRAP reagents was mixed and kept at 37°C for 6 min, then measured spectrometrically at 595 nm. To calculate the Fe^{2+} equivalent (%), we used the equation:

$$Fe^{2+} \text{ equivalent (\%)} = (\text{Ax})/(\text{Ay}) \times 100$$

Ax = sample's absorbance; Ay = ferrous sulfate (1000 μM) solution's absorbance.

Molecular Docking Study

The molecular docking study was performed utilizing Autodock v4.2 (http://autodock.scripps.edu/) integrated LigandScout software 4.4.3.[19] The compounds were drawn using Marvinsketch (www.chemaxon.com), saved as smile format (.smi), and submitted to energy minimization according to the previous procedure.[20-21] The COX-1 and COX-2 structures co-crystallized with FLP1650 and S58701, respectively (PDB ID: 1CQE and 6COX), were used as the protein targets.[22-23] The protein targets were downloaded and run the energy minimization according to the previous procedure.[20-21] For the protocol's validation, the root-mean-square deviation (RMSD) values obtained by re-docking the native ligands should be not more than 2.0 Å.[24-25]

RESULTS AND DISCUSSION

Chemistry

The condensation reaction between 3-aminocyclohex-2-en-1-one (**1**) and nine aromatic aldehyde compounds (2a-i) in anhydrous acetic acid under reflux conditions obtained six decahydroacridine-1,8-dione compounds (3a-f) with low to high yields (Scheme-1). The results indicated that the electron-

withdrawing groups at the para or meta position in the aromatic aldehyde ring increased the aldehyde reactivity and enhanced the yields and vice versa for the presence of electron-donating groups.

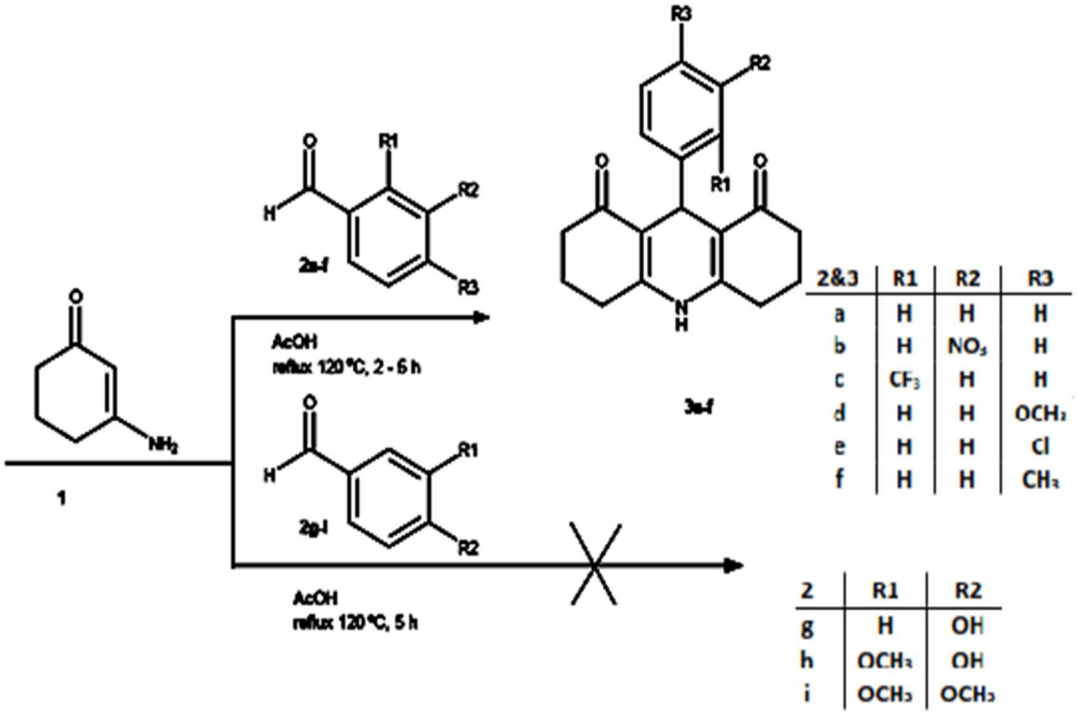

2&3	R1	R2	R3
a	H	H	H
b	H	NO_2	H
c	CF_3	H	H
d	H	H	OCH_3
e	H	H	Cl
f	H	H	CH_3

2	R1	R2
g	H	OH
h	OCH_3	OH
i	OCH_3	OCH_3

Scheme-1: The Synthesis of Decahydroacridine-1,8-dione Derivatives (**3a-f**).

The FTIR spectrum of compound 3a exhibited peaks at 3194, 3050, 2980, 1641, 1606, 1498, 1180, and 1130 cm^{-1} indicating amine, aromatic, aliphatic, carbonyl, ethylenic, CH_2, and C-N bonds. The ^{1}H-NMR spectrum showed the presence of N-H amine (s, 1H) at 9.44 ppm, five aromatic protons at 7.15 ppm (2H), 7.13 ppm (2H) and 7.03 ppm (1H), one proton of CH at 4.99 ppm, and aliphatic protons at 2.50 (overlap with DMSO, 4H), 2.17 (4H), 1.91 (2H), and 1.79 (2H). The ^{13}C-NMR spectrum exhibited the presence of two carbon of carbonyl at 194.8 ppm, ten double bond and aromatic carbon at 151.3-112.4 ppm, and seven carbon aliphatic at 36.8-20.8 ppm.[26-27] In the 2D Heteronuclear Single-Quantum Correlation (HSQC) spectra (Fig.-2a), the methylene group protons (CH_2), appear as two peaks at 1.79 ppm (2H) and 1.91 ppm (2H), were correlated with a peak of two carbons at 20.8 ppm, while the methylene group protons (CH_2) appearing at 2.17 ppm (m, 4H) were correlated with a peak of two carbons at 36.8 ppm. The methylene group protons (CH_2) appearing at 2.50 ppm (m, 4H, overlap with DMSO) were correlated with a peak of two carbons at 26.3 ppm. Protons of CH of the dihydropyridine ring connected to an aromatic ring, appearing as a single peak at 4.90 ppm (1H), were correlated with a carbon peak at 32.1 ppm. Four protons of an aromatic ring appearing at 7.13 ppm anda7.15 ppm were correlated with two carbon peaks at 127.5 and 127.8 ppm, while one proton of an aromatic ring appearing as a multiplet peak at 7.03 ppm was correlated with one carbon peak at 125.4 ppm. In the HMBC (Heteronuclear Multiple Bond Correlation) spectra (Fig.-2b), the methylene group protons (CH_2) appearing as two peaks at 1.79 and 1.91 ppm were correlated with carbon peaks at 26.3, 36.8, 151.3 and 194.8 ppm. The methylene group protons (CH_2) appearing at 2.17 ppm (m, 4H) were correlated with carbon peaks at 20.8, 26.3, and 194.8 ppm, while the methylene group protons (CH_2) appearing at 2.50 ppm (m, 4H, overlap with DMSO) were correlated with carbon peaks at 20.8, 36.8, 112.4, and 151.3 ppm. Protons of CH of the dihydropyridine ring connected to the aromatic ring appearing as a single peak at 4.90 ppm were correlated with carbon peaks at 112.4, 127.5, 147.4, 151.3, and 194.8 ppm. One proton of an aromatic ring appearing as a multiplet peak at 7.03 ppm was correlated with carbon peaks at 127.5 and 127.8 ppm; two protons of an aromatic ring appearing as triplet peaks at 7.13 ppm were correlated with carbon peaks at 125.4, 127.8, and 147.4 ppm; and two protons of an aromatic ring appearing as a doublet peak at 7.15 ppm were correlated with carbon peaks at 32.1, 125.4, 127.5, and 147.4 ppm. Meanwhile, the proton of amine (NH) was correlated with carbon peaks at 26.3,

112.4, 151.3, and 194.8 ppm.[26] The m/z in the mass spectrum obtained ultimately confirmed the expected structure of compound 3a. For elucidation of other prepared compounds' structures (3b-f) was done based on FTIR, ^{1}H-NMR, ^{13}C-NMR, and MS data. Those also confirmed the expected structures.

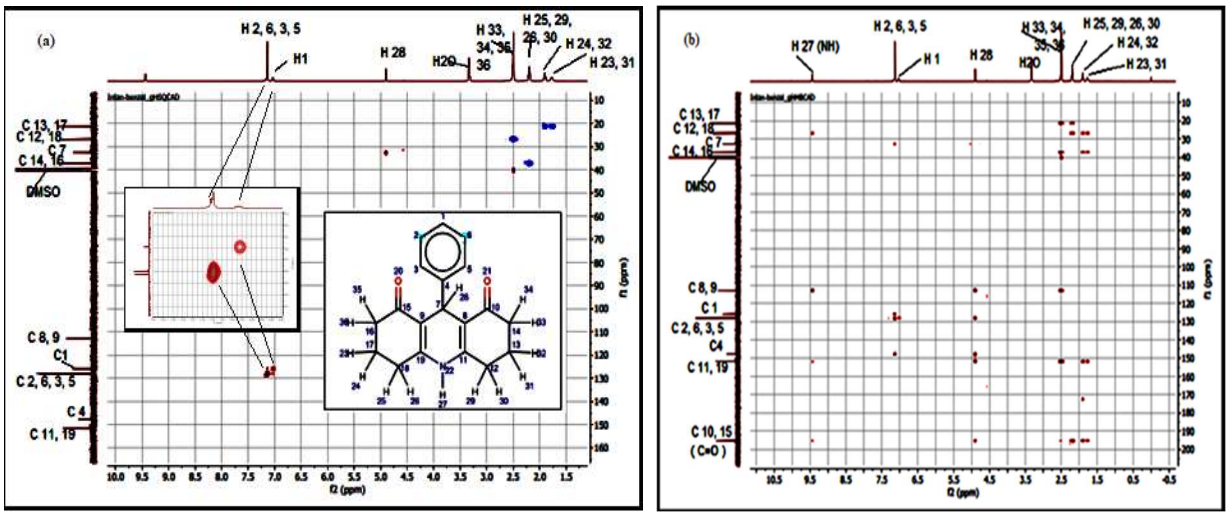

Fig.-2**:** The HSQC (a) and HMBC (b) spectra of compound 3a.

Antioxidant and Anti-inflammatory Properties

The antioxidant property of all prepared compounds was done using DPPH radical scavenging and FRAPimethods. In contrast, the anti-inflammatory activity was performed by a procedure of thermal-induced denaturation of protein. In a preliminary study, we observed that all prepared compounds had lower antioxidant activity than curcumin but higher anti-inflammatory activity than sodium diclofenac (Table-1). Therefore, we continued the anti-inflammatory activity test to determine the IC_{50}. The test compounds showed a dose-dependent relationship (Fig.-3) and compound 3a-d exhibited higher activity (IC_{50} = 0.125 - 0.316 μM) than diclofenac sodium (IC_{50} = 0.563 μM) (Table-2). Compound 3d having a 4-methoxy group at phenyl ring had the highest activity. It's in line with reported earlier on asymmetrical mono-carbonyl analogs of curcumin.[16] Inflammation has been involved in developing many diseases such as arthritis, lupus, and others. Protein denaturation produces auto antigens stimulating inflammatory response. NSAIDs are frequently applied to treat inflammatory conditions. They can bind with plasma protein and have shown a significant ability to inhibit protein denaturation.[28-32] The compound's ability to inhibit protein denaturation higher than diclofenac sodium implies an evident prospect as a potent anti-inflammation agent.

Molecular Docking Study

To predict the ligand-target and possible mechanism of action of the compounds at a molecular level, the molecular docking of title compounds has been done. Most NSAIDs inhibit inflammation by inhibiting the COX enzyme's catalytic activity, so we dock the compounds to that enzymes. The RMSD value obtained by re-docking native ligands to 1CQE and 6COX binding site for protocol's validation were 1.90 Å and 0.22 Å, confirming that the protocol has good performance for the docking (Fig.-4).[24-25] The results of the docking stated that all the compounds could interact with both enzymes. Almost all the compounds to both enzymes exhibited binding energy lower than diclofenac and curcumin (Table-2). Except for compounds 3e and 3f, this *in-silico* affinity was in line with their *in-vitro* activity. The ligand-amino acid interactions of the protein target are presented in Tables-3 and 4. Diclofenac forms hydrogen bonding with Tyr385 residue of COX-1 binding site. While in the COX-2 binding site, it creates hydrogen bonding to Ser530 and Tyr385. It also forms several hydrophobic interactions with hydrophobic residues. The results are in line with previous research.[33] The interaction between the ligand with Ser530 is essential for several compounds' inhibitory COX-2 activities.[33-34] The compound 3d forms hydrogen bonding with Tyr385 in the COX-1 binding site, and 3c forms hydrogen bonding with Ser530 in the COX-2 binding site. Except for 3b against COX-1, all the synthesized compounds and diclofenac form hydrophobic interaction with several identical residues.

Tabel-1: Preliminary Anti-inflammatory and Antioxidant Properties of the Title Compounds

Compds	Antioxidant		Anti-inflammatory
	25 ppm	3.33 ppm	15 µM
	DPPH	FRAP	% Inhibition ± SD
	% Scavenge ± SD	% Fe^{2+} equivalent	
3a	14.08 ± 0.96	30.16 ± 1.19	96.04 ± 0.006
3b	11.07 ± 0.23	26.92 ± 0.59	96.04 ± 0.004
3c	7.32 ± 0.29	26.27 ± 0.59	98.70 ± 0.001
3d	7.13 ± 0.62	29.64 ± 0.45	98.85 ± 0.001
3e	11.04 ± 0.56	27.57 ± 1.03	nd
3f	5.97 ± 0.23	30.29 ± 0.78	nd
Curcumin	78.38 ± 0.23	402.28 ± 3.32	97.64 ± 0.002
Diclofenac Sodium	nd	nd	69.79 ± 0.008

nd = no data

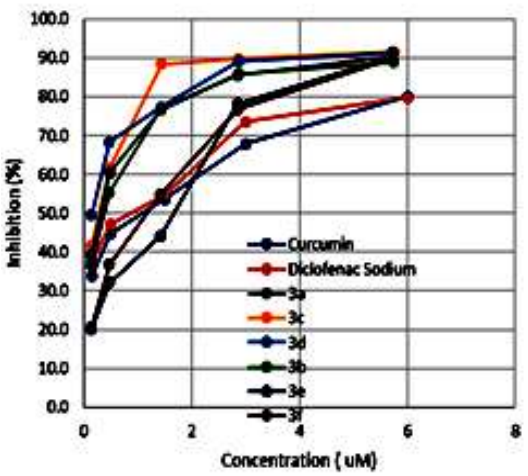

Fig.-3: Relation of Concentrations and Inhibition of Protein Denaturation Activity of Test Compounds

Table-2: The Title Compound's Anti-Inflammatory Activity and Binding Energy Interaction to COX-1 (1CQE) and COX-2 (6COX)

Compounds (Ligands)	IC_{50} (µM)	Binding Energy (Kcal/mol)	
		COX-1	COX-2
3a	0.316 ± 0.015	-8.83	-8.53
3b	0.258 ± 0.006	-10.32	-9.48
3c	0.203 ± 0.009	-7.55	-7.78
3d	0.125 ± 0.011	-8.32	-8.56
3e	0.942 ± 0.025	-8.46	-9.17
3f	0.811 ± 0.031	-9.79	-9.04
Diclofenac	0.706 ± 0.021	-7.70	-7.58
Curcumin	0.563 ± 0.017	-8.25	-7.70
FLP1650	-	-8.59	-
S58701	-	-	-10.6

*Inhibition of protein denaturation

Table-3: Ligand-Amino Acid Interactions in the COX-1 Binding Site and Their Bonds Type

Ligands	Amino Acids Residues/Interactions	
	Hydrophobic	Hydrogen Bond
FLP1650	Val116, Leu359, Leu531, Ile523, Val349, Leu352, Phe381, Tyr385, Ala527	Arg120, Tyr355
Diclofenac	Leu531, Val349, Leu352, Phe381, Ala527, Leu384	Tyr385
Curcumin	Val116, Leu359, Leu531, Val349 Ala527, Met113, Leu357	-
3a	Val349, Leu352, Tyr385, Tyr348	-
3b	Tyr355, Bog1702, Ile89	-
3c	Val349, Leu352, Phe381, Tyr385, Ala527, Leu384, Tyr348	-
3d	Val349, Leu352, Tyr348	Tyr385
3e	Val349, Leu352, Phe381, Tyr385, Tyr348, Phe205, Val344	-
3f	Val349, Leu352, Phe381, Tyr385, Ala527, Tyr348	-

Table-4: Ligand-Amino Acid Interactions in the COX-2 Binding Site and Their Bonds Type

Ligands	Amino Acids Residues/Interaction	
	Hydrophobic	Hydrogen Bond
S58701	Leu359, Val116, Leu531, Ala527, Val349, Leu384, Tyr385, Phe381, Leu352, Val523, Tyr355	Phe518, Gln192, Ser353
Diclofenac	Leu531, Ala527,Val349, Phe518, Leu352, Val523	Tyr385, Ser530
Curcumin	Ala527, Val349, Phe518, Leu352, Val523, Tyr355, Arg120	-

3a	Phe518, Leu352, Val523	-
3b	Phe518, Leu352, Val523	Tyr355
3c	Ala527, Val349, Phe518, Leu352, Val523, Tyr348	Ser530
3d	Phe518, Leu352, Val523	-
3e	Phe518, Leu352, Val523, Ala516, Ile517	-
3f	Phe518, Leu352, Val523, Ala516, Ile517	-

Fig.-4: Superpose Visualization of Co-Crystalline Ligand (blue) with Copy Ligand FLP1650 to COX-1 (1CQE) (a) and S58701 to COX-2 (6COX)

CONCLUSION

New decahydroacridine-1,8-dione derivatives have been successfully synthesized. All the compounds demonstrated higher activity to inhibit thermal-induced protein denaturation than diclofenac sodium but lower antioxidant activity than curcumin. Docking's study showed that all the prepared compounds could interact well with COX-1 and COX-2, and the majority showed lower binding energies than diclofenac and curcumin. The compounds promise to be a potent anti-inflammatory agent. However, the compounds should be further investigated to search for their in vivo activity and their toxicity.

ACKNOWLEDGMENT

We are full thanks to the Ministry of research and technology/NationallResearch &&Innovation Agency, Indonesia, which funded this study via PDUPT Grant on 2020; No.: NKB-91/UN2.RST/HKP.05.00/2020, the Molecular Structure Analysis Lab., ITB, Indonesia, and the Chemical Research Center, LIPI, Indonesia, measured NMR spectra and mass spectra.

REFERENCES

1. American College of Rheumatology, Enpowering Rheumatology Professionals, NSAIDs (nonsteroidal anti-inflammatory drugs) (2020), https://www.rheumatology.org/I-Am-A/Patient-Caregiver/Treatments/NSAIDs(accessed 21.08.21)
2. S. Wongrakpanich, A. Wongrakpanich, K. Melhado, J. Rangaswami, *Aging and disease*, **9(1)**, 143(2018), https://doi.org/10.14336/AD.2017.0306
3. K.G. Shilpa, K.H. Shivaprasad, and M.R. Archana, *Rasayan Journal of Chemistry*, **14(4)**, 2246(2021), http://doi.org/10.31788/RJC.2021.1446507
4. N. Ullah, F. Jamali, Z. Huang, F. Sanaee, A. Rodriguez-Dimitrescu, F. Aldawsari, F. Jamali, A. Bhardwaj, N.U. Islam, and C.A. Velázquez-Martínez, *Journal of Enzyme Inhibition Medicinal Chemisty*, **31(6)**, 1018(2016), https://doi.org/10.3109/14756366.2015.1088840
5. A.A. Abdelhamid, S.K. Mohamed, A. Maharramov, A. Khalilov and M. Allahverdiev, *Journal of Saudi Chemical Society*. **18**, 474(2014), https://doi.org/10.1016/j.jscs.2011.10.005
6. B. Zeynizadeh and M. Gilanizadeh, *Current Chemisty Letter,* **9**, 71(2020), https://doi.org/10.5267/j.ccl.2019.8.001
7. S. Sudha and M.A. Pasha, *The Scientific World Journal,* Article **ID 930787**, 6 pages(2013), https://doi.org/10.1155/2013/930787
8. M.M. Alam, A.T. Mubarak, M.A. Assiri, S.M. Ahmed, and A.M. Fouda. *BMC Chemistry,* **13**, 40(2019), https://doi.org/10.1186/s13065-019-0545-3

9. S.S. Mansoor, K. Aswin, K. Logaiya, and S.P.N. Sudhan, *Journal of Taibah University of Science,* **8**, 265(2014), https://doi.org/10.1016/j.jtusci.2014.03.003
10. J.-J. Xia and K.-H. Zhang, *Molecules*, **17**, 5339(2012), https://doi.org/10.3390/molecules17055339
11. G.M. Ziarani, S. Mousavi, N. Lashgari, A. Badiei, and M. Shakiba, *Iranian Journal of Chemistry and Chemical Engineering*, **32(4)**, 9(2013), https://doi.org/10.30492/IJCCE.2013.6739
12. G. Sujatha, V. Anusuya, and G.L. Balaji, *European Journal Molecule & Clinical Medicine*, **7(3),** 2211(2020)
13. M. Kidwai and D. Bhatnagar, *Tetrahedron Letter,* **51(20)**, 2700(2010), https://doi.org/10.1016/j.tetlet.2010.03.033
14. Y.-B. Shen and G.-W. Wang, *Arkivoc*, **xvi**, 1(2008)
15. H. Hayun, B.P. Maggadani, A. Kurnia, A. Hanifah, M. Yuliandi, I. Fitriyani and S.P. Hadrianti, *International Journal of Applied Pharmaceutics*, **11**, 246(2019), https://doi.org/10.22159/ijap.2019.v11s1.19448
16. T.N. Putri, A. Bachtiar and H. Hayun, *Journal of Applied Pharmaceutical Sciences,* **8(05)**, 019(2018), https://doi.org/10.7324/JAPS.2018.8503
17. T. Okselni, A. Santoni, A. Dharma and M. Efdi, *Rasayan Journal of Chemistry*, **11(3)**, 1211(2018), http://dx.doi.org/10.31788/RJC.2018.1133058
18. H. Hayun, I. Gavrila, S. Silviana, A.E.K. Siahaan, R.F. Vonna and M.I. Latifah, *Rasayan Journal of Chemistry*, **13(1)**, 131 (2020), https://doi.org/10.31788/RJC.2020.1315300
19. G. Wolber and T. Langer, *Journal of Chemical Information and Modeling,* **45(1)**, 160(2005), https://doi.org/10.1021/ci049885e
20. P. Tosco, N. Stiefl, and G. Landrum, *Journal of Cheminformatics*, **6**, 37(2014), https://doi.org/10.1186/s13321-014-0037-3
21. S. Megantara, M. Mutakin, E. Halimah, E. Febrina, and J. Levita, *Rasayan Journal of Chemisty*, **13(03)**,1321(2020), https://doi.org/10.31788/RJC.2020.1335766
22. D. Picot, P.J. Loll, and R.M. Garavito, *Nature*, **367**, 243(1997), https://doi.org/10.1038/367243a0
23. R.G. Kurumbail, A.M. Stevens, J.K. Gierse, J.J. Mcdonald, R.A. Stegeman, J.Y. Pak, D. Gildehaus, J.M. Miyashiro, T.D. Penning, K. Seibert, P.C. Isakson, and W.C. Stallings, *Nature,* **384,** 644(1996), https://doi.org/10.1038/367243a0
24. D. Ramírez and J. Caballero, *Molecules*, **23(5)**, 1038(2018), https://doi.org/10.3390/molecules23051038
25. H. Hariyanti, K. Kusmardi, A. Yanuar, and H. Hayun, *Indonesian Journal of Chem*isty, **21(1)**, 137(2021), https://doi.org/10.22146/ijc.54745
26. R.M. Silverstein, F.X. Webster, and D.J. Kiemle, Spectrometric Identification of Organic Compounds, 7th ed., John Wiley & Sons, Inc., New York, NY, USA, (2005)
27. MarvinSketch 20.8.0. ChemAxon Ltd., 1998–2020, http://www.chemaxon.com (accessed 14.11.20)
28. M. Marius, D. Amadou, A.A. Donatien, A. Gilbert, Y.N. William, K. Rauf, et al., *Gastroenterology Research and Practice,* Article **ID 4253174**, (2020), https://doi.org/10.1155/2020/4253174
29. N.I. Osman, N.J. Sidik, A. Awal, N.A.M. Adam, and N.I. Rezali, *Journal of Intercultural Ethnopharmacology*, **5(4)**, 343(2016), https://doi.org/10.5455/jice.20160731025522
30. E.L. Opie, *Journal of Experimental Medicine*, **115**, 597(1962), https://doi.org/10.1084/jem.115.3.597
31. L. Saso, G. Valentini, M.L. Casini, E. Grippa, M.T. Gatto, M.G. Leone, and B. Silvertini, *Archives of Pharmacal Research*, **24**, 150(2001), https://doi.org/10.1007/BF02976483
32. S. Yesmin, A. Paul, T. Naz, A.B.M.A. Rahman, S.F. Akhter, M.I.I. Wahed, T.B. Emran, and S.A. Siddiqui, *Clinical Phytoscience*, **6(59)**, 1(2020), https://doi.org/10.1186/s40816-020-00207-7
33. A.L. Blobaum and L.J. Marnett, *Journal of Medicinal Chemistry*, **50**, 1425(2006), https://doi.org/10.1021/jm0613166
34. H. Hayun, A. Yanuar, M. Hanafi, and P.W.S.S. Hudiyono, *Bioinformation*, **7(5)**, 246(2011), https://doi.org/10.6026/97320630007246

[RJC-6775/2021]

UNIVERSITAS MUHAMMADIYAH PROF. DR. HAMKA
FAKULTAS FARMASI DAN SAINS
Jl. Limau II, Kebayoran Baru, Jakarta 12130 Tel. (021) 7208177, 722886, Fax. (021) 7261226, 7256620
Islamic Centre, Jl. Delima II/IV, Klender, Jakarta Timur Tlp.: (021) 8611070, Fax. (021) 86603233
Website: www.ffs-uhamka.ac.id; E-mail: ffs@uhamka.ac.id

SURAT TUGAS
MELAKUKAN KEGIATAN PENELITIAN DAN PUBLIKASI
NO. 223/F.03.08/2022

Bismillahirrohmanirrohiim,
Yang bertanda tangan di bawah ini

N a m a	**Dr. apt. Hadi Sunaryo, M.Si.**
NIDN	0325067201
Pangkat /Jabatan Akademik	Penata Tk. I, III/d / Lektor Kepala
Jabatan	Dekan
Unit Kerja	Fakultas Farmasi dan Sains UHAMKA Jakarta

Memberikan tugas Penelitian dan Publikasi pada **tahun akademik 2021/2022** kepada:

N a m a	**Dr. apt. Hariyanti, M.Si.**
NID/NIDN	D.03.0606/ 0311097705
Pangkat /Jabatan Akademik	Penata/ III-C
Jabatan Fungsional	LEKTOR
Unit Kerja	Fakultas Farmasi dan Sains UHAMKA Jakarta

Untuk Melaksanakan Penelitian dan Publikasi sebagai berikut:

NO	JUDUL PENELITIAN DAN PUBLIKASI
1.	**"Molecular Docking Study of Isoflavonoid Erythrina variegata To Plasminogen Receptor as Thrombolytic Agent on Myocardial Infarction Disease"**

Demikian surat tugas ini diberikan kepada yang bersangkutan untuk dilaksanakan dengan penuh amanah dan tanggung jawab

Jakarta, 09 Maret 2022
Dekan,

Dr. apt. Hadi Sunaryo, M.Si., Apt.

Tembusan Yth:
1. Rektor UHAMKA Jakarta
2. Wakil Rektor I dan II UHAMKA Jakarta
3. Arsip

Jurnal Jamu Indonesia (2022) 7(1):12-19
ISSN 2407-7178 eISSN 2407-7763

Artikel Penelitian
DOI: https://doi.org/10.29244/jji.v7i1.172

Studi *Molecular Docking* Senyawa Isoflavonoid Dadap Ayam (*Erythrina variegata*) Terhadap Reseptor Plasminogen Sebagai Agen Trombolitik Pada Penyakit Infark Miokard

Molecular Docking Study of Isoflavonoid Erythrina variegata To Plasminogen Receptor as Thrombolytic Agent on Myocardial Infarction Disease

Penulis **Rizky Arcinthya Rachmania[1]*, Hariyanti Hariyanti[1], Dewi Susilawati[1]**

Afiliasi **[1]Program Studi Farmasi, Fakultas Farmasi dan Sains, Universitas Muhammadiyah Prof. DR. HAMKA (UHAMKA), Islamic Center Jln. Delima II/IV Klender, Jakarta Timur**

Kata Kunci
- dadap ayam
- plasminogen
- isoflavonoid
- trombolitik
- *docking*

Keywords
- *Erythrina variegata*
- *plasminogen*
- *isoflavonoid*
- *thrombolytic*
- *docking*

Diterima 3 Maret 2020
Direvisi 23 November 2021
Disetujui 18 Februari 2022

***Penulis Koresponding**
Rizky Arcinthya Rachmania
email:
rizky_arcinthya@uhamka.ac.id

ABSTRAK

Dadap ayam merupakan salah satu tanaman yang memiliki khasiat sebagai agen trombolitik. Senyawa isoflavonoid berpotensi memacu perubahan plasminogen yang berperan dalam proses pembentukan fibrin yang menyebabkan terbentuknya bekuan fibrin yang dapat menyumbat pembuluh darah arteri sehingga menyebabkan terjadinya infark miokard. Penelitian ini bertujuan untuk melihat interaksi senyawa isoflavonoid dari kulit batang dadap ayam yang diharapkan dapat menjadi kandidat obat trombolitik. Metode yang digunakan pada penelitian ini adalah molecular docking dengan menggunakan bantuan software Autodock Vina dan Pymol. Hasil penelitian menunjukkan nilai ΔG binding affinity streptokinase sebagai ligan standar -8,4 kkal/mol dan turunan isoflavonoid yang memiliki nilai ΔG binding affinity terendah terdapat pada folitenol -11,5 kkal/mol dan orientanol C -11,4 kkal/mol. Sehingga dapat disimpulkan turunan isoflavonoid dadap ayam mempunyai potensi ikatan lebih baik dibandingkan dengan streptokinase sebagai ligan standar.

ABSTRACT

Erythrina variegata is one of the plants that have efficacy as thrombolytic agent. Isoflavonoid compound has the potential to accelerate the changes of plasminogen which plays important role in the forming of fibrin, that causes the formation of fibrin clots that can clog the arteries thus causing myocardial infarction. This study aimed to look at the activity of isoflavonoid compounds from Erythrina variegata bark which are expected to be candidates for thrombolytic drugs. This research aims at looking for the interaction of isoflavonoid compounds of bark which is expected can be thrombolytic drug candidates. The method used in this research was the molecular docking with Autodock Vina and PyMOL software. The results showed that the value of ΔG binding affinity as ligands standard streptokinase -8.4 kcal/mol and isoflavonoid derivatives that have ΔG binding affinity value was lowest for the folitenol -11.5 kcal / mol and orientanol C -11.4 kcal/mol. Can be concluded that isoflavonoid derivatives in Erythrina variegata have better binding potential compared to streptokinase as standard ligands.

PENDAHULUAN

Trombosis merupakan suatu proses patologis, pada peristiwa ini agregasi trombosit dan bekuan fibrin menutup pembuluh darah. Trombosis arteri dapat menyebabkan *nekrosis ischemic* pada jaringan yang disuplai oleh arteri bersangkutan misalnya *infark miokard* (Majerus and Tollefsen 2001). Penyakit *Infark miokard* adalah kondisi terhentinya aliran darah pada arteri koroner yang mendarahi jantung (Simanjuntak *et al.* 2019). Penyakit ini ditandai dengan rasa sakit pada dada yang terjadi akibat sebagian otot jantung mati (Anies 2015; PERKI 2018). Salah satu penyebab terjadinya penyakit ini adalah terbentuknya aterosklerosis yaitu pengerasan dan penebalan dinding pembuluh darah arteri akibat plak (Anies 2015). Berdasarkan hasil Riset Kesehatan Dasar (RISKESDAS 2013) prevalensi penyakit *infark miokard* akut tertinggi terdapat di Sulawesi Tengah (0,8%) diikuti Sulawesi Utara, DKI Jakarta, dan Aceh, masing-masing 0,7% (Budiman dkk. 2015).

Obat-obat trombolitik merupakan suatu terapi untuk penyakit *infark miokard*. Golongan obat ini dapat melarutkan trombus yang sudah terbentuk dengan mengkatalisasi plasmin dari plasminogen. Obat-obat ini menimbulkan suatu keadaan pelarutan/lisis tergeneralisasi saat pemberian secara intravena (Hambleton & O'Reilly 2002). Golongan obat trombolitik terdiri dari streptokinase, urokinase, dan t-PA (Aktivator Plasminogen Jaringan). Streptokinase merupakan terapi pertama untuk mengembalikan aliran darah ke arteri koroner yang mengalami trombosis. Obat ini merupakan protein yang diperoleh dari *streptococcus* yang dapat mengubah plasminogen menjadi plasmin (Fletcher 2007). Streptokinase adalah sediaan protein yang diperoleh dari Streptococcus haemolyticus kelompok C. Senyawa ini mempunyai sifat dapat bergabung dengan plasminogen manusia membentuk aktivator plasminogen. Hal ini menyebabkan perubahan konformasi yang memajankan sisi aktif pada plasminogen untuk membentuk plasmin bebas (Majerus & Tollefsen 2001).

Reseptor plasminogen adalah bentuk prekursor dari serin protease plasmin yang beredar dalam bentuk inaktif. Plasminogen terdiri dari domain Pan-apple (PAP), lima domain kringle (KR 1-5), dan domain serin protease (SP). Domain kringle memediasi interaksi dengan gumpalan fibrin dan reseptor permukaan sel. Interaksi ini memicu plasminogen menjadi bentuk terbuka yang dapat dibelah dan dikonversi menjadi plasmin oleh tipe jaringan plasminogen aktivator dan jenis urokinase (Law R *et al*. 2012). Reseptor enzim plasminogen diubah menjadi plasmin dengan pemutusan ikatan peptida tunggal. Plasmin merupakan suatu protease yang relatif nonspesifik, senyawa ini mencerna bekuan fibrin dan protein plasma lainnya termasuk beberapa faktor koagulasi. Plasminogen dan plasmin memiliki ranah protein khusus (*kringles*) yang berikatan dengan lisin di bekuan fibrin dan memberikan spesifisitas bekuan terhadap proses-proses fibrinolitik (Zehnder 2012).

Terapi obat trombolitik cenderung melarutkan trombus patologis dan deposit fibrin pada pembuluh yang luka. Oleh karena itu obat-obat ini bersifat toksik dan menyebabkan efek samping berupa hemoragia (Majerus and Tollefsen 2001). Dalam hal ini pengobatan menggunakan herbal menjadi pilihan utama, dikarenakan minimnya efek samping yang didapat.

Salah satu jenis tanaman yang pernah diteliti sebagai agen trombolitik yaitu tanaman dadap ayam (*Erythrina variegata* L.). Bagian yang digunakan sebagai obat trombolitik adalah kulit batangnya (Shahriar 2015). Kandungan kimia yang terkandung didalam tanaman dadap ayam meliputi triterpenoid, steroid dan turunan isoflavonoid (Herlina *et al*. 2012). Hasil dari penelitian Aprilia (2021) menunjukkan bahwa pada daun dadap ayam menghasilkan kelima senyawa yaitu alkaloid 15,35 %, flavonoid 3,501 %, saponin 6,67 %, steroid 3,11 % dan tanin 0,14 %. Kandungan dalam kulit batang dadap ayam yang diduga berkhasiat sebagai agen trombolitik yaitu senyawa isoflavonoid. Berdasarkan penelitian Miao *et al*. (2013) flavonoid beraktivitas sebagai trombolitik dan dapat meningkatkan jenis aktivator plasminogen jaringan. Penelitian sebelumnya menunjukkan bahwa tanaman dadap ayam memiliki aktivitas sebagai antikolesterol (Balamurugan and Shantha 2010), antibakteri (Tanaka *et al*. 2004) dan antifertilitas (Tjiphanata *et al*. 2017). Berdasarkan pada penelitian-penelitian di atas, maka mendesak untuk segera menemukan kandidat obat alami penyakit Infark Miokard yang berpotensi dan berpeluang besar untuk dijadikan obat Infark Miokard.

Penelitian dan studi tentang tanaman dadap ayam di atas juga menjelaskan bahwa keragaman tanaman dadap ayam memiliki potensi yang berkualitas baik dalam menangani penyakit Infark Miokard. Hal ini disebabkan oleh adanya senyawa-senyawa aktif dalam tanaman dadap ayam yaitu senyawa-senyawa isoflavonoid. Senyawa-senyawa isoflavonoid (**Gambar 1**) yang diperkirakan memiliki afinitas ikatan dan interaksi trombolitik ini dapat diteliti dengan metode penambatan molekul (*molecular docking*). Metode *molecular docking* adalah studi interaksi beberapa

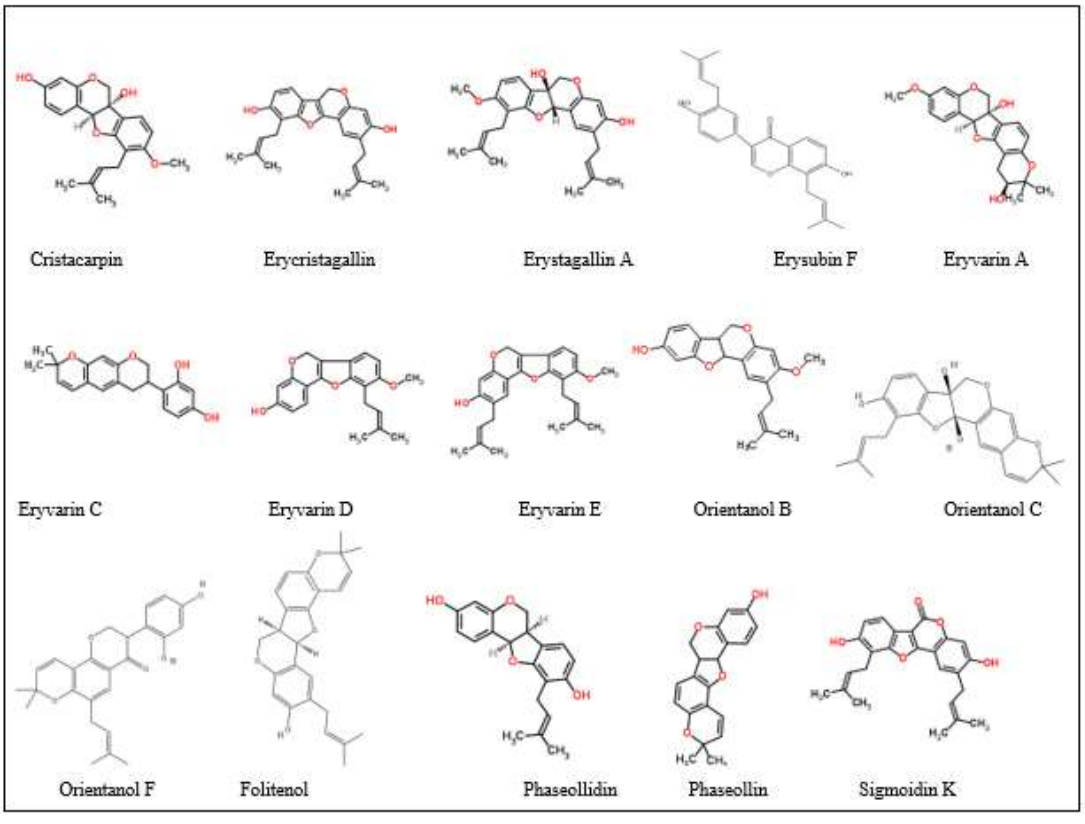

Gambar 1. Struktur Ligan Tanaman Dadap ayam (Situs *PubChem*)

senyawa bahan alam yang diketahui dapat berikatan dengan molekul protein yang menggunakan aplikasi computer secara *in silico* pada tingkat molekuler. Metode ini digunakan untuk membantu menentukan senyawa yang akan ditapis. *Molecular docking* pada penelitian ini menggunakan perangkat lunak *Autodock Vina* serta *PyMol* sebagai perangkat visualisasi.

Penelitian ini bertujuan untuk mengetahui afinitas ikatan dan interaksi diantara senyawa isoflavonoid dari kulit batang dadap ayam (*Erythrina variegata* L.) dengan reseptor plasminogen (4DUU) secara *in silico* melalui studi *molecular docking* untuk menentukan kandidat obat trombolitik. Terminologi *in silico* diantaranya dikenal sebagai penapisan virtual. Pendekatan secara virtual ini menjadi alternatif karena dapat digunakan untuk melakukan penapisan senyawa biologis.

METODE

Alat dan Bahan

Alat yang digunakan dalam penelitian ini berupa perangkat keras dan perangkat lunak.Peragkat keras dilengkapi dengan *processor* AMD A8-6410 APU *with* AMD Radeon R5 *Graphics* CPU GHz, RAM4 GB dan system operasi *Microsoft Windows* 8. 1 Pro 64-bit, Monitor HP® 24 inci, dan jaringan internet *speedy* 10 Mbps. Perangkat lunak dilengkapi dengan paket MGL *Tools* 1.5.6 yang terdiri dari *Autodock Vina*, *Autodock Tools*, CLC *Drug Discovery Workbench* 2.5, *Pymol* (DeLano Scientific LLC.), *Vegazz* 3.0.3.18, dan *Protein Bank Data* pada situs http://www.rcsb.org/pdb.

Bahan yang digunakan adalah struktur 3D dari reseptor plasminogen diunduh dari *Protein Bank Data* dengan situs http://www.rcsb.org/pdb. yang berformat .pdb yaitu *human* plasminogen (PDB ID: 4DUU), dan struktur 3D senyawa turunan isoflavonoid, antara lain cristacarpin, erycristagallin, erystagallin A, erysubin F, eryvarin A, eryvarin C, eryvarin D, eryvarin E, folitenol, orientanol B, orientanol C, orientanol F, phaseollidin, phaseollin, dan sigmoidin K (Tanaka *et al*, 2002).

Prosedur Penelitian

Penyiapan Struktur Plasminogen

Pengunduhan plasminogen dari *Protein Bank Data* pada situs http://www.rcsb.org/pdb yang berformat .pdb. Pemisahan makromolekul dari molekul yang tidak diperlukan menggunakan program *Discovery studio* 4.5. Hasil pemisahan tersebut disimpan dalam format .pdb.

Perancangan Struktur Ligan Tiga Dimensi

Perancangan struktur ligan dilakukan dengan *software Vegazz* dengan format gambar MDL *molfile*. Kemudian diubah menjadi bentuk .pdb.

Penentuan *Cavity* pada Reseptor

Penentuan *cavity* dilakukan untuk mengenali residu yang membentuk *cavity* pada reseptor. Penentuan *cavity* dilakukan dengan menggunakan *software offline* CLC *Drug Discovery Workbench* 2.5.

Preparasi *File Docking*

Preparasi *ligan* dilakukan dengan mengatur *number of action torsion* dan mengubah format menjadi .pdbqt, sedangkan preparasi reseptor dilakukan dengan menambahkan *hydrogen polar*, mengatur *grid box* agar diketahui posisi dari *binding site* dan mengubah format menjadi .pdbqt. Preparasi *file docking* ini menggunakan *software Autodock Tools*. *File* ini disimpan didalam satu *folder* di dalam *drive* C pada komputer.

Proses *Molecular Docking* dengan *Autodock Vina*

Autodock Vina yang berisi ligan dan protein yang berformat .pdbqt disimpan di *drive* C. Kemudian ligan dan protein tersebut disalindan diubah ke dalam bentuk *notepad* disimpan dengan nama *conf*. Untuk menjalankannya menggunakan program *command prompt*.

Analisis *Molecular Docking*

Analisis *molecular docking* dilakukan dengan melihat nilai Energi bebas ikatan hasil *docking,* dilihat pada *output* dalam format log.txt. Kompleks ligan-reseptor yang dipilih adalah kompleks yang memiliki nilai energi bebas ikatan terendah kemudian dilakukan analisis lebih lanjut.

Visualisasi *Molecular Docking*

Visualisasi *molekular docking* dilakukan dengan menggunakan *software PyMol*. Tujuannya untuk melihat interaksi antara ligan dengan residu asam amino pada reseptor.

HASIL & PEMBAHASAN

Plasminogen merupakan makromolekul yang akan dijadikan sebagai target *docking* yang diunduh dari *Protein Data Bank* (PDB) pada RCSB (http://www.rcsb.org/pdb). PDB ID plasminogen yaitu 4DUU yang berasal dari *Protein Data Bank* terdiri dari 791 residu asam amino yang merupakan struktur kristal sinar x dengan resolusi 5,2 Å, ditemukan pada *Homo sapiens* dan merupakan rantai tunggal tanpa ada ligan alami. PDB ID 4DUU dipilih karena merupakan plasminogen yang berfungsi lebih efisien dalam konteks bekuan fibrin (Law *et* al. 2012).

Penentuan *cavity* dilakukan untuk mengenali residu yang membentuk *cavity* dan *pocket* pada target (reseptor). Tujuannya untuk mendapat efek pemacuan terhadap reseptor plasminogen. *Cavity* merupakan suatu celah yang dimiliki oleh reseptor, sedangkan *pocket* merupakan ruang yang berada di dalam *cavity* sebagai akses terjadinya ikatan antara ligan dengan reseptor sehingga menghasilkan efek yang diharapkan. *Cavity* yang ditemukan pada reseptor target biasanya lebih dari satu *cavity*. Oleh karena itu perlu dilakukan evaluasi *cavity* untuk melihat kemungkinan *cavity* menjadi *binding site* yang sebenarnya.

Hasil pencarian *cavity* pada reseptor plasminogen, terdeteksi banyaknya *cavity* berada pada daerah – daerah reseptor plasminogen (**Gambar 2**). Hal ini menjadikan perlu dilakukannya evaluasi *cavity* dengan cara *setup binding site* pada program kerja *software* CLC *Drug Discovery Workbench* 2.5. Setelah dilakukan evaluasi *cavity*, daerah reseptor plasminogen yang telah terdeteksi banyaknya *cavity* menunjukkan suatu area lebih spesifik yang menggambarkan *cavity* sebenarnya sebagai *binding site* (**Gambar 3**). Area ini yang nantinya merupakan tempat terjadinya interaksi antara residu asam amino pada reseptor dengan ligan yang akan dijadikan area *gridbox*. Pada kode reseptor 4DUU tidak terdapat ligan alami sehingga area gridbox ditentukan dengan penentuan *cavity binding site* dengan software CLC *Drug Discovery Workbench* 2.5.

File struktur 15 ligan dadap ayam dan streptokinase yang berada dalam bentuk .pdb diubah ke dalam bentuk .pdbqt pada *software offline Autodock Tools* yang berasal dari MGL*Tools* 1.5.6 (*Scripps Research Institute*). Sebelum ligan diubah dalam format .pdbqt, ligan perlu diatur angka *torsion*nya untuk mempercepat kerja *docking* pada *Vina*. Torsi diubah pada opsi *Ligand-Torsion Tree*. Setelah torsi diubah, ligan baru disimpan dalam format .pdbqt pada opsi *Ligand-Output*. Plasminogen yang sudah dibersihkan sebelumnya perlu ditambahkan hidrogen dengan tujuan agar kondisi reseptor tersebut sesuai dengan pH fisiologis (pH~7) (Drie 2005). Sama seperti ligan, plasminogen juga diubah formatnya menjadi bentuk .pdbqt.

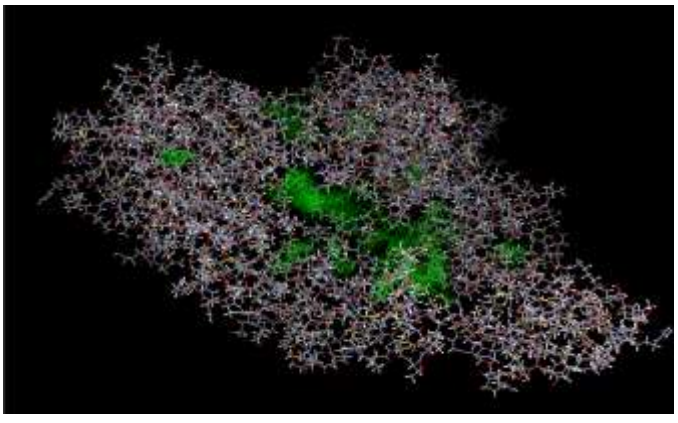

Gambar 2. Hasil Deteksi *Cavity* Reseptor Plasminogen (CLC *Drug Discovery Workbench* 2.5)
Keterangan: Area yang ditandai dengan spot-spot warna hijau merupakan area *cavity*

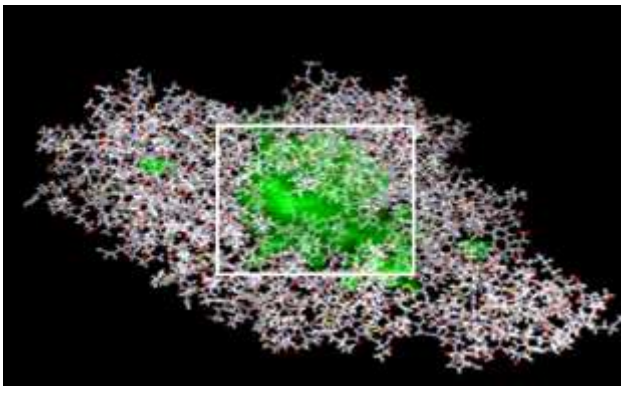

Gambar 3. Hasil Deteksi *Binding Site* Reseptor Plasminogen (CLC *Drug Discovery Workbench* 2.5)
Area yang berada pada kotak putih merupakan *cavity* sebenarnya sebagai *binding site* pada reseptor

Pada reseptor harus pula ditentukan *gridbox. Gridbox* merupakan tempat dimana ligan akan berinteraksi pada target reseptor (enzim) dan digambarkan dalam bentuk kubus. *Gridbox* tersebut juga diatur dalam *software offline Autodock Tools*. Penentuan *gridbox* dilakukan berdasarkan hasil dari penentuan *cavity binding site* dari software CLC *Drug Discovery Workbench* 2.5 berada pada koordinat *center* x= 5.108, y= -6.619, z= 33.731, *size* x= 40, y= 40, z= 40, dan *spacing* (amstrong)= 1.

Proses *docking* senyawa isoflavonoid dadap ayam dan pembanding streptokinase dijalankan dengan menggunakan *command prompt* yang sebelumnya diatur konfigurasinya menggunakan *notepad* yang sudah tersedia pada *accessories* komputer. Konfigurasi yang diatur harus mencantumkan nama reseptor, nama ligan, *file out* dengan format .pdbqt, *grid center, grid size*, dan *exhaustiveness*. Konfigurasi tersebut harus diatur dengan benar agar *command prompt* bisa membaca program tersebut. Konfigurasi disimpan dalam *folder vina* yang berada pada *drive* C *windows*. Syarat untuk melakukan *docking* dengan *Autodock Vina* adalah ligan dan reseptor harus dengan format .pdbqt dan terdapat *gridbox.*

Analisis hasil *molecular docking* pada penelitian ini adalah nilai ΔG *binding affinity*, serta interaksi ligan dengan residu protein. Berdasarkan hasil *docking* antara ligan dengan reseptor diperoleh sembilan konformasi ligan dengan nilai *binding affinity*. Penentuan konformasi ligan dapat dilihat dari hasil yang keluar pada *command prompt*, dari sembilan konformasi ligan dipilih satu konformasi ligan dengan energi terkecil. *Binding affinity* merupakan parameter *docking* menggunakan *Autodock Vina*. Nilai yang dilihat adalah nilai ΔG *binding affinity* (kkal/mol). Semakin kecil nilai ΔG *binding affinity* maka afinitas antara reseptor dengan ligan semakin tinggi, sebaliknya semakin besar nilai ΔG *binding affinity* maka afinitas antara reseptor dengan ligan semakin rendah (Pebiansyah dkk. 2013).

Tabel 1 menunjukkan bahwa ke lima belas ligan tanaman memiliki kestabilan yang lebih baik dibandingkan dengan ligan standarnya yang dilihat dari nilai energi bebas. Nilai energi bebas yang digunakan adalah nilai yang paling rendah dikarenakan nilai energi

bebas rendah menunjukkan afinitas yang tinggi pada proses penambatan molekul. Ligan tanaman yang memiliki kestabilan paling baik ditunjukkan oleh folitenol dengan nilai ΔG sebesar -11.5 kkal/mol. dan orientanol C dengan nilai ΔG sebesar -11.4 kkal/mol. Hal ini menunjukkan bahwa senyawa folitenol dan orinetanol C mempunyai interaksi yang lebih baik terhadap reseptor plasminogen dibandingkan dengan streptokinase.

Untuk melihat interaksi/afinitas antara residu asam amino dengan ligan hasil *molecular docking* dilakukan menggunakan *software offline PyMol*. Pada *software* tersebut dapat dilihat ikatan hidrogen dan residu apa saja yang terikat.

Tabel 2 menunjukkan interaksi antara residu asam amino dengan ligan tanaman. Pada dasarnya interaksi antara reseptor dengan ligan akan menghasilkan jarak ikatan dan residu asam amino yang berikatan. Ikatan yang terjadi dapat berupa ikatan hidrogen yang merupakan gaya yang terjadi antara atom yang memiliki kelektronegatifan yang tinggi dengan atom hidrogen yang terikat secara kovalen pada suatu atom

Tabel 1. Hasil *Docking* Ligan Standar dan Ligan Tanaman terhadapReseptor Plasminogen (4DUU)

Ligan		ΔG *binding affinity* (kkal/mol)
Ligan	Standar	-8,4
Streptokinase		-11,5
Ligan 1	Folitenol	
Ligan 2	Orientanol C	-11,4
Ligan 3	Eryvarin A	-10,9
Ligan 4	Erysubin F	-10,7
Ligan 5	Phasollin	-10,7
Ligan 6	Eryvarin C	-10,6
Ligan 7	Erystagallin A	-10,2
Ligan 8	Orientanol B	-10,0
Ligan 9	Phaseollidin	-10,0
Ligan 10	Sigmoidin K	-10,0
Ligan 11	Eryvarin E	-9,9
Ligan 12	Orientanol F	-9,9
Ligan 13	Cristacarpin	-9,8
Ligan 14	Erycristagallin	-9,7
Ligan 15	Eryvarin D	-9,3

Tabel 2. Hasil Visualisasi *Docking* Jarak Ikatan dan Residu Asam Amino Antara Ligan Standar dan Ligan Tanaman terhadap Reseptor Plasminogen (4DUU) Menggunakan *Software PyMol*

Ligan	Jarak Ikatan Hidrogen (Å)	Residu Asam amino yang Berikatan	Gugus Fungsi yang Berikatan
Streptokinase	2,7	Val 72	-OH
	3,1	Val 72	-OH
	3,2	Gly 11	-OH
Folitenol	2,8	Met 69	-OH
	3,0	Trp 427	-OH
	3,0	Val 72	-O
	3,3	Val 72	-O
Orientanol C	2,9	Met 69	-OH
	3,1	Trp 427	-OH
	3,5	Gln 10	-OH
	3,3	Gly11	-OH
	3,1	Val 72	-OH

elektronegatif seperti Flour (F). Nitrogen (N). dan Oksigen (O) (Glowacki *et al*. 2013). Interaksi antara ligan standar yaitu streptokinase dengan protein plasminogen menunjukkan adanya ikatan hidrogen dari gugus –OH dengan Val72, Val72, dan Gly11. Untuk ligan kulit batang dadap ayam yang mempunyai afinitas lebih tinggi yaitu folitenol dan orientanol menunjukkan adanya ikatan hidrogen yang mirip dengan ligan standar yaitu folitenol (**Gambar 4**) berikatan dengan Val72, Val72, Met69, dan Trp427, sedangkan orientanol C (**Gambar 5**) berikatan dengan Gly11, Val72, Gln10, Met69, dan Trp427.

SIMPULAN

Senyawa turunan isoflavonoid yang tedapat pada kulit batang dadap ayam (*Erythrina variegata*) yaitu folitenol dan orientanol C menghasilkan nilai energi bebas -11.5 kkal/mol dan -11.4 kkal/mol lebih rendah dibandingkan dengan streptokinase sebagai ligan standar yaitu -8.4 kkal/mol. Sehingga dapat disimpulkan bahwa ligan folitenol dan orientanol C tersebut memiliki afinitas yang lebih baik dari streptokinase.

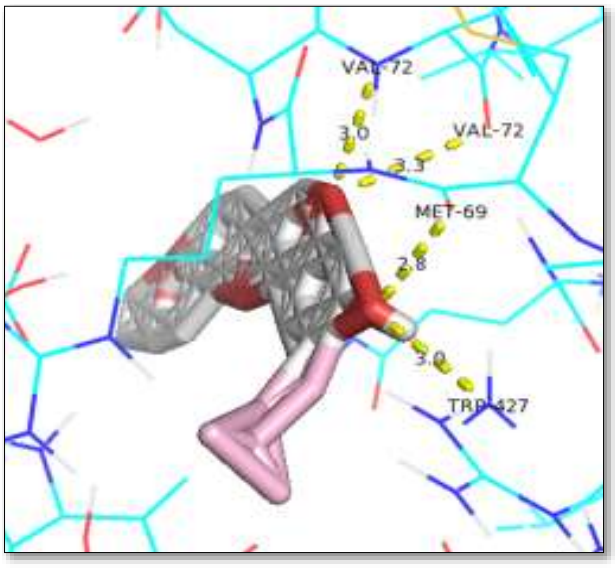

Gambar 4. Kontak Residu Ligan Folitenol dengan Reseptor 4DUU (*Software PyMol*). Ligan berwarna abu-abu-merah dan asam amino pada reseptor berwarna biru

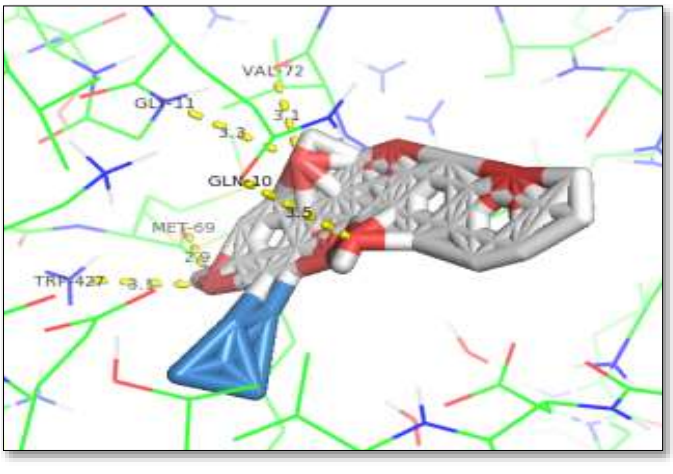

Gambar 5. Kontak Residu Ligan Orientanol C dengan Reseptor 4DUU (*Software PyMol*). Ligan berwarna abu-abu-merah dan asam amino pada reseptor berwarna hijau**.**

UCAPAN TERIMAKASIH

Penulis berterima kasih kepada Program Studi Farmasi, Fakultas Farmasi dan Sains UHAMKA yang telah mendukung penelitian ini mulai dari tahap awal penelitian hingga tahap publikasi.

DAFTAR PUSTAKA

Anies. 2015. *Kolestrol dan Penyakit Jantung Koroner*. Ar-Ruzz Media. Jogjakarta. Hlm. 55. 57-58. 105-108.

Aprilia, EA. 2021. Uji Kadar Fitokimia Daun Tumbuhan Dadap Ayam (Erythrina variegata L.) Yang Berpotensi Sebagai Obat. Skripsi thesis, Universitas Muhammadiyah Palembang.

Balamurugan G. Shantha A. 2010. Effect of *Erythrina variegata* Seed Extract on Hyperlipidemia Elicited by High-Fat Diet in Wistar Rats. *Journal of Pharmacy and Bioallied.* 2(4): 350-355.

Brooijmans N. 2009. Docking Methods. Ligand Design and Validating Data Sets in The Structural Genomics Era. Dalam: Gu J. Bourne PE (Eds). 2009. *Structural Bioinformatics*. New York. Hlm. 645-646.

Budiman F. Mulyadi. Lolong J. 2015. Faktor-Faktor yang Berhubungan dengan Tingkat Kecemasan pada Pasien Infark Miokard Akut di Ruangan CVCU RSUP Prof. Dr. R. D. Kandou Manado. *E-Journal Keperawatan*. 3(3): 1-7.

Drie JH. 2005. Pharmacophore-Based Virtual Screening: A Practical Perspective. Dalam: Alvarez J. Shoichet B (Eds). 2005. *Virtual Screening in Drug Doscovery*. CRC Press. Boca Raton. Hlm. 169.

Fletcher G. 2007. *Sindrom Koroner Akut-Farmakologis*. Terjemahan: Diana lyrawati.https://lyrawati.files.wordpress.com/2008/11/koroner-akutinfarkmiokard_obat_hosppharm.pdf. Diakses 26 Maret 2018

Glowacki ED. Vladu MI. Bauer S. 2013. Hydrogen Bonds in Molecular Solid from Biological Systems to Organic Electronics. *Journal of MaterialChemistry*. 1: 3742-3753.

Hambleton J. O'Reilly A. 2002. Obat-Obat yang Digunakan Pada Gangguan-Gangguan Pembekuan Darah. Dalam: Katzung BG. 2002. *Farmakologi Dasar dan Klinik Buku 2 Edisi 8.* Terjemahan: Bagian Farmakologi Fakultas Kedokteran Universitas Airlangga. Salemba Medika. Jakarta. Hlm. 403.

Herlina T. Syafruddin. Udin Z. 2012. Senyawa Aktif Antikanker Payudara dan Antimalaria dari Tumbuhan Dadap ayam (*Erythrina variegata*) Secara in Vitro. *Jurnal Manusia dan Lingkungan*. 19 (1): 30-36.

Law RHP. Caradoc-Davies T. Cowieson N. Norvath AJ. Encarnacao JA. Steer D. Cowan A. Zhang Q. Lu BGC. Pike RN. Smith AI. Coughlin PB. Whisstock JC. 2012. The X-ray Crystal Structure of Full-Length Human Plasminogen. *Cell Reports*. **1**: 185-190.

Majerus PW. Tollefsen DM. 2001. Obat-Obat Antikoagulan. Trombolitik. dan Antiplatelet. Dalam: Hardman JG. Limbird LE (Eds). 2001. Goodman and Gilman *Dasar Farmakologi Terapi Edisi 10 Vol 4*. Terjemahan: Tim Alih Bahasa Sekolah Farmasi ITB. Buku Kedokteran EGC. Jakarta. Hlm 1490. 1502-1503.

Miao M. MD. Zhang X. Wang L. 2013. Persimmon Leaf Flavonoid Induces Brain Ischemic Tolerance in Mice.*Neural Regeneration Research.* 8(28): 2625-2632.

Pebiansyah A. Purwanto. Priatna E. 2013. Sintesis Senyawa 3-(4-metilbenzoil)-1-Feniltiourea Sebagai Kandidat Antikanker (Studi Interaksi dan Toksisitas Secara *in Silico*). *Jurnal Penelitian Skripsi*. STIKes Bakti Tunas Husada. Tsikmalaya. Hlm. 8-9.

PERKI. 2018. Pedoman Tata Laksana Sindrom Koroner Akut. Edisi keempat. Indonesian Heart Association.

Simanjuntak GV. Simamora M. Sitorus HF. 2019. Perbandingan outcome pasien infark miokard akut dengan dan tanpa diabetes mellitus. Jurnal Kebidanan dan Keperawatan 'Aisyiyah'. 15 (2): 111-116

Tanaka H. Sato M. Fujiwara S. Hirata M. Etoh H. Takeuchi H. 2002. Antibacterial Activity of Isoflavonoids Isolated from *Erythrina variegata* Against Methicillin-Resistant *Staphylococcus aureus*. *Journal Microbiology*. 35: 494-498

Tjiphanata S. De Queljoe E. Sudewi S. 2017. Pengaruh Pemberian Ekstrak Etanol Daun Dadap Ayam (Erythrina variegata L.) Terhadap Kualitas Spermatozoa Tikus Putih Jantan Galur Wistar (Rattus norvegicus). PHARMACON Jurnal Ilmiah Farmasi. 6(3) : 91-98

Zehnder JL. 2012. Obat yang Digunakan Pada Gangguan Koagulasi. Dalam: Katzung BG. Masters SB. Trevor AJ (Eds). 2012. *Farmakologi Dasar dan Klinik Edisi 12 Vol 2.* Terjemahan: Pendit BU. Buku Kedokteran EGC. Jakarta. Hlm. 687.

UNIVERSITAS MUHAMMADIYAH PROF. DR. HAMKA
FAKULTAS FARMASI DAN SAINS
Jl. Limau II, Kebayoran Baru, Jakarta 12130 Tel. (021) 7208177, 722886, Fax. (021) 7261226, 7256620
Islamic Centre, Jl. Delima II/IV, Klender, Jakarta Timur Tlp.: (021) 8611070, Fax. (021) 86603233
Website: www.ffs-uhamka.ac.id; E-mail: ffs@uhamka.ac.id

SURAT TUGAS
MELAKUKAN KEGIATAN PENELITIAN DAN PUBLIKASI
NO. 809/F.03.08/2022

Bismillahirrohmanirrohiim,
Yang bertanda tangan di bawah ini

N a m a	**Dr. apt. Hadi Sunaryo, M.Si.**
NIDN	0325067201
Pangkat /Jabatan Akademik	Penata Tk. I, III/d / Lektor Kepala
Jabatan	Dekan
Unit Kerja	Fakultas Farmasi dan Sains UHAMKA Jakarta

Memberikan tugas Penelitian dan Publikasi pada **tahun akademik 2022/2023** kepada:

N a m a	**Dr. apt. Hariyanti, M.Si.**
NID/NIDN	D.03.0606/ 0311097705
Pangkat /Jabatan Akademik	Penata/ III-C
Jabatan Fungsional	LEKTOR
Unit Kerja	Fakultas Farmasi dan Sains UHAMKA Jakarta

Untuk Melaksanakan Penelitian dan Publikasi sebagai berikut:

NO	JUDUL PENELITIAN DAN PUBLIKASI
1.	**"Nanosuspension of Carica papaya L. Seed extract for anti-hyperlipidemic propyl lipids in hyperlipidemic hamsters"**

Demikian surat tugas ini diberikan kepada yang bersangkutan untuk dilaksanakan dengan penuh amanah dan tanggung jawab

Jakarta, 04 September 2022
Dekan,

Dr. apt. Hadi Sunaryo, M.Si., Apt.

Tembusan Yth:
1. Rektor UHAMKA Jakarta
2. Wakil Rektor I dan II UHAMKA Jakarta
3. Arsip

NANOSUSPENSION OF *CARICA PAPAYA* L. SEED EXTRACT FOR ANTI-HYPERLIPIDEMIC PROPYL LIPIDS IN HYPERLIPIDEMIC HAMSTERS

Hadi Sunaryo[a]*, Elly Wardani[b], Pramulani Mulya Lestari[c], Haryanti[d], Susilo[e]

Article History: **Received**: 26.07.2022 **Revised**: 25.08.2022 **Accepted**: 14.09.2022

Abstract: *Carica papaya* seeds contain flavonoid compounds, saponins, tannins, and anthocyanins that function as anti-hyperlipidemic. This study aims to determine the effect of giving nanosuspension *C. papaya* seed extract on reducing levels of total cholesterol, LDL-cholesterol, triglycerides, and an increase in HDL-cholesterol in hamster blood induced by high-fat feed. The animals carried out for testing were randomly divided into seven treatment groups, namely the standard group, the opposing group was only given high-fat flour, the positive group was assigned atorvastatin 2.42 mg/kg body weight, and three test groups were given consistent preparations of *C. papaya* seed extract at a dose of 2.4% each; 4,8%; 9.6% and the test group was assigned a trial of *C. papaya* seed extract of 240 mg/kg body weight. Activities the administration of test preparations is carried out for 14 days. Measurement of lipid propyl levels using a clinical spectrophotometer. Test data analysis using one-way ANOVA statistics. All doses of *C. papaya* seed extract nanosuspension preparations were significantly able to lower levels of total cholesterol, LDL-cholesterol, and triglycerides, and increase HDL-cholesterol ($p \leq 0.05$) compared to negative controls in hyperlipidemia hamsters. Dose 3 nanosuspension preparations (9.6%) were significantly able to lower levels of total cholesterol, LDL, and triglycerides and increase HDL-cholesterol levels ($p \leq 0.05$) compared to negative controls and were comparable to positive controls of atorvastatin ($p \geq 0.05$).

[a]. Department of Pharmacology, Faculty of Pharmacy and Sciences, Universitas Muhammadiyah Prof. Dr. HAMKA, Jl. Delima II/IV Klender, Jakarta, Indonesia 134602
[b]. Department of Pharmacology, Faculty of Pharmacy and Sciences, Universitas Muhammadiyah Prof. Dr. HAMKA, Jl. Delima II/IV Klender, Jakarta, Indonesia 134602
[c]. Department of Technology Pharmacy, Faculty of Pharmacy and Sciences, Universitas Muhammadiyah Prof. Dr. HAMKA, Jl. Delima II/IV Klender, Jakarta, Indonesia 134602
[d]. Department of Pharmaceutical Chemistry, Faculty of Pharmacy and Sciences, Universitas Muhammadiyah Prof. Dr. HAMKA, Jl. Delima II/IV Klender, Jakarta, Indonesia 134602
[e]. Department of Biology Education, Universitas Muhammadiyah Prof. Dr. HAMKA, Jl. Tanah Merdeka, Jakarta Timur, Indonesia

***Corresponding Author**

E-mail: hadi_sunaryo@uhamka.ac.id

DOI: 10.31838/ecb/2022.11.07.002

INTRODUCTION

Coronary Heart Disease (CHD) has become the leading cause of death in the world. One of the other risk factors for coronary heart disease is hyperlipidemia (Sulistyowati, 2009). Hyperlipidemia is a condition of excess fats (lipids) in the blood, including cholesterol and triglycerides. Hyperlipidemia, in general, is divided into two subcategories: hypercholesterolemia and hypertriglyceridemia (Harikumar et al., 2013).

Plants that can reduce hypertriglyceridemia include *C. papaya* seeds. *C. papaya* seeds have benefits where the compounds contained in *C. papaya* seeds, namely tannins, saponins, and flavonoids, have the potential as antioxidants (Zhou et al., 2011). The content of compounds found in *C. papaya* seeds includes fatty acids, crude protein, crude fiber, *C. papaya* oil, campaign, benzyl isothiocyanate, benzyl glucosinolate, glucotropacolin, benzylthiourea, caring hentriacontane, β-sitosterol, and the enzyme tyrosine (Yogiraj et al., 2014). Phytochemical analysis of *C. papaya* showed the presence of saponins, alkaloids, tannins, flavonoids, cardiac glycosides, anthraquinones, phlobatinins, anthocyanosides, and phenols (Srivastava & Singh, 2016). Previous studies have shown *C. papaya* seed water extract can lower glucose levels, lipid profiles, or total cholesterol and blood triglycerides in male rats of *Sprague Dawley* (Lusiana et al., 2011; Dawane et al., 2015). The same thing done by Nwangwa & Ekhoye (2013) showed that *C. papaya* seed water extract reduced blood lipid levels in albino rats. According to Inneh et al. (2019), the *C. papaya* seed extract has anti-hyperlipidemic and anti-atherogenic activity

The activity of medicinal plants depends on the release of biologically active compounds. Most of the extracts' active components cannot pass through the lipid membrane of the cells (Ajazuddin & Saraf, 2010). These constraints cause some excerpts not to be used clinically, so optimizing the preparation of natural materials with nanotechnology is necessary. The manufacture of nanostructured systems is

expected to strengthen the action of herbal extracts (Bailey & Berkland, 2009). Nanotechnology is an approach to producing particles in nano-size (Chingunpituk, 2007). The manufacture of extract nanoparticles is carried out with a ball mill tool. Milling is carried out inside the chamber with small balls rotating inside. The *C. papaya* seed extract is a viscous extract with Etonol as a solvent; milling is carried out with ethanol carriers. Particle size reduction of *C. papaya* seed extract with Ballmill tool. Particle size reduction results in particles measuring 410.4 nm. This study aims to determine the nanosuspension activity of ethanol extract of 70% *C. papaya* seeds against prolyl lipids of hamster hyperlipidemia.

RESEARCH METHODS

Seeds Extraction

Fresh *C. papaya* seeds are cleaned of adhering impurities and then washed with water. Soaked seeds are drained, then dried by oven at 60ºC to dry and carry out dry sorting. After drying, the simplicia is mashed using a pollinator until it becomes powder and then sifted with a sieve mesh number 40 weighed. After extraction by maceration, 500 g of *C. papaya* seed powder is put into the macerator, then 70% ethanol solvent is added. Separated macerate using filtration. Do the repetition three times. The Maserati obtained is concentrated using a vacuum rotary evaporator until a viscous extract is received, then evaporated in a water bath with a temperature of 50ºC until a thick section of Ethanol 70% *C. papaya* seeds is obtained.

Examination of Extract Characteristics

The examination of extract characteristics includes an organoleptic test examining the shape, color, smell, and taste of ethanol extract of 70% *C. papaya* seeds. The calculation of amendment is calculated by calculating the amount of section obtained divided by Simplicia powder and then multiplied by 100% (Departemen Kesehatan RI, 2000). Determination of water content using the toluene distillation method (Departemen Kesehatan RI, 2008). The decision of the total level of the calculation against the weight of the test material is expressed in % b / b. This phytochemical screening test was carried out to see the chemical content in the form of alkaloids, flavonoids, tannins, saponins, terpenoids, and steroids contained in the range of *C. papaya* seed extract (Hanani, 2015).

Manufacture of *C. papaya* Seed Extract Nanosuspension

The nanosuspension formula of the *C. papaya* seed extract can be seen in Table 1.

Table 1. Nanosuspension Manufacturing Formula

Ingredient Name	Formula I	Formula II	Formula III	Function
C. papaya seed extract	2,4	4,8	9,6	Active substances
HPMC	1	1	1	Viscosity increase
Tween 80	1	1	1	Surfactant
Nipagin	0,1	0,1	0,1	Preservatives
Na.metabisulfit	0,1	0,1	0,1	Antioksidants
Aquadest ad	100ml	100ml	100ml	Solvent

The manufacture of *C. papaya* seeds nanosuspension extract is carried out by Ready *C. papaya* seed extract, put into ball milling by wet milling method. Then, a nanoparticle of ethanol extract is formed, 70% *C. papaya* seed extract. HPMC is dispersed in hot water at a temperature of 70ºC until it expands. Nipagin is dissolved in hot water first until it becomes a solution. Sodium metabisulfite is dissolved first with water, then HPMC and nipagin solution, stirring until homogeneous. Put tween 80 as a surfactant, enter the *C. papaya* seed extract's nanoparticle results, then go until homogeneous After mixing all, justify the volume with equates until the limit mark (Iskandarsyah & Mutakim, 2010).
Evaluation of the physical properties and physical stability of the nanosuspension *C. papaya* seed extract was carried out for six weeks, including particle size, potential zeta, polydispersity index, particle morphology, viscosity, and acidity of the nanosuspension preparation to determine the character and stability of the nanosuspension particles.

Manufacture of High Cholesterol Feed

High-fat feed comprises 40% quail egg yolk, 10% white butter, and standard meal (hamster pellets) 50%. For the manufacture of high-fat feed, raw quail egg yolks are separated by the whites, then quail egg yolks are added with white butter that has been heated and mixed with hamster standard feed until dough is formed is made into pellets. Feed hamsters 80 g in 1 day about 10 g (Smith et al., 1995).

Test Animal Treatment

The treatment of test animals has received approval from the Ethics Committee for Health Research, Faculty of Medicine, University of Indonesia, No: KET-1257 / UN2. F1/ETIK/PPM.00.02/2019. This study was conducted experimentally with a complete randomized design, using 28 male *Syrian* hamsters divided into seven groups of 4 hamsters per group. The division of the group of hamsters is as follows:

a) Group 1: Normal control, given standard feed.
b) Group 2: Positive control, given high cholesterol feed and Atorvastatin 2,422 mg/kg body weight.
c) Group 3: Negative control, given high cholesterol feed and CMC Na.
d) Group 4: D introduction of *C. papaya* seed extract using a dose of 240mg/kg body weight.
e) Group 5: D introducing high-cholesterol feed and a 2.4% dose of extract nanosuspension preparations.
f) Group 6: Given high cholesterol feed and nanosuspension preparation, extract dose of 4.8%.
g) Group 7: Given high cholesterol feed and nanosuspension preparation, extract dose of 9.6%.

Blood Serum Collection

Hamster blood collection is carried out two times, namely on day 29 and day 43, through the orbital sinuses in each group of hamsters. Hamsters are treated using ketamine until unconscious. Previously male hamsters were satisfied first for 12 hours. Blood is put into the microtube and centrifuged for 5 minutes at a speed of 6000 rpm; blood serum will be obtained to check the total cholesterol levels, LDL, HDL, and Triglycerides (Vogel, 2008).

RESULTS AND DISCUSSION

Phytochemical screening is carried out in the thick extract of *C. papaya* seeds, including alkaloids, flavonoids, saponins, tannins, terpenoids, and steroids. The results of phytochemical screening can be seen in Table 2. The compounds in *C. papaya* seeds are tannins, saponins, and flavonoids that function as antioxidants. According to Ulyarti et al., (2017), flavonoids and tannins can be used as biopharmaceutical raw materials.

Table 2. Phytochemical screening results of ethanol extract 70% *C. papaya* seeds

No.	Types of Testing	Results
1.	Alkaloids	+
2.	Saponins	+
3.	Tannins	+
4.	Phenol	+
5.	Flavonoid	+
6.	Triterpenoid	+

+ = exists
- = none
Organoleptic tests and drying shrinkage are carried out to find out the characteristics of powders and extracts. Results can be seen in Table 3.

Table 3. The Characteristic Yield of 70% *C. papaya* Seeds Ethanol Extract

No.	Type	Organoleptic Test			
		Shape	Odor	Taste	Color
1.	Powder	Fine Powder	Distinctive	Bitter	Dark Brown
2.	Extract	Dry	Distinctive	Bitter	Dark Brown

Table 4. Test Results of Water and Ash Content of 70% *C. papaya* Seeds Ethanol Extract

No	Type	Result (%)
1.	Moisture Content	9,84
2.	Ash Content	17,54

***C. papaya* Seed Extract Nanosuspension**

The manufacture of extract nanosuspension is carried out with a ball mill tool. Milling is carried out in the chamber with a small ball rotating inside—particle size reduction results in particles measuring 410.4 nm (Gupta et al., 2012). Meanwhile, the particle test results on the nanosuspension have an average particle diameter size of 300.2 nm - 455.5 nm.

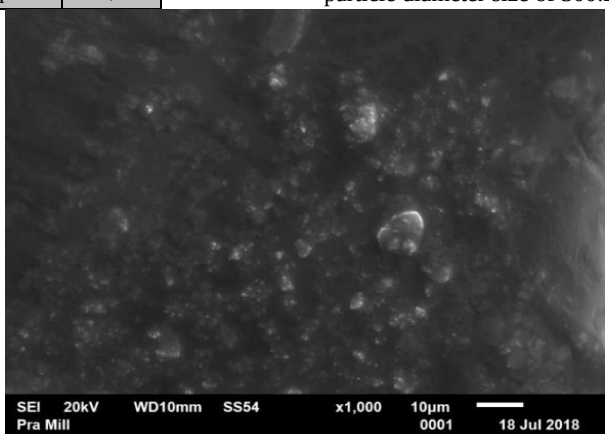

Figure 1. *C. papaya* Seed Extract Before Milling

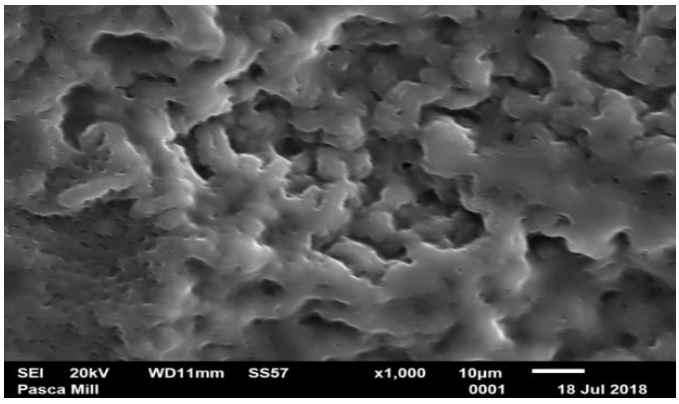

Figure 2. *C. papaya* Seed Extract After Milling

***C. papaya* Seed Extract Nanosuspension Preparations**

Nanosuspension is colloidal dispersions of drug particles in nano-size (Patravale et al., 2004). It can also be defined as a biphasic system consisting of pure drug particles dispersed in an aqueous polymer where the diameter of the suspended particles is less than 1μm in size. Consistency is prepared by mixing *C. papaya* seed extract nanoparticles with HPMC and Tween 80 as a stabilizer that reduces the system's free energy by lowering the interfacial voltage in the design. Besides that, this stabilizer can also prevent nanoparticle aggregation by electrostatic or steric stabilization. The large surface area of *C. papaya* seed extract due to the small particle size produces a high interfacial voltage that can increase the free energy in the system; this shows that the nanosuspension of *C. papaya* seed extract is unstable thermodynamically unstable.

Nanoparticles with a zeta potential of ± 30 mV can prevent aggregation between particles due to charges on the surface of the nanoparticles (Patel et al., 2016). In the formula, there is no potential value of zeta above the ± 30 mV; this means that the procedure can produce a weak repulsive force, as a result of which particles can merge to form aggregates that can precipitate.

The polydispersity index is a parameter that expresses the particle size distribution with values of 0.01 - 0.7 nanoparticles with a narrow distribution and more than 0.7 extensive size distribution (Nidhin et al., 2009). The smaller the value of its polydispersity index, the more homogeneous the particle size spread (Yuan et al., 2008). All formulas obtained a polydispersity index of 0.571, still in the 0.01 - 0.7. This indicates a relatively narrow or homogeneous particle size distribution. No change occurs during six weeks of storage at room temperature.

Viscosity also affects the stability of a suspension system. If the particle charge is negligible, then according to Stoke's law, the sedimentation rate is affected by the diameter and suspending agent. The larger the particle size, the higher the speed of sedimentation rate; on the contrary, the higher the viscosity, the smaller the sedimentation rate. However, if the viscosity is too high, it can cause caking, making the suspension difficult to redispersion (Priyambodo, 2007). The result of the viscosity inspection using the viscometer type first RM spindle no one formula viscosity is 250 rpm. Viscosity is the resistance of a liquid to flow; the higher the viscosity, the more excellent the opposition (Martin et al., 1993). The results of pH measurements in the three formulas carried out; there was no significant difference where the pH of the preparation ranged from 6.5 - 6.7, whereas the standard pH of the suspension, according to Kulshreshta et al. (2009), was between 5-7.

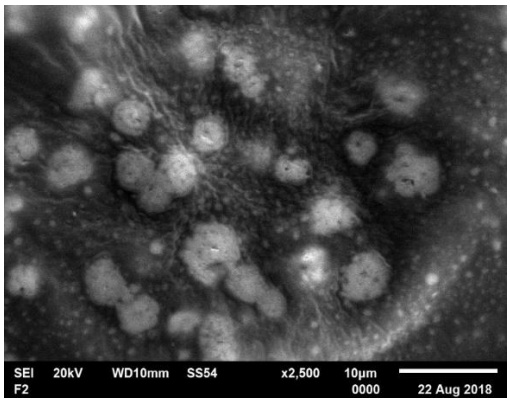

Figure 3. Morphology of Nanosuspension Particles of *C. papaya* Seed Catalysis

Particle surface can be observed using SEM (Scanning Electron Microscopy) with a magnification of 2,500 times; nanosuspension particles look spherical. The particle size in nanosuspension is the most critical parameter because it is responsible for physical stability. Nanosuspension may change the crystal structure, which may become amorphous or polymorphic due to high-pressure homogenization.

Hyperlipidemia Hamsters

The study used experimental animals of male Syrian hamsters of the same age and environmental conditions to avoid differences in biological activity. The hamster used is a healthy hamster with signs of clear eyes, clean fur, and regular and active behavior. The selection of hamster model animals is because hamsters have a lipoprotein profile that is more like humans than rats. Hamsters also have an atherogenic lipoprotein profile that can circulate into a non-HDL form and a cholesterol ester transport protein (CETP). This receptor mediates the uptake of LDL lipoproteins through LDL receptors that play a role in producing B-100 apolipoproteins (apo) in the liver and the production of Apo B in the intestine (Smith et al., 1995). Thus, hamsters develop hypercholesterolemia and hypertriglycerides faster when fed cholesterol-rich foods.

The standard feed used contains a moisture content of 13%, protein 21%, ash 7%, crude fat 7%, crude fiber 5%, calcium 0.90%, phosphorus 0.60%. The butter used is Anchor Pure New Zealand Unsalted Butter 10%, each serving (15 g) containing 7 g of saturated fat, 2.5 g of monounsaturated fat, 0.5 g of trans fat, and 30 mg of cholesterol. Butter is one of the saturated fatty acids derived from animal products that contain high fats and is a source of trans fats in the body that are harmful if consumed excessively. Trans fatty acids inhibit the activity of the enzyme Lecithin Cholesterol Acyl Transferase (LCAT), causing a decrease in cholesterol esterification accompanied by an increase in the transfer of cholesterol esters from HDL to LDL. This increases LDL cholesterol levels and decreases HDL cholesterol levels (Mozaffarian et al., 2006).

Total Cholesterol Levels

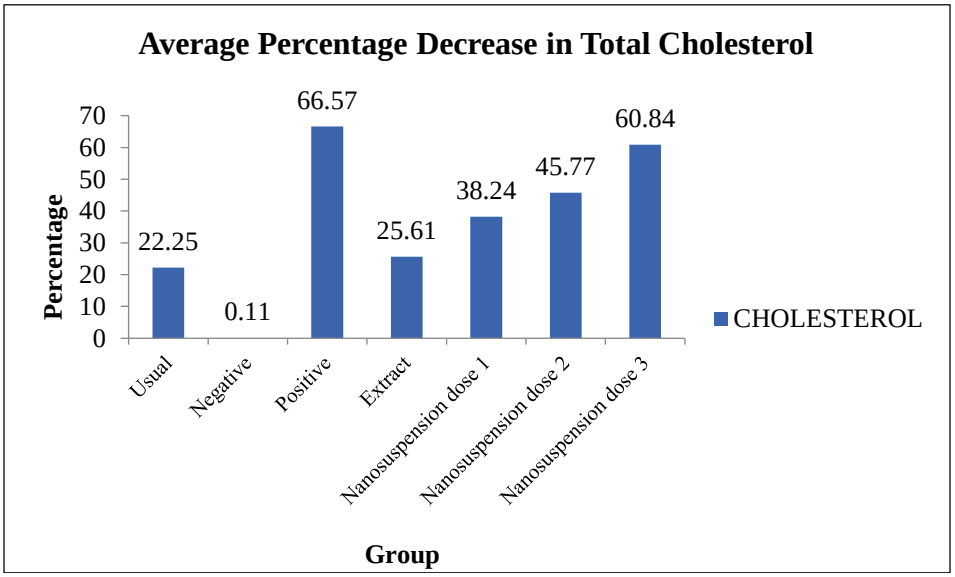

Figure 4. Average percentage decrease in total cholesterol levels

The data results on the percentage of hamsters' total cholesterol levels are entered into the statistics and tested for the normality of the data and their homogeneity. The statistical results show that the data on total cholesterol levels are distributed normally (p = 0.200) and homogeneously (p = 0.274). Then proceed with the analysis using a one-way ANOVA. From the results of the ANOVA table, the percentage of total cholesterol levels is processed p-value = 0.000 < 0.05. These results show that the provision of nanosubscribed *C. papaya* seed extract has a meaningful effect on hamster cholesterol levels. The data is then continued with the Tukey test. The Tukey test showed that the percentage decrease in total cholesterol levels was obtained by the nanosuspension group dose III (60.84%), which was comparable to the positive control (66.57%), and differed significantly from the nanosuspension group dose I (38.24%) and dose II (45.77%).

LDL-cholesterol levels

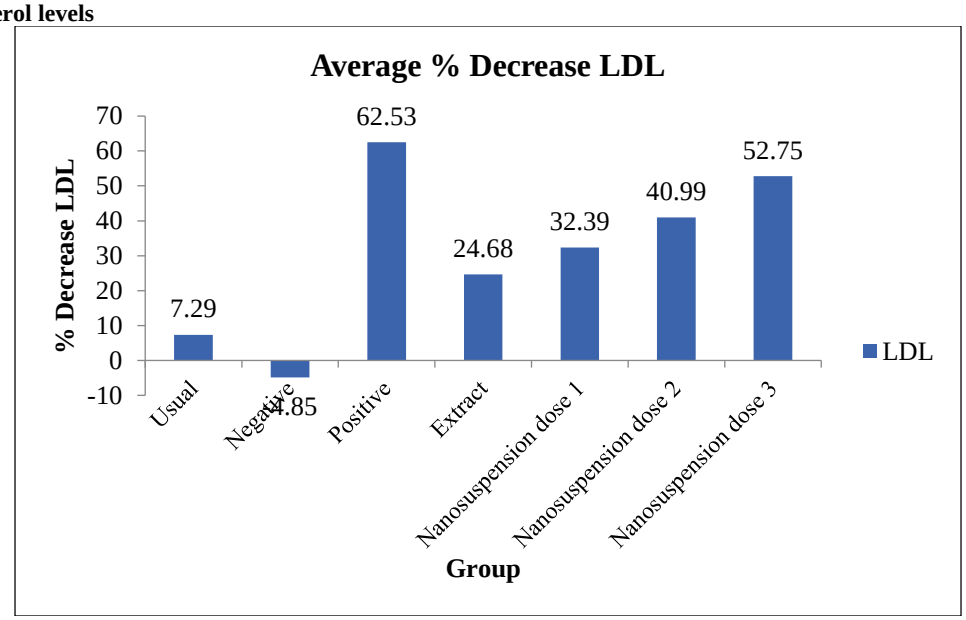

Figure 5. Average percentage decrease in LDL cholesterol levels

The average percentage decrease in LDL levels in figure 2 shows that the positive control group (62.53%) gave the most significant percentage decrease compared to other groups. The negative group showed a percentage decrease of -4.85%,

which means that the negative group experienced a continuous increase in LDL levels because the negative group was not given test preparations, only given high fat diet foods. The nanosuspension group at dose 3 (52.75%) gave the largest percentage reduction in LDL levels when compared to the nanosuspension group at doses 1, 2 and the extract group. This also shows that there is an increase in the decrease in LDL levels after being made into nanosuspension preparations when compared to extract preparations.

Data LDL levels were statistically tested, and the normality test results obtained Asymp values. Sig. (2-tailed) = 0.200>α (0.05), the data is normally distributed. The homogeneity test results obtained a Sig value of 0.293 > α (0.05) so that the data varied homogeneously, then continued with analysis using one-way ANOVA. The results of the ANOVA table against the percentage decrease in LDL levels obtained sig values. 0.000 < 0.05. This shows that there are significant differences between treatments. According to Legis (2017), Phenolic compounds in natural ingredients have been shown to have antioxidant effects and can inhibit the oxidation of LDL (Saputri et al., 2017). It can be concluded that the administration of test preparations influences the decrease in hamster LDL levels. Then the analysis continued with the Tukey test. For the Tukey test, the decrease in LDL levels data showed that the negative group differed significantly from the group given the test preparation and the normal group. It can be concluded that the dose three nanosuspension groups have an activity of lowering LDL levels equivalent to atorvastatin as a comparison substance. Phenol extract can also lower glucose, triglyceride, and LDL cholesterol levels and increase energy expenditure and oxidation of weight loss (Terra et al., 2009; Sari et al., 2021). Thus, the nanosuspension of ethanol extract of 70% *C. papaya* seeds dose III lowered LDL levels equivalent to the positive control, with a percentage of reducing LDL cholesterol levels by 52.75%.

Triglyceride Levels

Based on the statistical tests using SPSS, the normality test results obtained Asymp values. Sig. (2-tailed) = 0.054 > 0.05) so the data is distributed normally. The homogeneity test results obtained a Sig value of 0.173 > 0.05) so the data varied homogeneously, then continued with analysis using a one-way ANOVA. The Tukey test results showed a difference in the percentage of the significant decrease in triglyceride levels in the entire group of test preparations. A negative group obtained a Sig value of α < (0.05). This shows that nanosuspension preparations of the *C. papaya* seed extract can significantly reduce triglyceride levels against hamster hyperlipidemia induced by a high-fat diet.

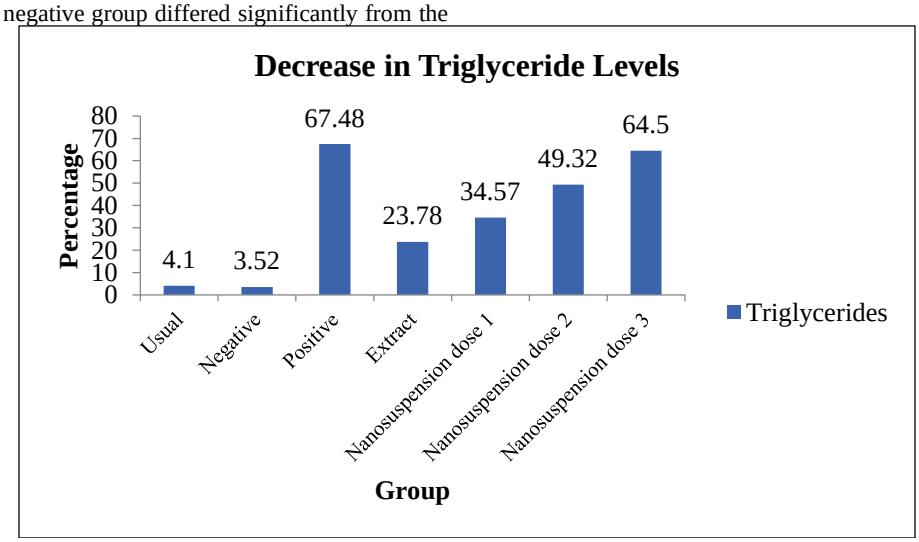

Figure 6. Average percentage decrease in Triglyceride levels

Based on the Tukey test, when compared to the negative group, there was also a significant decrease in the percentage of triglyceride levels in all groups except the normal group. The decrease in triglycerides is not very specific because there is also a decrease in triglyceride levels in the normal group. These results showed that the administration of nanosuspension preparations of *C. papaya* seed extract dose 3 had a meaningful effect on reducing hamster blood triglyceride levels because it was comparable to the positive control of atorvastatin. Based on figure 6, it can be seen that the percentage decrease in triglyceride levels increased in the nanosuspension preparation group of *C. papaya* seed extract of all dose variations (34.57%; 49.32%, and 64.50%) and the positive control group (67.48%) when compared with the negative group (3.52%) and the normal group (4.1%).

HDL-cholesterol levels

The average percentage increase in HDL levels was then carried out normality and homogeneity tests. Based on the data obtained from the results of the standard distribution test for HDL levels (α = 0.071), the homogeneity test (α = 0.233) shows that the distributed data is regular and homogeneous (α >0.05).

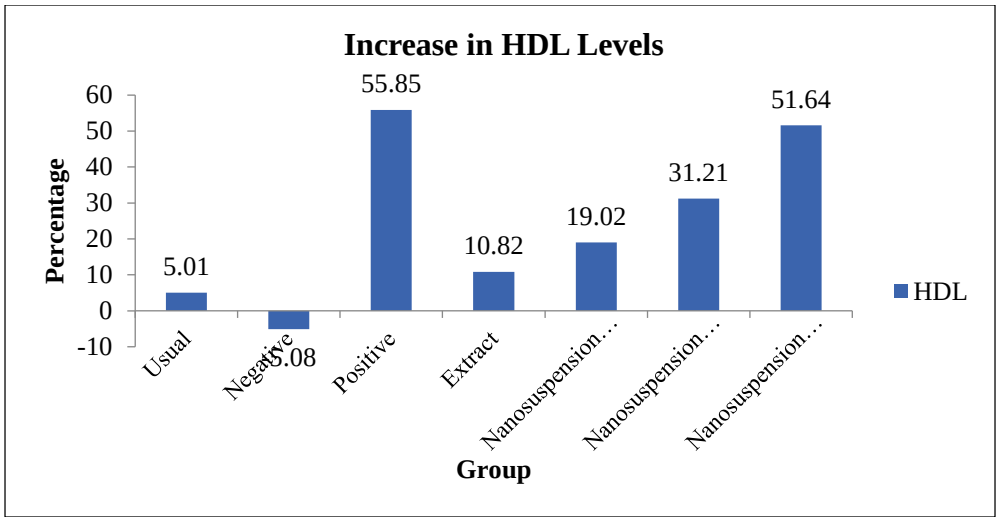

Figure 7. Average percentage increase in HDL cholesterol levels

Data on the percentage increase in HDL levels continued with a one-way ANOVA test with a significance level of 95% (α = 0.05) and obtained a Sig value. 0.000<0.05 indicates the effect of treatment or meaningful differences on the increase in HDL levels of each group. Based on the results of the Tukey test, there was a significant difference (<0.05) between the negative control group and the positive control; all extract preparations and nanosubscribed nanosuspension of doses 1, 2, and 3. There was a significant difference between nanosuspension doses 1, 2, and 3 indicating a difference in the activity of the three doses. In this case, the nanosubstitution group of dose three *C. papaya* seed extract had a movement of increasing HDL levels comparable to the positive control group. Figure 7 shows that the negative control group showed the smallest percent increase in HDL levels compared to the other group of -5.08%. The small percentage is due to the induction of high-fat feed but not given test preparations. N-standard control occurs due to physiological factors in hamsters who are not given test preparations or a low-fat diet.

All groups of test preparations showed different results with hostile control groups on reducing total cholesterol levels, LDL cholesterol, triglycerides, and increasing HDL cholesterol levels. *C. papaya* seeds have benefits where the compounds contained in *C. papaya* seeds, namely tannins, saponins, and flavonoids, have the potential as antioxidants (Zhou et al., 2011). Flavonoids are phenol compounds among the secondary metabolites in plants that function as antioxidants (Ningrum et al., 2021; Zuraida et al., 2017). Flavonoids are antioxidants that capture radicals and maintain a balance between oxidants and antioxidants in the body. Flavonoids can improve the endothelial function of blood vessels and are hypolipidemic, anti-inflammatory, and antioxidants. According to Sari et al. (2021), flavonoids can decrease the accumulation of lipids in the heart, reduce glucose absorption, and inhibit the breakdown of polysaccharides into monosaccharides. The high flavonoid content in *C. papaya* seeds can lower total liver cholesterol, blood triglycerides, and LDL cholesterol in hamster hypercholesterolemia. Antioxidant compounds in *C. papaya* seeds are thought to increase the secretion of bile acids to reduce levels of total cholesterol, triglycerides, and LDL cholesterol.

CONCLUSION

The nanosuspension of the *C. papaya* seed extract can be made through a suspension with the combined stabilizer formula of HPMC and Tween 80, which has the highest viscosity with the smallest particle size. All doses of nanosubstantial preparations of *C. papaya* seed extract were significantly able to lower levels of total cholesterol, triglycerides, LDL cholesterol, and increase HDL cholesterol compared to negative controls ($p \leq 0.05$) in hyperlipidemia hamsters. Nanosuspension preparation dose 3 (9.6 %) was significantly able to lower levels of total cholesterol, LDL cholesterol, and triglycerides and increase HDL cholesterol levels compared to the positive control of atorvastatin ($p \geq 0.05$).

ETHICAL APPROVAL

All experimental protocols were approved by the Ethics Committee for Health Research, Faculty of Medicine, University of Indonesia, No: KET-1257/UN2. F1/ETIK/PPM.00.02/2019 and were performed in accordance with ethical standards for the care and use of laboratory animals.

FUNDING

This study was funded by the Directorate of Research and Community Service, Directorate General of Research and Development Strengthening of the Indonesian Ministry of Research, Technology and Higher Education.

Conflict of interest: We declare this study no potential conflict of interest.

Informed consent: Informed consent was obtained from all participants included in the study.

AUTHOR CONTRIBUTIONS

All authors made substantial contributions to the conception and design, analysis, and interpretation of data, and critical review of the manuscript. HD conception and interpretation of the results, and wrote the manuscript. EW carried out the design of the study, performed the statistical analyses, and the revision of the manuscript. PML performed statistical analyses and helped rewrite the manuscript substantially during the revision process. HH was involved in drafting the manuscript. SS helped revise the manuscript. All authors have been involved in revising the manuscript critically for important intellectual content. All authors have read and agreed to the published version of the manuscript.

REFERENCES

i. Ajazuddin, & Saraf, S. (2010). Applications of novel drug delivery system for herbal formulations. *Fitoterapia*, *81*(7), 680–689. https://doi.org/10.1016/j.fitote.2010.05.001

ii. Bailey, M. M., & Berkland, C. J. (2009). Nanoparticle formulations in pulmonary drug delivery. *Med Res Rev*, *29*(2), 196–212. https://doi.org/10.1002/med.20140.

iii. Chingunpituk, J. (2007). Nanosuspension Technology for Drug Delivery. *Walailak Journal of Sci & Tech*, *4*(2), 139–153.

iv. Dawane, J. S., Pandit, V., Deshpande, S., & Kuvalekar, A. (2015). Evaluation of Anti-Diabetic Activity of Nishamlaki on Streptozotocin-Induced Type II Diabetic Rats. *International Journal of Phytomedicine*, *6*(4), 595–600. https://doi.org/10.5138/ijpm.v6i4.1545

v. Departemen Kesehatan RI. (2000). *Buku Panduan Teknologi Ekstrak*. Direktorat Jenderal Pengawasan Obat dan Makanan.

vi. Departemen Kesehatan RI. (2008). *Farmakope Herbal Indonesia Edisi 1*. Direktorat Jendral Badan Pengawasan Obat dan Makanan.

vii. Gupta, N., Mudgil, M., Nagpal, M., & Pawar, P. (2012). Nanotechnology: A New Approach For Ocular Drug Delivery System. *International Journal Of Pharmacy And Pharmaceutical Sciences*, *4*(2), 105–112.

viii. Hanani, E. (2015). *Analisis Fitokimia*. Buku Kedokteran EGC.

ix. Harikumar, K., Althaf, S. A., Kishore, B., Ramunaik, M., & Suvarna, C. H. (2013). A Review on Hyperlipidemic. *International Journal of Novel Trends in Pharmaceutical Sciences*, *3*(4), 59–70.

x. Inneh, C., Uhonmoibhi, S., & Oghenakhogie, M. (2019). Effect of Aqueous Seed Extract of Carica *C. papaya* on Lipid Profile and Anti-Atherogenic Index of Wistar Rat Following Cholesterol Administration. *The FABES Journal*, *33*(S1). https://doi.org/10.1096/fasebj.2019.33.1_supplement.522.10

xi. Iskandarsyah, & Mutakim, A. (2010). Preparasi dan Karakterisasi Nanosuspensi Dengan Polivinilpirolidon (PVP) sebagai Pembawa Nanopartikel senyawa Asam Mefenamat. *Majalah Ilmu Kefarmasian*, *7*(2).

xii. Kulshreshta, Singh, & Wall. (2009). *Pharmaceutical Suspensions From Formulation Development to Manufacturing*. Springer New York Dordrecht Heidelberg London.

xiii. Lusiana, K., Magatra, P., & Martono, Y. (2011). Ekstrak Limbah Biji Pepaya (Carica *C. papaya* Seeds) Anti Penyakit Jantung Koroner. *Prosiding Seminar Nasional Sains Dan Pendidikan Sains VII UKSW*, 194–198.

xiv. Martin, A., Swarbrick, J., & Cammarata, A. (1993). Farmasi Fisik: Dasar-dasar Farmasi Fisik dalam Ilmu Farmasetik. In *Edisi Ketiga. Penerjemah: Yoshita.* UI-Press.

xv. Mozaffarian, D., Katan, M. B., Ascherio, A., Stampfer, M. J., & Willett, W. C. (2006). Trans Fatty Acids and Cardiovascular Disease. In *New England Journal of in KK-Ay Diabetic Mice.* www.pubmed.gov.

xvi. Nidhin, M., Indumathy, R., Sreeram, K., & Nair, B., U. (2009). Synthesis of Iron Oxide Nanoparticles of Narrow Size Distribution on Polysaccharide Templates. Buletin. *Material Scence*, *31*(1), 93–96.

xvii. Ningrum, A. M., Christina, M., Putri, T. R., & Simamora, C. J. K. (2021). Probability Induction of Kratom Plant Bioactive Components in Antidiabetic and Antiobesity Studies. *Bioeduscience*, *5*(3), 234–240. https://doi.org/10.22236/j.bes/536900

xviii. Nwangwa, E. K., & Ekhoye, E. I. (2013). Anti-Hyperlipidemic Activity of Aqueous Extract of Carica *C. papaya* Seed in Albino Rats fed with High Fat Diet. *Current Trends in Technology and Sciences*, *2*(3), 262–266.

xix. Patel, M., Bhumi, B. P., & Chainesh. (2016). Nanosuspension: A Novel Approach to Enhance Solubility of Poorly Water-Soluble Drugs - A review. *International Journal of Advances in Pharmaceutics*, *5*(2), 21–29.

xx. Patravale, V. B., Date, A. A., & Kulkarni, R. M. (2004). Nanosuspensions: a promising drug delivery strategy. *J Pharm Pharmacol*, *56*(7), 827–840. https://doi.org/10.1211/0022357023691

xxi. Priyambodo, B. (2007). *Manajemen Farmasi Industri*. Global Pustaka Utama.

xxii. Saputri, L. O., Satriyasa, B. K., & Yasa, W. P. S. (2017). Ekstrak Air Biji Pepaya (Carica *C. papaya*) dapat Menurunkan Kadar Kolesterol Total dan Kadar Serumglutamat Piruvat Transaminase (SGPT) pada Tikus Putih Jantan Galur Wistar yang Hiperkolesterolemia. *Warmadewa Medical Journal*, *2*(1). https://doi.org/10.22225/WMJ.2.1.73.1-10

xxiii. Sari, D. R., Afra, A., Sembiring, E. Y. F. S. B., & Simamora, C. J. K. (2021). Fat-Rich Food Review on Obesity Control through Induction Enzyme Inhibitors. *Bioeduscience*, *5*(3), 211–217. https://doi.org/10.22236/j.bes/526211

xxiv. Smith, D. E., Osqood, D. P., & Lichtenstein, A. H. (1995). The Effect of Fasting on Plasma Lipids in an Animal Model for The Study of Diet-Induced Atherosclerosis (The FIB Golden Syrian Hamster). Canadian Assoc. *Canadian Assoc: Lab Animal Svi*, *30*, 78–79.

xxv. Srivastava, A. K., & Singh, V. K. (2016). Carica *C. papaya*- A Herbal Medicine. *International Journal of Research Studies in Biosciences*, *4*(11), 19–25. https://doi.org/10.20431/2349-0365.0411004

xxvi. Sulistyowati, T. (2009). Role of HDL-Cholesterol on Cardiovascular Disease and Diabetes Mellitus. *Gizi Indonesia*, *32*(1), 69–76. https://doi.org/10.36457/gizindo.v32i1.70

xxvii. Terra, X., Montagut, G., Bustos, M., Llopiz, N., Ardèvol, A., Bladé, C., Fernández-Larrea, J., Pujadas, G., Salvadó, J., Arola, L., & Blay, M. (2009). Grape-seed procyanidins prevent low-grade inflammation by modulating cytokine expression in rats fed a high-fat diet. *The Journal of Nutritional Biochemistry*, *20*(3), 210–218. https://doi.org/10.1016/J.JNUTBIO.2008.02.005

xxviii. Ulyarti, Nazarudin, & Sari, D. W. (2017). The study of functional properties of Nypa fruticans flour. *AIP Conference Proceedings*, *1823*(March). https://doi.org/10.1063/1.4978100

xxix. Vogel, H. G. (2008). *Drug Discovery and Evaluation Pharmacological*. Springer.

xxx. Yogiraj, V., Goyal, P. K., Chauhan, C. S., Goyal, A., & Vyas, B. (2014). Carica *C. papaya* Linn: An Overview. *International Journal of Herbal Medicine*, *2*(5A), 1–8.

xxxi. Yuan, Y., Gao, Y., Zhao, J., & Mao, L. (2008). Characterization And Stability Evaluation of B-Carotene Nanoemulsions Prepared by High-Pressure Homogenization Under Various Emulsifying Conditions. *Food Research International*, *41*(1), 61–68. https://doi.org/10.1016/j.foodres.2007.09.006

xxxii. Zhou, K., Wang, H., Mei, W., Li, X., Luo, Y., & Dai, H. (2011). Antioxidant activity of *C. papaya* seed extracts. *Molecules*, *16*(8), 6179–6192. https://doi.org/10.3390/molecules16086179

xxxiii. Zuraida, Z., Sulistiyani, S., Sajuthi, D., & Suparto, I. H. (2017). Fenol, Flavonoid, dan Aktivitas Antioksidan pada Ekstrak Kulit Batang Pulai (Alstonia scholaris R.Br). *Jurnal Penelitian Hasil Hutan*, *35*(3), 211–219. https://doi.org/10.20886/jphh.2017.35.3.211-219

UNIVERSITAS MUHAMMADIYAH PROF. DR. HAMKA
FAKULTAS FARMASI DAN SAINS
Jl. Limau II, Kebayoran Baru, Jakarta 12130 Tel. (021) 7208177, 722886, Fax. (021) 7261226, 7256620
Islamic Centre, Jl. Delima II/IV, Klender, Jakarta Timur Tlp.: (021) 8611070, Fax. (021) 86603233
Website: www.ffs-uhamka.ac.id; E-mail: ffs@uhamka.ac.id

SURAT TUGAS
MELAKUKAN KEGIATAN PENELITIAN DAN PUBLIKASI
NO. 810/F.03.08/2022

Bismillahirrohmanirrohiim,
Yang bertanda tangan di bawah ini

N a m a	**Dr. apt. Hadi Sunaryo, M.Si.**
NIDN	0325067201
Pangkat /Jabatan Akademik	Penata Tk. I, III/d / Lektor Kepala
Jabatan	Dekan
Unit Kerja	Fakultas Farmasi dan Sains UHAMKA Jakarta

Memberikan tugas Penelitian dan Publikasi pada **tahun akademik 2022/2023** kepada:

N a m a	**Dr. apt. Hariyanti, M.Si.**
NID/NIDN	D.03.0606/ 0311097705
Pangkat /Jabatan Akademik	Penata/ III-C
Jabatan Fungsional	LEKTOR
Unit Kerja	Fakultas Farmasi dan Sains UHAMKA Jakarta

Untuk Melaksanakan Penelitian dan Publikasi sebagai berikut:

NO	JUDUL PENELITIAN DAN PUBLIKASI
1.	**"Bioassay guided isolation of artoindonesianin C with antidiabetic activity from Artocarpus elasticus Reinw. ex. Blume bark"**

Demikian surat tugas ini diberikan kepada yang bersangkutan untuk dilaksanakan dengan penuh amanah dan tanggung jawab

Jakarta, 04 September 2022
Dekan,

Dr. apt. Hadi Sunaryo, M.Si., Apt.

Tembusan Yth:
1. Rektor UHAMKA Jakarta
2. Wakil Rektor I dan II UHAMKA Jakarta
3. Arsip

Bioassay guided isolation of artoindonesianin C with antidiabetic activity from *Artocarpus elasticus* Reinw. ex. Blume bark

Cite as: AIP Conference Proceedings **2493**, 070025 (2022); https://doi.org/10.1063/5.0110147
Published Online: 05 December 2022

Sofa Fajriah, Hariyanti, Angie Elviani, et al.

Bioassay Guided Isolation of Artoindonesianin C with Antidiabetic Activity from *Artocarpus elasticus* Reinw. Ex. Blume Bark

Sofa Fajriah[1,a)], Hariyanti[2], Angie Elviani[2], Mariyana Sanusi[2], and Megawati[1]

[1]*Research Center for Chemistry, National Research and Innovation Agency Republic of Indonesia Kawasan PUSPIPTEK Serpong, Kota Tangerang Selatan, Banten, Indonesia.*

[2]*Faculty of Pharmacy and Sciences, University of Muhammadiyah Prof. DR. HAMKA Jl. Limau II, Kebayoran Baru, Jakarta Selatan, Jakarta, Indonesia*

[a)]Corresponding author: sofafajriah@gmail.com; sofa002@lipi.go.id

Abstract. *Artocarpus elasticus* Reinw. ex Blume is a member of the Moraceae tribe, which contains prenylated phenolic compounds, especially flavonoids with different structural variations such as flavanones, flavones, xanthones, chalcone, and stilbene. This research aims to isolate, identify, and evaluate their antidiabetic activity from *A. elasticus* Reinw. ex Blume bark. The research method consisted of isolation by column chromatography based on bioassay-guided fractionation, characterization of isolate using UV-Vis, FTIR, LC-MS, and NMR spectroscopy and *in vitro* antidiabetic activity assay against α-glucosidase enzyme. This study obtained artoindonesianin C with the molecular formula of $C_{26}H_{22}O_8$. Antidiabetic activity against α- glucosidase inhibitor showed significant activity with IC_{50} value of 31.88 µg/mL.

Keywords: *Artocarpus elasticus Reinw.* ex Blume, antidiabetic activity, artoindonesianin C, α-glucosidase enzyme

INTRODUCTION

Diabetes mellitus (DM) is a metabolic disorder characterized by hyperglycemia associated with abnormalities of carbohydrate, fat, and protein metabolism caused by decreased insulin secretion or decreased insulin sensitivity, or both and causes chronic and neuropathic complications [1]. The cause of diabetes mellitus is a lack of insulin, which functions to allow glucose to enter cells to be metabolized (burned) and thus utilized as an energy source. As a result, glucose builds up in the blood (hyperglycemia) and is eventually excreted in the urine without being used (glycosuria). Another cause is the decreased sensitivity of cell receptors to insulin (insulin resistance) caused by overeating and obesity [2].

Recently, some herbal medicines have been useful to treat diabetes and have been used empirically as antidiabetic remedies. One of the plant families known to have many benefits is Moraceae, a fairly large plant family consisting of 1180 species and 38 genera [3]. One of the genera belonging to the family Moraceae is Artocarpus. This plant is widely distributed throughout the archipelago, and several species are endemic to South Sulawesi. Artocarpus contains prenylated phenolic compounds, especially flavonoids with various structural variations such as flavanones, flavones, xanthones, chalcones, and stilbenes. The prenyl group on the flavonoid is in the C-3 position and the oxygenated B ring at the C-4' or C-2', C-4' or C-2', C-4', C-5' position. In addition, prenylation can also occur at positions C-6, C-8, and C3' [4,5,6]. *A. elasticus* also has a unique structure of flavonoids and produces broad physiological effects such as artonin E, artobiloxanthone, cycloartobiloxanthone, artoindonesian W, artoindonesianin P, and artoflavone B as α-glucosidase inhibitors [7, 8]. Therefore, the purpose of this study was to isolate α-glucosidase inhibitory compounds

Proceedings of the 7th International Symposium on Applied Chemistry 2021
AIP Conf. Proc. 2493, 070025-1–070025-6; https://doi.org/10.1063/5.0110147
Published by AIP Publishing. 978-0-7354-4265-8/$30.00

from *A. elasticus* barks using bioassay-guided fractionation techniques and identify the isolate using spectroscopic methods.

MATERIALS AND METHODS

Materials

General

UV/Vis analysis was recorded on Agilent Technology, Cary 60, and FTIR spectrum was measured with Shimadzu-Prestige 21. 1D and 2D NMR spectra were recorded with JEOL ECZR500 operating at 500 MHz using $CDCl_3$ as a solvent. Molecular weight was obtained from LCMS data with ESI system (Mariner Biospectrometry). Column chromatography was performed on silica (60-230 mesh, Merck) and sephadex LH-20 (Sigma Aldrich). Preparative TLC and TLC was analysis on GF_{254} plates (Merck). α-Glucosidase was obtained from yeast *Saccharomyces cerevisiae* (EC 3.2.1.20).

Plant material

The barks of *Artocarpus elasticus were* collected from Mekongga Forest, South East Sulawesi, Indonesia and identified by a botanist from Research Center for Biology LIPI. A voucher specimen was deposited in the herbarium with voucher specimen UHA46.

Methods

Extraction and Fractionation

The dried bark of *A. elasticus* was extracted by maceration. A portion of 800 grams powder was macerated with methanol solvent with ratio 1: 3 (simplicia : solvent) for 3 x 24 hours. The combined methanol extracts were evaporated to dryness with a rotary evaporator at a temperature of 40-50°C to give methanol extract (47.67 g). Furthermore, about 30 grams methanol extracts were fractionated by solvent extraction method in a ratio of 1:1 using a separating funnel with n-hexane, ethyl acetate and n-butanol for 3 times, then each fraction was evaporated under reduce pressure to yield n-hexane (7.57 g), ethyl acetate (9.72 g), *n*-butanol (3.01 g) and residue (water, 3.04 g) fractions.

Isolation and Purification

The amount of 7 grams ethyl acetate fraction (the active fraction) was further purified using VLC (Vacuum Liquid Chromatography) with gradient elution (*n*-hexane-ethyl acetate-methanol) to obtain nine main fractions. Fraction 4 was subjected to a silica gel (Kieselgel 60, 60-230 mesh) column chromatography eluted with gradient elution (*n*-hexane-ethyl acetate-methanol) to afford nine sub-fractions (SF1-SF9). Sub-fraction SF5 further was purified using sephadex LH-20 eluted with dichloromethane-methanol (1:1) to give 8 sub-fractions ($SF_{5.1}$ – $SF_{5.8}$). Furthermore, $SF_{5.5}$ was purified using preparative TLC with *n*-hexane:ethyl acetate (9:1) as mobile phase to afford a pure compound **1** (8 mg). Compound **1** was characterized with UV/Vis, FTIR, LCMS and FT-NMR spectrometers, and its α-glucosidase inhibitory activity assay was examined.

α-Glucosidase Inhibitory Activity Assay

The α-glucosidase inhibitory activity assay was evaluated according to the previous method with minor modifications [9, 10]. A total of 5 µL sample dissolved in DMSO at various concentrations was added with 495 µL of phosphate buffer pH 7.0 and p-nitrophenyl-α-D-glucopyranoside (PNPG) solution of 5 mM as much as 250 µL, then incubated for 5 minutes at 37°C. The reaction was started by adding 250 µL of enzyme solution to the sample, followed by incubation for 15 minutes at 37°C. After the incubation period was completed, the reaction was stopped by adding 1000 µL Na_2CO_3. The absorbance of the sample was measured using a UV-Vis spectrophotometer at a

wavelength of 400 nm. Furthermore, blanks were prepared to correct background absorbance where the enzyme was replaced with 250 µL of phosphate buffer. The percent inhibition of α-glucosidase inhibitory activity was calculated using the following formula: % Inhibition= (A - B)/A x 100, where A was the absorbance of the control reaction and B was the absorbance in the presence of the sample. The value of IC_{50} was calculated from the main inhibitory values by applying linear regression analysis. Quercetin and α-mangostin were used as reference standard.

RESULTS AND DISCUSSION

The extraction process of the dried barks of *A. elasticus* yielded 5.96% of methanol extract. This extract exhibited high activity as an α-glucosidase inhibitor with IC_{50} 1.95 µg/mL. Furthermore, the fractionation process of methanol extract yielded 25.25% of *n*-hexane fraction, 32.41% of ethyl acetate fraction, 10.05% *n*-butanol fraction, and 13.12% residue (water) fraction. These fractions were further assayed their α-glucosidase inhibitory activity, and all had a strong activity with IC_{50} 8.67, 8.67, 1.24, 9.30 µg/mL with quercetin as the positive control (IC_{50} 9.30 µg/mL). Further studies were conducted on ethyl acetate fraction. This fraction was purified using a gravity chromatography column with silica gel 60 GF_{254} as the stationary phase with gradient elution using solvents with different polarities ranging from 100% non-polar solvents to 100% polar solvents (*n*-hexane, ethyl acetate, and methanol). All subfractions obtained were identified by Thin Layer Chromatography (TLC), and the spots were observed under UV light at λ 254 nm and 365 nm afforded nine sub-fractions (SF1-SF9). These subfractions were analyses for their α-glucosidase inhibitory activity shown in Table 1. Since SF5 showed the highest activity, it was selected for the next purification process. This subfraction further was subjected to Sephadex LH-20 column chromatography and by Preparative Thin Layer Chromatography and obtained the active compound **1** as a yellow powder (8 mg). The structure of **1** was determined by using UV-Vis spectrophotometry, FTIR, LC-MS, and NMR.

TABLE 1. α-Glucosidase Inhibitory Activity of extracts, fractions, and subfractions from *A. elasticus* barks

Sample	IC_{50} (µg/mL)	Sample	IC_{50} (µg/mL)	Sample	IC_{50} (µg/mL)
Quercetin (positive control)	9.30	Residue (water) fraction	9.30	SF5	1.38
Methanol Extract	1.95	SF1	132.95	SF6	1.42
n-hexane fraction	8.67	SF2	11.47	SF7	4.10
Ethyl acetate fraction	8.67	SF3	8.85	SF8	8.74
n-butanol fraction	1.24	SF4	1.39	SF9	8.08

The UV-Vis spectrophotometry analysis of compound **1** showed two absorption bands at the maximum wavelength (λmax) of 265 nm and 395 nm, and it was characteristic for xanthone derivative [11]. The FTIR spectrum also showed typical of hydroxyl, aliphatic, carbonyl and benzene groups at absorption λ 3437, 2862, 1641 and 1458 nm, respectively. The ESI-MS data showed that compound **1** has molecular weight *m/z* 462.47 with a molecular formula of $C_{26}H_{22}O_8$.

Based on ^{1}H-NMR data ($CDCl_3$, 500 MHz), it showed the presence of an intramolecular hydroxyl group (OH) at chemical shift δ_H 12.60 ppm (1H, s, OH-1). A 2,2-dimethylchromene was shown with the presence of two methyl groups at chemical shift δ_H 1.50 and 1.49 (6H, s, Me-14 and Me-15) and two olefinic protons at δ_H 7.04 (1H, d, J= 10 Hz, H-11) and 5.70 (1H, d, J = 10 Hz, H -12). Isoprenyl group was showed with the presence of methyl group at δ_H 2.13 (3H, s, Me-20) and a terminal methylene protons at δ_H 4.86 & 5.28 (2H, s, H-21). Sharp singlets at δ_H 6.31 (1H, s, H-2), and 8.26 ppm (1H, s, H-8) indicated two aromatic protons in ring B and D. Signals of a hydroxyl group also showed at δ_H 7.06 (1H, s, OH-18), an isolated methylene group at δ_H 4.86 and 5.28 (2H, s, H-21). A methoxy group was showed at δ_H 3.74 (3H, s, - OCH_3), 7.04 (1H, d, J= 10 Hz, H-11) $\delta_{H\,7}$ one singlet proton at the H-8 position with a chemical shift of H 8.26 one singlet proton at the hydroxyl position (-OH) with a chemical shift of 7.06 (1H, s, OH-18), one singlet protons at position H-2 with a shift of 6.31 two singlet protons at position H-21 with a chemical shift of 4.86 and 5.28 (2H, s, H-21), three singlet protons at the methoxy position with a chemical shift of 3.74 (3H, s, 23-OCH_3).

The ^{13}C-NMR ($CDCl_3$, 125 MHz) of compound **1** contained 26 carbons, consists of 4 methyl (-CH_3), 4 methine (-CH), 2 methylene (-CH_2), 13 quaternary carbons and 3 carbonyl (C=O). The methyl groups consist of a typical methoxy group (O-CH_3) at a chemical shift δ_C 52.1 ppm, methyl sp3 at δ_C 25.4 ppm (C-20) and methyl at C-14 and C-15 with δ_C C 28.7 ppm. The methylene groups (-CH_2) were presented at δ_C 54.0 (C-17) and δ_C 117.7 ppm (C-21).

The methine (-CH) group were showed in δ_C 100.1 (C-2), 132.9 (C-8), 115.0 (C-11), and 128.1 (C -12). Quaternary carbons showed at δ_C 161.8 (C-1), 160.0 (C-3), 100.2 (C-4), 150.9 (C-4a), 125.6 (C-5), C 156.7 (C-6), 141.9 (C-7), 121.9 (C-8a), 104.1 (C-9a) , 151.4 (C-10a), 79.1 (C-13), 76.9 (C-18), and 138.1 ppm (C-19). The carbonyl groups (C=O) showed at δ_C 179.4 ppm (C-9), C 197.0 ppm (C-16) and C 174.5 ppm (C-22).

TABLE 2. ^{1}H, ^{13}C, HMQC and HMBC data of compound **1**

Position	HMQC	Artoindonesianin C [11]		HMBC
	δ_H (ppm, multiplisitas, J(Hz))	δc (ppm)	δc (ppm)	δc (ppm)
1	-	161.8	162.1	
2	6.31 (*s*)	100.1	99.1	C-9a
3		160.0	160.6	
4		100.2	101.1	
4a		150.9	150.9	
5		125.6	124.3	
6		156.7	158.6	
7		141.9	141.0	
8	8.26 (*s*)	132.9	131.3	C-6, C-9, C-10a
8a		121.9	120.7	
9		179.4	178.9	
9a		104.1	103..5	
10a		151.4	150.1	
11	7.04 (*d*, *J* = 10)	115.0	113.8	C-13
12	5.70 (*d*, *J* = 10)	128.1	128.4	C-2
13		79.1	78.9	
14	1.50 (*s*)	28.7	28.0	-
15	1.49 (*s*)	28.7	28.0	-
16		197.0	198.0	
17	3.20 (*d*, *J* = 18)	54.0	52.6	C-16, C-18
18	7.06 (*s*)	76.9	76.3	-
19		138.1	137.6	
20	2.13 (*s*)	25.4	24.5	C-8, C-19, C-21
21	4.86 (*s*); 5,28 (*s*)	117.7	117.5	C-19, C-20
22		174.5	172.6	
23	3.74 (*s*)	52.1	52.4	174.5

Two-dimensional NMR analysis was performed with HMQC and HMBC. The HMQC spectrum showed a direct correlation between protons and carbon ($^{1}J_{C,H}$). HMQC data showed a chemical shift at δ_H 8.26 ppm correlated with carbon at δ_C 132.9 ppm, δ_H 7.10 ppm to carbon at δ_C 115.0 ppm, δ_H 5.70 ppm to carbon at δ_C 128.1 ppm, δ_H 1.26 ppm to carbon at δ_C 28.7 ppm, δ_H 3.20 ppm to carbon at δ_C 52.1 ppm, δ_H 7.08 ppm to carbon at δ_C 76.9 ppm, δ_H 2.13 ppm to carbon at δ_C 25.4 ppm and δ_H 4.86 ppm for carbon at δ_C 117.7 ppm. HMQC correlation can be seen in Table 2.

The HMBC spectrum showed an indirect correlation between proton and nearby carbon with a distance of two to three bonds ($^{2,3}J_{CH}$). HMBC data showed that the methyl groups on Me-14 and Me-15 correlate with the quaternary carbons C-7 and C-19 and with the C-21 methylene group. The methoxy group (O-CH_3) at C-23 has a correlation with

the carbonyl group (C=O) at C-22. The H-8 position correlates with the carbonyl (C=O) at C-9 and two quaternary carbons at C-6 and C-10a. The H-21 position correlates with the methine group at C-8 and the methyl group at C-20. The methylene group at position H-17 has a correlation with the carbonyl group (C=O) at C-16 and the alcohol (C-OH) and ester (R-CO_2) groups at C-18. At the H-12 position has a correlation with methyl at C-14 and C-15 and quaternary carbon at C-4. The H-11 position correlates with the oxygenated quaternary carbon at the C-13 position. Besides, the H-2 position correlated with C-9a. HMBC correlation can be seen in Figure 1.

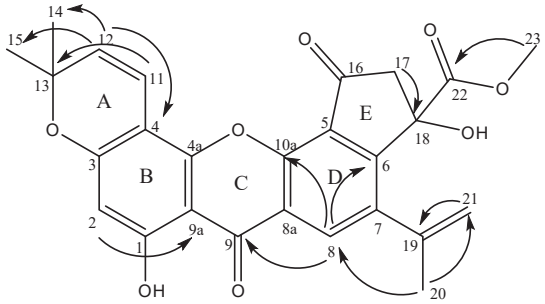

FIGURE 1. HMBC correlation of compound **1**

Based on the results of the analysis of ^{1}H-NMR, ^{13}C-NMR, HMQC and HMBC data as well as UV-VIS, FTIR and LC-MS spectrometer and supported with literature [11] it was concluded that compound **1** is a xanthone derivative, Artoindonesianin C. This compound was first report in *A. elasticus* and found in the species *A. teysmanii* Miq [11].

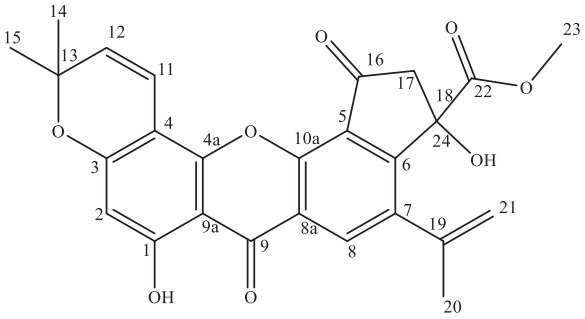

FIGURE 2. Artoindonesianin C isolated from *A. elasticus* barks.

The antidiabetic activity of artoindonesianin C was evaluated using α-glucosidase from the yeast *S. cerevisiae*. α-Glucosidase inhibitors might reduce a blood sugar level and lead to suppressed postprandial hyperglycaemia responsible for diabetes [7]. In this study, α-mangostin (IC_{50} 14.55 µg/mL) was used as positive control because it is a xanthone group and known to have α-glucosidase inhibitor activity [12]. The results showed that artoindonesianin C have potential to inhibit α-glucosidase enzyme with IC_{50} 31.88 µg/mL. The activity decreased compared to SF-5 since there was a synergistic activity between the compounds in the fraction level, therefore artoindonesianin C which is a pure compound has a lower ability to inhibit α-glucosidase enzyme.

CONCLUSIONS

The present study revealed that artoindonesianin C has been successfully isolated from *A. elasticus* barks and potential to be developed as an antidiabetic agent. Besides, the extracts and fractions from *A. elasticus* also have potential source as herbal medicine for antidiabetic type 2 remedies [7].

ACKNOWLEDGEMENT

This work was supported by a grant from LIPI. Authors were grateful thanks to Ms. Puspa Dewi N. Lotulung for measuring MS spectroscopy.

REFERENCES

1. Y.M. Kim, M.H. Wang and H.I. Rhee. Carbohydrate Research **339**, 715-717 (2004).
2. P. Phukhatmuen, A. Raksat, S. Laphookhieo, R. Charoensup, T. Duangyod, W. Maneerat. Heliyon **6**:e03625, 1-8 (2020).
3. J.M. Christenhusz, J.W. Phytotaxa **261** (3), 201-217 (2016).
4. A.K. Gupta, U. Pathak, M. Medhi, A. Mastinu, M.S. Sikarwar, P. Mishra. Agric. Rev. **41** (4), 305-316 (2020).
5. M. Daus, P. Chaithada, S. Phongpaichit, R. Watanapokasin, A.R. Carroll, W. Mahabusarakan. Phytochem. Lett. **19**, 226-230 (2017).
6. F. Ramli, M. Rahmani, I.S. Ismail, M.A. Sukari, M.A. Rahman, A. Zajmi, A.M. Akim, N.M. Hashim, R. Go. Nat. Prod. Communication **11** (8), 1103-1106 (2016).
7. J. Jenis, A. Baiseitova, S.H. Yoon, C. Park, J.Y. Kim, Z.P. Li, K.W. Lee, K.H. Park. J. Enzyme Inhib. Med. Chem. **34** (1), 1623-1632 (2019).
8. E.W.C. Chan, S.K. Wong, J. Tangah, H.T. Chan. Sys Rev Pharm. **9**(1), 58-63 (2018).
9. D.S. Lee, S.H. Lee. FEBS Letters **501**, 84-8 (2001).
10. R.T. Dewi , S. Tachibana, S. Fajriah, M. Hanafi, Med. Chem. Res. **24**(2), 737-743 **(**2015).
11. L. Makmur, Syamsurizal, Tukiran, S.A. Achmad, N. Aimi, E.H. Hakim, M. Kitajima, H. Takayama. J. Nat. Prod. **63,** 243-244 (2000).
12. H.W. Ryu, J.K. Cho, M.J. Curtis-Long, H.J. Yuk, Y.S. Kim, S. Jung, Y.S. Kim, B.W. Lee, K.H. Park. Phytochem. **72** (17), 2148-2154 (2011).